Doctoral Dissertation

Doctoral Program in Electronic and Telecommunication Engineering (30th cycle)

Communication Networks in CubeSat Constellations: Analysis, Design and Implementation

By

Luca Zanette
******

Supervisor(s):

Prof. L.M. Reyneri, Supervisor

Doctoral Examination Committee:

Prof. Rizwan Mughal, Referee, Institute of Space Technology, Islamabad
Prof. Stefano Speretta, Referee, Delft University of Technology
Prof. Marco Luise, Università di Pisa
Prof. Claudio Passerone, Politecnico di Torino
Prof. Alberto Vallan, Politecnico di Torino

Politecnico di Torino

2018

Declaration

I hereby declare that, the contents and organization of this dissertation constitute my own original work and does not compromise in any way the rights of third parties, including those relating to the security of personal data.

Luca Zanette

2018

To my Grandmother,
Still I can see the half-smile of yours, followed by a silence.
So much it meant to those who knew you..

Abstract

CubeSat constellations are redefining the way we approach to space missions, from the particular impact on scientific mission possibilities, constellations potential is growing with the increasing accessibility in terms of low development and launch costs and higher performances of the available technologies for CubeSats.

In this thesis we focus on communication networks in CubeSat constellations: the project consist of developing a clustering algorithm able to group small satellites in order to create an optimized communication network by considering problems related to mutual access time and communication capabilities we reduce the typical negative effects of clustering algorithms such as ripple effect of re-clustering and optimizing the cluster-head formation number.

The network creation is exploited by our proposed hardware system, composed by a phased array with up to 10dB gain, managed by a beamforming algorithm, to increase the total data volume transferable from a CubeSat constellation to the ground station. The total data volume earned vary from 40% to a peak of 99% more, depending on the constellation topology analyzed

Contents

List of Figures

List of Tables

Chapter 1

Introduction

1.1 CubeSat

CubeSat is a standard for miniaturized satellites developed by Cal Poly State University and Stanford University in 1999 [1]. This standard quickly became a valid solution to provide a low-cost and methodological approach to satisfy the growing interest from universities in design of small satellites for space research purposes.

A CubeSat satellite is made up by one or more 10x10x10 cm cubic units (1U) often designed and build by using commercial-off-the-shelf (COTS) components for the electronics and the structure. According to the CubeSat design specifications, the number of single unit (1U) joined classify the size of CubeSat, most common structures are 1U, 2U and 3U; in recent years, larger CubeSat platforms has been proposed, such as the 6U (10x20x30 cm) and 12U (20x20x30 cm) to extend the capabilities and test more complex systems and payloads. CubeSat specifications was initially intended for Earth observation, amateur radio or technology instrumentation test missions in low Earth orbit (LEO). Many CubeSat has been build to demonstrate spacecraft technologies targeted for small satellite use, for scientific missions and for academic purposes by several universities.

The interest in CubeSats design has rapidly grown due to their flexibility, fast design and realization process, low cost development and launch; moreover, they represent a useful solution for missions with high risk rate, where expensive satellites cannot be employed.

Despite the great advantages, CubeSats present several critical factors related to

dimensions, power supply, communication capabilities, propulsion systems, computing power, etc...

The use of COTS micro controller includes commercially available PIC, MSP, and ARM controllers of 8-33 MHz, 16-32 bit typically [2] [3] that guarantees higher data processing capabilities compared to space qualified components, however higher risks of faults must be considered due to higher susceptibility to space radiations and interferences.

CubeSats attitude determination must face the lack of high sensitivity star tracking systems, the best performing technology for attitude determination are miniaturized sun sensors usually used in combination with magnetometers that can achieve less than 2° accuracy [4]. CubeSats attitude control technologies are based on magnetic control or reaction wheels, usually with 5° accuracy [5] [6].

Communication systems represent one of the most important critical factor we want to focus on. Bouwmeester and Guo work [2] shows that 75% of CubeSats investigated use UHF with a maximum typical data rates of 9600 bps while only 15 % work in S-band and reach a maximum, data rate of 256 kbps. The remaining CubeSats missions work in VHF with data rates similar to UHF. The typical transmission power range for downlink is 0.1 W to 1W so data rates values are primarily limited by available link power budget rather than by the existence of available electronics. Available transmission power and communication capabilities represent the key factors to define the efficiency of a CubeSat mission. The total data volume transferable between CubeSat and ground station depends from the communication capabilities and from the orbit characteristics of CubeSats, i.e. the total access with the ground station and the ability of CubeSat to maintain its orbit, if propulsion system available.

1.2   CubeSat Constellations

A defined set of CubeSats that cooperate together to achieve specific goals form a constellation, the cooperation of two or more CubeSats allows to achieve results that a single monolithic system is unable reach. There is a growing interest among science community in using distributed systems of small satellites for space science missions, with a special focus on Earth observation missions. Constellation architectures have been studied and optimized for decades, they are typically designed

to provide a wide and optimized coverage over a specific area or guarantees the higher visibility between satellites and ground station/s. The number of satellites that form the constellation and orbit parameters of each of them define the coverage and visibility characteristics of the constellations. Particular importance assumes the communication among satellites of the constellation: the ability to establish an inter-satellite link modify the entire mission data and command send/receive strategy. Thanks to hop-to-hop communication, satellites can be seen as nodes of a network and single CubeSat can be reached by the ground station despite it not results in the GS's field of view.

Beside great advantages in terms of coverage and visibility, the use of a distributed structure avoids catastrophic single point failures, in case of failure of a single satellite the entire system can still be operational and, with the support of an adequate control strategy, a strategical satellite can be replaced by another candidate able to sustain specific requirements.

1.3   Thesis Structure and Goals

In this thesis a complete study and design on CubeSat constellations in term of communication networks is performed.

We start by introducing high level constellation management algorithms: the clustering algorithms. These algorithms are used to create links between satellites and define specific roles that each satellite must assume. The goal is to develop an algorithm able to manage CubeSat constellations and assign to each CubeSat a specific role to create a communication network in the constellation able to optimize communication and provide the longer and reliable access between all constellation's elements and the ground station.

After the network creation we focus on the communication hardware by considering the mosts suitable antenna for CubeSats and we perform a link budget analysis to define constellation limits in terms of communication capabilities and physical extension.

The link budget analysis will be the key factor to define a proper antenna configuration and in which spatial boundaries we can establish inter-satellite links in order to maximize the total daily data volume from constellation to ground station.

After the link budget analysis we design and realize the hardware communication

system based on a phased array and we introduce the hardware control strategy able
to employ this antenna in order to estimate the direction of arrival of the received
signal during the receive mode or steer the array toward a specific direction during
the transmit mode with the purpose to optimize the communication during the data
transfer. This process will be managed by a beamforming algorithm.

Our final goal is to create two complementary systems that alternately work to
manage the constellation's communication phase: the cluster system contribute to
the network creation and link type optimization, the communication system exploit
the proposed CubeSat hardware communication sub-system to optimize data transfer
and improve the total data volume that a normal constellation can download toward
the ground station. We provide an independent constellation management system
able, thanks to our proposed clustering algorithm, to create a communication network
among CubeSat of the same constellation and to define if establishing inter-satellite
links with the high gain proposed antenna system can bring advantages in terms of
data volume and constellation visibility.

In chapter 2 existing clustering algorithms are introduced and analyzed: they
are employed to manage CubeSat constellations at high level. Thanks to clustering
algorithms each satellite of the constellation can assume a specific role in order to
create a communication network and optimize data and command transfer among
CubeSats.

In chapter 3 a selection of antennas that fit CubeSats spatial and performance restriction is presented.

In chapter 4 a set of antenna configurations to establish communication links is
proposed and, for each configuration, a detailed link budget analysis is performed.
Considering the proposed antenna configurations we focus on the EIRP to understand
data rate levels achievable by establishing communication links among CubeSats
(inter-satellite links) and from CubeSats to Ground Station (Up/Down-links).

In chapter 5 a set of constellation topologies is proposed with the purposes to analyze
the total daily volume transferable toward ground station by establishing only direct
downlink communications. These results will be compared with the total daily
volume downloadable by establishing also space-links. The final goal is to define if
establishing space-links brings advantages in terms of data volume or not.

In chapter 6 we present the hardware designed to establish space-links according to
previous consideration and communication strategy. Chapter 7 presents the hardware

control strategy and the signal direction of arrival estimation algorithm utilized to improve the mutual physical position estimation process and optimize the inter-satellite communication link.

In chapter 8 and 9 our proposed clustering algorithm is presented, implemented, simulated and simulations results are analyzed and explained.

Chapter 10 present the proposed antenna configuration for CubeSat constellation and the total data improvements achievable by establishing space-links.

Chapter 2

Clustering Algorithm for CubeSat Constellations

Satellite constellation management is strictly related to the constellation topology and its evolution in time in terms of mutual physical position and speed. If we consider propulsion systems available on satellites is possible to avoid orbiting problems (e.g. orbit drift) and perform formation flight of satellites. In this case, satellites can maintain specific distances and it's possible to create stable, time-invariant communication links that change in case of previously defined communication strategies or because of unexpected malfunctions.

When propulsion systems are not available, the topology in satellite constellations results less stable, orbit modification due to external factors results hard to prevent and control. External mobility variations influence on constellation's elements, energy management strategies and mission priorities of the single element of the constellation makes impossible to define a priori an optimized inter satellite link creation strategy able to manage a CubeSat constellations. Therefore, a dynamic control strategy able to consider all factors that affect the space-links capability and allows to optimize communication between satellites results a fundamental factor in constellation communication management.

In this chapter we present existing control strategies adopted to manage networks of mobile nodes, we analyze their strengths and weaknesses and we try to select a series of existing methodologies and approaches in order to design an algorithm that fit our requirements and create a useful solution to manage CubeSat constellations.

2.1 Mobile ad-hoc networks (MANETs)

Mobile ad-hoc networks (MANET) are autonomous systems of mobile terminals / nodes connected between them by wireless ad-hoc connections, systems of autonomous and mobile routers with their hosts connected to form a graph.

In a complex scenario where nodes have strong differences in performances, motilities and where existing communication infrastructures are expensive or inconvenient to develop, wireless links can still provide to nodes to communicate tanks to the formation of a MANET [7][8].

Dynamic routing represents one of the most critical issue in MANETs: since there is not a physical communication infrastructure, nodes of MANETs are expected to cooperate to establish, implement and maintain a reliable network in a dynamically manner and guarantee the communication by routing packets through the most efficient path with the purpose to cover all the extension of the network, allowing nodes to communicate over multiple hops.

MANETs architecture can be *flat* or *hierarchical*: in a flat MANET all nodes have equal functionalities and tasks, while a hierarchical network is more complex, nodes can assume specific roles based on a set of parameters and perform tasks with different complexity levels. Nevertheless, it should be noted that a flat structure cannot satisfy the routing requirements represented by complex scenarios and / or large dynamic MANETs [9][10].

Mobility of nodes, complexity or dimension of the messages exchanged between nodes are primary factors that could easily compromise the structure and functionality of MANETs. These factors can lead to the saturation of the network, generating delay and / or messages losses, in particular when network is composed by nodes with high mobility or when MANETs presents specific physical conditions. Consequently, hierarchical architectures are essential to achieve basic performances in large-scale or high-mobility MANETs [7].

2.2 Clustering Algorithms

Formation and management of MANETs is related to several factors: the initial physical displacement of terminals, mobility behaviors of each element like individual

and mutual speed, nodes dispersion, communication features and, more generically, hardware features of nodes, etc.. represent just a selection of critical variables that can be considered to create a maintain a stable structure of a MANET.

Many algorithms has been developed to form, manage and maintain MANETs structures: the **clustering algorithms**.

Main goal of clustering algorithms is to autonomously create and maintain MANETs in specific work environments. The general strategy consist to group nodes in virtual sub-groups based on specific grouping parameters (e.g. proximity) with the purpose of optimize the organization between nodes of the whole MANET.

Depending on the grouping strategy, nodes can assume different functionalities and status such as *cluster-head*, *cluster-member* or *cluster-gateway*. Figure 2.1 shows a generic cluster representation with cluster-heads (CH), cluster-members and nodes with gateway capabilities.
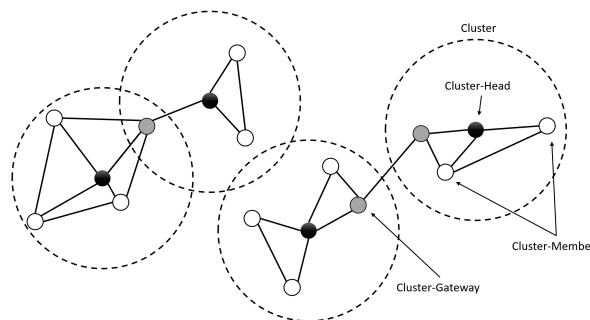
Fig. 2.1 Generic Cluster Structures

Usually, a cluster-head (CH) is a local administrator of its cluster: depending on global or local purposes and nodes abilities, CH coordinates its group (local cluster) to achieve specific goals useful for the cluster or for the whole network. Furthermore, CH usually manages the data flow inside and outside the cluster and is responsible for *invite* new member to join its group. However, functionalities and privileges of CHs vary depending on the clustering algorithms.

A cluster-member (CM) is a node connected to a cluster-head: speed, position, hardware features, communication abilities, etc.. are the typical constraints that define when the CM can link to a cluster-head. We will further analyze several clustering algorithms to understand the most common aggregation mechanisms used for CMs.

A cluster-gateway (CG) is a cluster-member with the ability to communicate with

members belonging to other clusters, also for CG, functionalities are defined by constraints that vary depending on algorithm selected for MANETs management. Sometimes gateway functionality is available only for cluster-heads, sometimes only for cluster-members, sometimes is not required nor performed.

2.3 Strengths and weaknesses of Clustering

Clustering algorithms guarantee a certain level of performances when they are exploited to handle MANETs especially when a large number of mobile nodes are involved [7][11]. The use of these algorithms offer great benefits, however every algorithm has its own limitation and costs.

2.3.1 Routing

The structures formed by clustering algorithms introduces the ability to route messages between nodes of the same cluster and perform inter-cluster communication. By working on the routing protocols [12] [13] is possible to determine an optimal routing configuration to perform communication between elements of the whole network thanks to the creation of a virtual dynamic backbone though the network. That is, elements of cluster with gateway ability allow to form a communication channel backbone over the MANET, allowing to route information according to a specific optimization strategy. The costs of routing capabilities are intrinsic: depending on the adopted strategy, a certain level of complexity is introduced in the system on the routing layer.

2.3.2 Physical Behavior and Re-Clustering

Grouping MANET in smaller sub-groups means splitting the network so to make it more stable and easier to manage: the mobility variations and differences in terms of relative position and mutual speed can bring to situations where a node needs to switch its cluster affiliation, this process is called "node *re-affiliation*".
When a node re-affiliation needs to be performed, a flooding effect can affect the entire network: some clustering schemes may cause side effects and the cluster

structure may need to be completely rebuilt if some important events occur to strategic nodes (e.g. a Cluster-Head "die" or gives up his status). This event is called *ripple effect of re-clustering* [14–22]. The ripple effect in a cluster structure represent one of the most critical issue and can compromise the functioning of the entire system.

Some clustering algorithms limit this effect warning only the interested clusters about the re-affiliation process procedure [23, 24]. This concept can be extended to manage every significant event in the cluster: our design process will include these strategies to mitigate the ripple effect of re-clustering as much as possible.

2.3.3 Clusters Formation

Is possible to distinguish two different phases in clustering algorithms: cluster formation and cluster maintenance. The cluster formation phase is the most critical: during this phase a neighborhood analysis must be carried out to define the initial node conditions and planning next steps. Most of the clustering schemes usually assume that mobile nodes must be in static condition to facilitate the formation process. A finite number of messages must be exchanged to define which role must be assumed by every node, therefore a frozen period of motion must be kept to define the first configuration of clusters. However, this is in total contrast with our scenario: the initial static period cannot be guaranteed in small-satellite constellations. Computational round is another important parameter that must be considered during the clusters formation phase: it represents the number of rounds in which the cluster formation procedure must be completed. Computational round must be kept as low as possible in order to conclude the formation process in short time without an excessive data exchange. Static assumption and computational round are two critical parameters that must be considered to define the efficiency of a clustering algorithm.

2.3.4 Structures Maintenance

In order to maintain a cluster structure, an explicit control messages exchanging phase is generally required [25][14–18, 26, 19–21]: depending on the algorithm, large number of control messages can be necessary to maintain the network structure, this brings to a significant bandwidth occupation and to energy consumption. The

explicit control message parameter evaluates the efficiency of communication for clusters maintenance action in relation to total data flow.

2.3.5 Resources Reuse

As introduced before, the local master (cluster-head) can coordinate transmissions inside and outside clusters to save resources and energy, avoid crosstalk and, more generically, allow a tasks redistribution to sensibly reduce the individual communication requirements to nodes. System capabilities are one of the key factor to be evaluated, the spatial reuse of resources allows to increase the system potential [25, 27]. In our specific use case the resource reuse, allows not-neighbor clusters to communicate over the same frequency and / or same code without communication interferences issues [28].

2.3.6 Clustering Evaluation Parameters

In conclusion, total computational round, ripple effect of re-clustering and stationary assumption are key factors that affect the efficiency of a clustering algorithm. Table 2.1 summarizes the generic evaluation parameters described in this section. We will further analyze the formation and maintenance phases of clusters and address the general problems related to structures in order to design an algorithm able to work efficiently in our scenario, able to deal with problems and satisfy our mission requirements.

Table 2.1 Clustering Evaluation Parameters

Costs of Clustering	Descriprion
Stationary Assumptions	To set up the cluster structures a frozen period is required to establish the first configuration of every node and the whole configuration of the system. The frozen period of motion depends from factors related to the nodes and to the clustering algorithm in use.
Explicit Control Messages	Represents the total number of messages necessary to maintain the structure of the cluster.
Ripple Effect	Is the "Domino effect" that a re-election of a Cluster-Head may cause on the entire cluster structure. When is not kept under control it can entirely modify the structure of the cluster, compromise the efficiency and cause a flood of the control messages necessary to maintain or create the cluster.
Computational Round	Computational rounds are number of rounds necessary to set up the clusters structures. They represent the total number of actions (steps) required to complete the clusters formation phase. Computational round can be fixed or vary depending on clustering algorithm and structures.
Computational TIme	Computational Time represent the required time to create cluster structures.
Cluster Maintenance Complexity	Total amount of messages used to maintain the cluster structure, it affect the total available bandwidth.

2.4 An Overview on Main Clustering Algorithms

By analyzing the characteristics of principal clustering algorithms, appears evident that each of them is suitable for a specific operational area, scenario or for a defined use case. Usually, once the operating boundaries are overcomes, algorithms present low efficiency and negative and / or harmful aspects for the network, e.g.: Passive Clustering (PC) presents an energy waste in case of low density distribution of nodes. A comprehensive survey of the main clustering algorithms can be found in[29]: Jane Y. Yu and Peter H.J. Chong classified algorithms under six main categories, selected depending on their working principle and their operational mode as shown in table 2.2 [29]. In next sections, we describe some of them, their working principle and their features.

Some features and methodologies from developed clustering algorithms has been selected as starting point to develop our algorithm: starting from similar concepts or from specific features that better fit to space environment requirements, we unified the strengths and we introduced new concepts during the design process to minimize weakness points and to be coherent with our concepts of simplicity, flexibility and energy saving. The selected algorithms are:

- Passive Clustering [22]

- On-Demand WCA (Weighted Clustering Algorithm) [21]

- 3-hop Between Adjacent Clusters [17]

- MOBIC [18]

Table 2.2 Clustering Algorithms Typologies

Tipology	Descriprion
DS-Based clustering	Find a dominating set of to reduce the number of nodes participating in route search or routing maintenance.
Low-mainteinance clustering	Minimizes the clustering-related maintenance cost and provide a cluster structure for the upper layer applications.
Mobility-aware clustering	Utilizes mobility of nodes as fundamental parameter for the cluster construction and maintenance. It assign nodes with similar relative speed to the same cluster.
Energy-efficient clustering	Avoids unnecessary energy consumption and balance the energy consumption with the purpose to prolong the lifetime of mobile node, consequently keep the network more stable and durable.
Load-balancing clustering	Limits the number of mobile node that can join to a cluster in order to distribute the total workload of the network.
Combined-metric based clustering	Considers multiple parameters of nodes (node degree, mobility, battery energy, cluster size, etc.) and combine them to obtain a discriminating factor used to configure the entire cluster structure. These parameters are combined together using weight factors in order to make the algorithm flexible for different application scenario.

2.4.1   Passive Clustering (PC)

Generally, clustering algorithms require to nodes to broadcast information repeatedly with other nodes to maintain a stable cluster structure. Consequently, number of messages to maintain cluster become an important source of overhead over bandwidth. In PC [22], like for other algorithms, nodes can be at different states such as Initial, Gateway, Head, etc.. When a node at Initial state has something to communicate, it declares itself as cluster-head and send a *head-claim* in broadcast. Neighbors that receive the claim automatically become ordinary nodes while node that receive more claims become gateway. Thus, means that in PC a single claim sent from a node is sufficient to start the process of cluster formation and stimulates the other nodes to independently change their status in any moment. When an ordinary node does not receive any communications from his cluster-head for a given period set its status to initial.

The fundamental characteristic of passive clustering is that explicit clustering-related messages are not involved to maintain the cluster structure, nodes are responsible of their own cluster status.

As a result, PC strongly reduces communication complexity. Cluster maintenance is traffic-dependent, thus eliminates control overhead messages for clustering allowing communication in networks with limited channel capacity and/or high mobility. Moreover, PC brings great advantages during the cluster formation phase: given the independent behavior of nodes computation rounds is unnecessary to consider. Furthermore, the cluster formation process in most algorithms requires nodes stationary assumption, meaning that nodes must not be in motion and their position must be known. In PC, the initial neighboring learning and the cluster construction can be performed while nodes are moving.

Despite these great advantages, PC does not guarantee a complete functional solution for our application. Problems inherent to the PC algorithm reflect negatively on our CubeSat cluster, these limitations involve that:

- A node becomes gateway only if a certain number of head-claims are detected, this mechanism reduces the generated duplicate communication traffic and supports a good connectivity between clusters. However, how to decide the optimal number of claims to receive to become gateway is not addressed in PC.

- For networks with discontinuous traffic, clusters are difficult to maintain. This can occur when elements must be in "no-transmit mode", e.g.: prohibited transmission points (e.g.: dark side of the moon), transmission interruptions due to using of sensible payload, etc.

- Ripple effect of re-clustering is not addressed. This could bring to a flood effect on cluster compromising the entire network structure.

- Creation of unnecessary Cluster-Heads can occurs: energy saving is one of primary aspect that must be considered in space environment as a consequence, Cluster-Heads number must be appropriate: they are responsible for the cluster structure and its goals, representing the communication junction between nodes and / or clusters, this role imply a greater amount of energy spent to communicate. High number of Cluster-Head is useful to distribute the communication activity and reduce the energy budget required for the single CH. However, to many Cluster-Heads corresponds an increasing of the structure complexity, consequently, to a greater energy consumption due to control messages required to manage it.

- Energy consumption is not optimized in PC. Nodes consume energy to transmits claims for undefined time. The singularity comes when nodes without neighbors try to communicate: it declares itself as cluster-head and start to send claims for undefined time generating an unless waste of energy.

Figure 2.2 shows an example of a PC formation scheme.
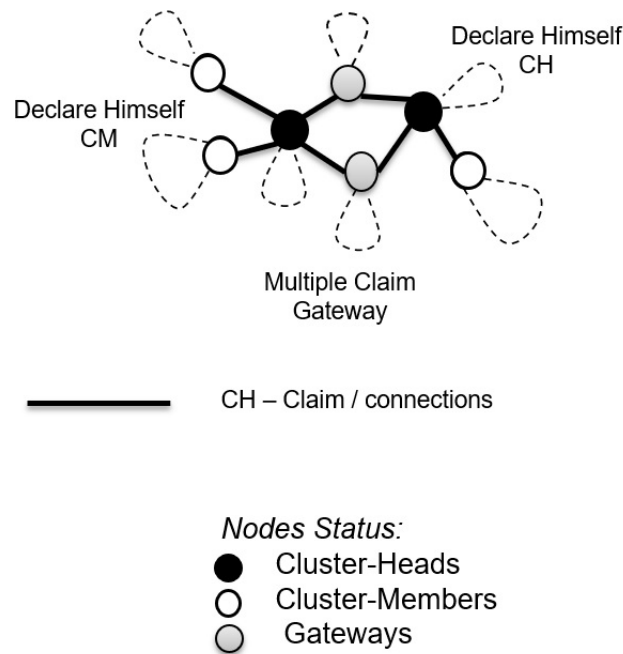
Fig. 2.2 PC Generic scheme.

Table 2.3 summarizes main advantages and disadvantages of Passive Clustering. We decided to take some advantages from in consideration to develop our algorithm.

Table 2.3 Passive Clustering: Pros and Cons

Passive Clustering	
Advantages	**Disadvantages**
Explicit control messages not required: bandwidth saving	Optimal claim number to become gateway not addressed
Stationary assumption for cluster formation not required	Cluster maintenance problems with discontinuous traffic
Constant computational round unnecessary to consider	Ripple-effect not addressed
Reduces the Communication Complexity	Energy and complexity optimization problems

2.4.2   Passive Clustering: Contributions to Our Algorithm

The head-claim broadcast phase previously described introduces the concept of *hello messages*: a broadcast message utilized from nodes to explore the neighborhood. Is possible to find a similar concept also in Wu's Connected Dominating Set algorithm [14]. In Wu's algorithm, a sort of hello message is used by nodes for maintenance purposes, any moving node continuously send beacon messages every t seconds and related mobile nodes perform monitoring activity to maintain the cluster structures. The weak point of claim messages in PC and beacon messages in Wu's algorithm is the energy requirements for continuous message broadcast: in case of low density of network, nodes send an unnecessary or not listened sequence of hello messages causing energy wasted for transmission.

On the other hand, in case of high density clusters, continuous broadcast imply risk of network congestion affecting the transmission efficiency. Moreover, a cluster structure maintenance system based on hello messages imply a large amount of message exchange especially if nodes are characterized by high mobility.

However, hello messages represent a powerful tool for the neighborhood exploration, our goal is to re-create a behavioral dualism with the hello messages commonly used in communication protocols at routing layer for classical static networks where the hello messages are exploited to determining the network connectivity [30]. We decided to exploit hello messages strategy in our algorithm with the introduction of some modifications to overcome the presented limitations. The functional modifications to the existing techniques and our proposed clustering algorithm are presented in chapter 8.

2.4.3   On-Demand Weighted Clustering Algorithm

Most of algorithms consider only one key parameter as reference to elect their cluster-heads and set up the cluster structures. On-Demand Weighted Clustering Algorithm (WCA) [21] combines a defined set of parameters to form the cluster structures with the purpose of elect the most suitable cluster-head of a local area. In On-Demand WCA preselected parameters are combined by weighting factors, therefore is possible to preset during the design phase the influence that parameters will have on cluster-head election process in order to fit the specifics of the mission. Four key parameters are considered for the cluster-head election process, they are:

- *Dv* - Degree-difference: indicates the ability of nodes to become CH in relation to the neighborhood and to its abilities, is given by:

$$Dv = |dv - M| \qquad (2.1)$$

  where *dv* is the number of neighbors of a mobile node and *M* is the number of nodes that a cluster-head can handle.

- *Pv* - Sum of the distance with all neighbors: this parameter gives indication about the relative position of neighbor nodes. It will be used to locate a central node to elects as cluster-head.

- *Mv* - Average moving speed: indicates the relative speed between nodes in order to group in the cluster nodes with similar mobility. This parameter allows to create clusters of nodes with similar movement parameters, that imply a more stable structure considering the evolution of the nodes movements.

- *Tv* - Cluster-head serving time: based on many factor, it is possible to estimate or establish a priori the serving time that a cluster-head can guarantee. Being a cluster-head requires a greater amount of energy, this parameter helps to elect the best cluster-head considering the need of durability over time.

These four parameters are processed to obtain the combined weight factor *Iv*, calculated as shown in 2.2:

$$Iv = c_1 Dv + c_2 Pv + c_3 Mv + c_4 Tv \qquad (2.2)$$

where:

$$c_1 + c_2 + c_3 + c_4 = 1 \qquad (2.3)$$

On-Demanding WCA will elect as cluster-head nodes with minimum value of Iv in their local area, all nodes covered by elected cluster-heads cannot participate to further cluster-head elections. This procedure will be repeated until each node assumes a status of cluster-head if electable or is connected to its cluster-head somehow.

Despite the great flexibility introduced from the consideration of multiple parameters and from the weight factors, also On-Demand WCA presents negative aspects:

- The cluster formation is based on the stationary assumption and is in contrast with space environment requirements: initially, a long frozen-period is required since each node needs to measure and collect an important amount of data and elaborate them to obtain the weight factor *Iv*. This is not acceptable since our algorithm must be able to setup clusters with nodes already in motion and integrate them after the cluster formation stage.

- In On-Demand WCA How to select the parameter *M* is not addressed explicitly in [21].

- Is not easy to establish mutual average moving speed: it depends from the technology available or from informations available from the system that is responsible of the nodes monitoring, if exists. In any case, a precise measurement of relative speed can be a great issue to overcome. If nodes are able to estimate the relative speed of neighbors, high computational costs results necessary, therefore the explicit control messages for cluster maintenance influence the channel bandwidth. High control messages exchange can bring communication channel saturation, making impossible using the channel for data transfer.

- The Cluster-head serving time (*Iv*) value can vary over a wide range depending on the node communication requirements, a dynamic adjustment of this value affect the cluster stability in case of energy waste peaks, to overcome this problem, a first survey of the general clusters behavior must be done, affecting the flexibility concept.

- When a mobile node moves to a region not covered, the cluster-head re-election will be performed based on the minimum *Iv* as described above. The re-election causes a ripple effect over the entire cluster structure, therefore the re-clustering destroys current network architecture involving a considerable number of control messages to re-build it. Therefore, the effectiveness of this algorithm can be doubted.

- The diameter of cluster is 1-hop: thus, means that inter-cluster communication must be performed from cluster-heads, involving a highest amount of energy consumption. Moreover, the cluster-head represent a bottleneck for the inter-cluster communication.

Figure 2.3 shows an example of a On-Demand WCA formation scheme.
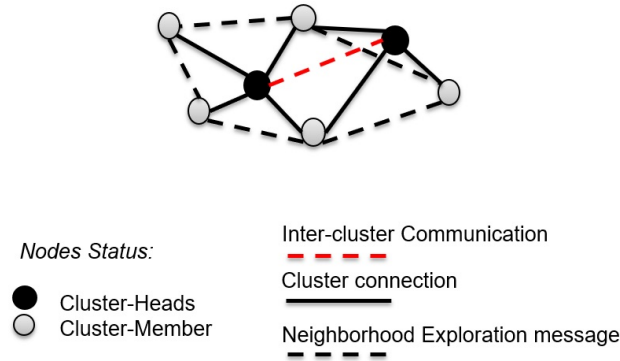
Fig. 2.3 On-Demand WCA Generic scheme.

Table 2.4 summarizes the weakness and the strength of On-demand WCA described in this section.

Table 2.4 On-Demand WCA: Pros and Cons

On-Demand Weighted Clustering Algorithm	
Advantages	**Disadvantages**
High flexibility for the mission requirements	Stationary assumprion for cluster formation required
Strategic cluster-head election gives flexibility to the algorithm	The maximum number of nodes that a cluster-head can handle is not defined from any procedure
Customizable behavior of nodes	Average relative moving speed hard to define: risk of flood of communication channel
	Dynamic cluster-head serving time can affects the cluster stability
	Ripple-effect limitation and management not addressed
	Cluster-heads communications problems and energy wasting

2.4.4   On-Demand WCA: Contributions to Our Algorithm

Despite the weakness mentioned above, on-demand WCA represents an important part of our clustering algorithm.

With On-Demand WCA, the cluster-head election process and, more in general, the whole cluster formation process becomes customizable and more flexible. This flexibility introduced from the weighting factors allows nodes with different features and abilities to easily cooperate each other. Is possible to overcome hardware features of nodes and, more important, to add an abstraction level.

To overcome a massive ripple effects of re-clustering, we introduce the limit that nodes connected with a cluster-head cannot participates to further cluster-head elections. Moreover, when a cluster-head dies or is unable to serve as CH, the re-election process is performed between nodes who was connected to that cluster-head. Thus, affects the efficiency in terms of total cluster-head number and CH optimization choice, but limits ripple-effect. Only in a second phase an optimization of the cluster-head number can be performed thank to a merging action, if necessary. Similar concept is introduced by *3hBAC* algorithm, it eliminates the ripple effect of the re-clustering by containing the re-clustering process only for the interested clusters.

2.4.5   3hBAC - 3-hop Between Adjacent Clusters

3hBAC [17] forms 1-hop-diameter non-overlapped structures with a 3-hops distance between neighbor cluster-heads. In 3hBAC clusters construction procedures start from the neighborhood of node with the lowest ID: in this neighborhood, mobile node with higher ID become the first cluster-head, all the direct neighbors assume the status of cluster-members. When a node assume CM status he cannot participate to next cluster-head elections. After the formation of the first cluster the procedure to form the other clusters can be performed in parallel in the network: cluster-members affiliated to different cluster-head that can communicate each other assumes the role of gateway in order to form create the network and backbone of MANET.

The most interesting feature of 3hBAC is the introduction of a new status that a node can assume: *the cluster-guest* (CG). Cluster-heads in 3hBAC try to stay at

2-hop distance so they can maintain the structure of the entire network without any significant change in the node status assignment. When two cluster-heads move into the working range of each other one of these two must give up the cluster-head role. In this case a re-clustering procedure starts to define the new cluster configuration, thanks to cluster-guests ripple effect of the re-election is influences only the interested clusters. In case a mobile node moves outside from cluster, it can join to other clusters as cluster-guest if detects a cluster-member, also this capability contributes to avoid re-clustering procedures and consequent effect of instability on the network. Figure 2.4 shows an example of a 3hBAC scheme and member re-affiliation.
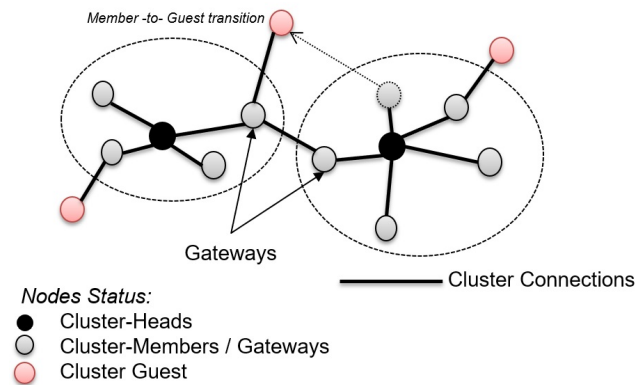
Fig. 2.4 3hBAC Generic scheme and member re-affiliation

Table 2.5 summarizes pros and cons of 3hBAC.

Table 2.5 3hBAC: Pros and Cons

3-hops Between Adjacent Clusters	
Advantages	**Disadvantages**
No Ripple-effect of re-clustering	Stationary assumprion for cluster formation required.
Limited communication complexity	More feasible in a dense scenario
No ripple-effect when cluster-member change their affiliation.	Unconstant computational round
High flexibility and stability thanks to the cluster-guest	Cluster-member are choosen based on their position without considering their mobility
Parallel cluster formation	2-hop distance manteinance involve a sort of mobility control actuator. Otherwise the cluster merging is invoked
	Re-election in case of immediate cluster-head overlapping in 2-hop range

2.4.6   3hBAC: Contributions to Our Algorithm

3hBAC presents great advantages if considering cluster stability and ripple effect containment: the introduction of cluster-guests guarantees great flexibility in case of intense and dynamic node re-affiliation without any impact on cluster structures.

We will exploit the concept of cluster-guest to take advantages from the consequent stability and the attenuation of ripple effect of re-clustering, moreover cluster-guests help to extend the working range of our algorithm.

Thanks to the cluster-guest status that a node can assume we are able to allow nodes with very different mobility characteristics to join to clusters without any impact on the network structure.In 3hBAC a cluster-member cannot participate to further cluster-head election; this restriction will be bypassed with the purpose of limit further the ripple effect in case of a cluster-head is unable to maintain its role. Therefore the re-election will be performed only among nodes who was connected to the "died" cluster-head. Substantially, 3hBAC with some modifications represents a basic part

of the cluster maintenance strategy of our algorithm.

In 3hBAC when a cluster-head overlaps on the working range of another cluster-head a re-clustering process start: we will use the same principle but, unlike 3hBAC we will wait before starting the process. A sort of re-clustering timer is introduced to avoid a continuous re-clustering oscillation behavior due to particular node mobility condition.

A similar concept is expressed in the cluster maintenance phase presented in MOBIC [18], it introduces a timer to avoid unnecessary cluster-head re-election. We will describe MOBIC in next section.

2.4.7   MOBIC Algorithm

Nodes mobility is the central characteristic that affects performances of every clustering algorithm: mobility affects network topology, communication, data flow. etc.. An entire category of clustering algorithms, the mobility-aware clustering algorithms, consider mobility factor as the main element to form clusters and manage MANETs. The idea of mobility-aware algorithms is to group mobile nodes with similar speed into same clusters. MOBIC [18] suggests to take into account mobility parameters of nodes, in particular during the cluster-head election process. The working principle suggests that cluster-head election must be considered as a local activity, every cluster-head should be elected depending on mobility characteristics of its neighborhood. Essentially, nodes with low relative speed are electable to become cluster-head. In MOBIC, the speed variance of mobile node is estimated, nodes with lowest variance result to moves less than its neighbors, therefore it can takes the role of cluster-head of its neighborhood.

The cluster maintenance phase in MOBIC follows the Least Cluster Change (LCC) [15] with some variations. LCC is based on Lowest ID Clustering (LIC) [31] or on Highest ID Clustering (HCC) [16]. LCC performs cluster maintenance by referring to the ID values of nodes. The re-clustering is invoked only in two cases: first, when a cluster-head moves into the working range of another, one of these two must give up the role. Second, when a node is unable to join any cluster-head it rebuilds the cluster structure according to LIC. The difference of MOBIC with LCC is represented by the introduction of the CCI timer. This timer is used to avoid unnecessary re-clustering actions when two cluster-heads converge in the same working range for

a brief period. Hence, a cluster-head gives up its role to the other competitor only if they stay in the same area for period longer than CCI thus helping to reduce the cluster-head changes rate.

Main problem in MOBIC is that the mobility behaviors are considered during the clusters formation phase but not over time: cluster maintenance phase gives ever less importance to variance of speed in time, in MANETs where moving nodes position is in continuous evolution, this algorithm become less and less efficient. Cluster formation characteristics and difficulties to interpret node mobility evolution make this algorithm suitable for MANETs with nodes that share a similar group mobility behavior, in a scenario where nodes move in same direction with similar speed: in case of randomly node directions and / or variation in mobility behavior, a degradation in performances could be verified. Figure 2.3 shows an example of a MOBIC formation scheme.
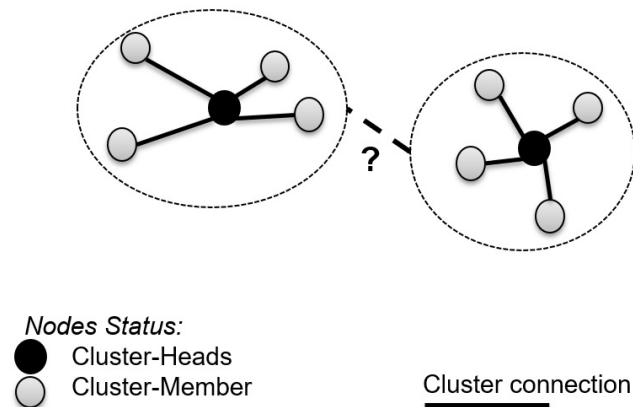
Fig. 2.5 MOBIC Generic scheme.

2.4.8   MOBIC: Contributions to Our Algorithm

As described before, the conditions in which MOBIC performances are optimized occur when nodes move in the same direction and with similar speed: a scenario with shared group mobility behaviors can reflect small-satellite constellations. The greater feature that makes MOBIC suitable for our purposes is the ability to create clusters no need of nodes stationary assumption: this allows to perform cluster formation phase in any time after launch, reducing the complexity needed for cluster formation phase. This part of MOBIC represents a precious strategy that we can exploit in

our algorithm. On the other hand, MOBIC presents some significant difficulties if it purely applied to a CubeSat constellation: first of all, the estimation of relative speed variance that all nodes must perform imply that nodes are equipped with hardware able to perform these measures, a certain level of complexity is introduced.

The second weakness of MOBIC lies in the maintenance phase: the re-clustering of node is called too often if some nodes change their mobility behavior or when nodes join to a cluster for brief periods. In case of CubeSat with difference orbit characteristics, clusters will be formed from nodes with continuous and dynamic mobility variation, maybe only a few of them will results able to join to cluster in a stable manner, causing continuous modification requirements in network organization.

In conclusion, MOBIC solves problems related to the cluster formation and maintenance phase, unfortunately it doesn't guarantee flexibility outside its optimal working range. In our algorithm, we will exploit the strategies proposed in MOBIC regarding the cluster formation by speed variance estimation. This strategy will support both cluster formation and maintenance phase of our algorithm, with the difference that we will try to mitigate the degradation of its efficiency over time by considering constantly mutual speed and positions during the maintenance phase. However, relative speed won't represent the only element to define cluster maintenance strategy: some modifications are introduced thanks to concept expressed in previous algorithms. Table 2.6 summarizes pros and cons of MOBIC.

Table 2.6 MOBIC: Pros and Cons

MOBIC Algorithm	
Advantages	**Disadvantages**
Takes into account the mobility of nodes to create clusters	Requires to nodes the ability to estimate the relative speed of their neighbours
Stationary assumptions not required	Weak cluster manteinace strategy
CCI timer to avoid unnecessary re-clustering actions	Mobility bheaviour evolution of node not considered. Degradation risks
	Ripple effect of re-clustering
	Explicit control messages for the cluster formation and mainteinance is invoked

Chapter 3

Antenna Selection

In this chapter we propose different antenna types and dimensions with the purpose of establish a wide operating range in terms of communication capabilities. We perform a complete study on the ground-link and space-link. All configurations are compared in order to optimize the communication while respecting typical CubeSats surface limitations.

3.1 Antennas

We select the *S-Band* as working frequency during all the simulations and measurements because it represent one of the free available frequencies for communication links. In particular, 144 MHz, 437 MHz and 2,4 GHz are the selectable frequencies. 2,4 GHz will be the selected frequency for our projects. Referring to ITU Radio regulations 2016 [32], there are available chunks dedicated to space-to-Earth communications. On the Ground station two parabolic antennas are selected:

- GS Antenna 0: Parabolic d = 3 m

- GS Antenna 1: Parabolic d = 5 m

A three meter diameter parabolic antenna is physically available at Politecnico di Torino, it is used to establish the communication in S-Band with CubeSats of the AraMiS [33] mission lead by the Department of Electronic and Telecommunication.

The five meter parabolic antenna is selected as ground station. A two or three meter parabolic antennas would be more appropriate for CubeSat mission, we refer to a five meter antenna to oversize the ground station contribute on link budget. Selected antenna types for CubeSats are:

- CubeSat Antenna (*O*): Omni-directional

- CubeSat Antenna (*P*): Patch (side length: 3,556 cm)

- CubeSat Antenna (*Par*): Parabolic

- CubeSat Antenna (*PA1 to PA4*): Phased Array(s)

3.2   Parabolic Antenna (Gain considerations)

The parabolic antenna gain vary depending on dimensions according to equation 3.1:

$$G = \frac{4\pi A}{\lambda^2} e_A = \left(\frac{\pi d}{\lambda} \right)^2 e_A \tag{3.1}$$

where:

A is the area of the antenna aperture. For a circular dish antenna, $A = \pi d^2/4$, giving the second formula above.

d is the diameter of the parabolic reflector, if it is circular.

λ is the wavelength of the radio waves.

e_A is a dimensionless parameter between 0 and 1 called the aperture efficiency. The aperture efficiency of typical parabolic antennas is 0.55 to 0.70. We assume a fixed efficiency of 0.55.

Therefore, for the selected parabolic antenna on ground station gain levels are:

Table 3.1 Parabolic-antenna-gain

Antenna Diameter [m]	Antenna Gain [dBi]
2	31
3	35
5	39

3.3   Patch Antenna

The selected patch antenna is developed by *Antenna Development Corporation (AntDevCo) [34]*, it has been designed and manufactured for many spacecraft programs, including CubeSat. This antenna is capable to support high data rates and at least 10 Watts of transmitted power. Applications include GPS, USAF SGLS, NASA space flight tracking and data networking (STDN) including TDRSS forward / return pairs, radar transponder, and the NASA DSN.

This antenna is supplied in a number of standard form factors, given the modular nature of the AraMiS project we select a standard dimension of 1,4" x 1,4" in order to fit in one AraMiS standard module. The patch antenna is feed from the bottom side and supports S-band.

Figure 3.1 shows a picture of the selected antenna:
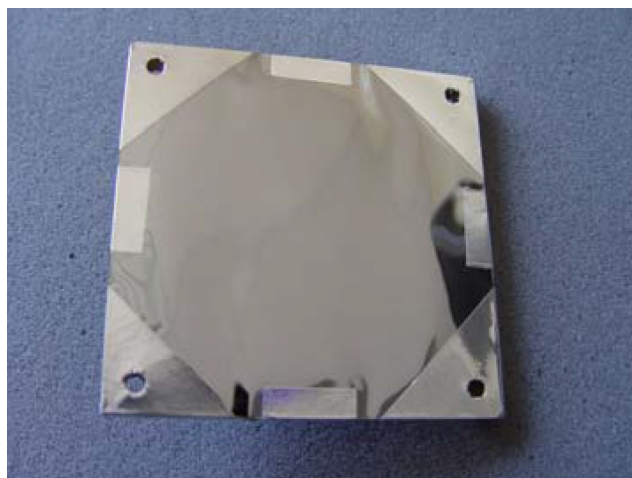
Fig. 3.1 Selected patch antenna.

Figure 3.2 shows the radiation pattern of the selected patch antenna: maximum gain is 2 dB, 2dB per division.
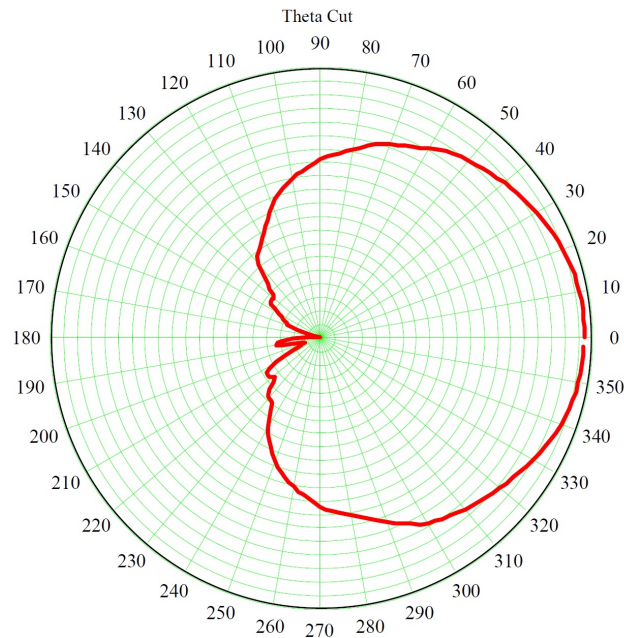
Fig. 3.2 Typical radiation pattern for full size patch antenna - 2200MHz.

3.4   Isotropic Omni-directional Antenna

By observing a generic radiation pattern of isotropic omni-directional antenna it's evident that provides high flexibility, reducing the global complexity in terms of communication strategy, it can ideally communicate over a 360° deg field of view, simplifying the global CubeSats attitude control strategy without consider the interference of the support. Figure 3.3 shows half spheric radiation pattern of this antenna, we assume that CubeSat limits the radiation pattern to a field of view of 180° with a gain of 0 dBi assigned to it by default.

Usually, antenna dipole or spiral antennas are mounted inside CubeSats and deployed after launch, many deployment techniques has been developed making the omni-directional antenna a solid solution for CubeSat missions. Despite their limitation in communication, omni-directional-like antennas result to be one of the most adopted solution in CubeSat missions.
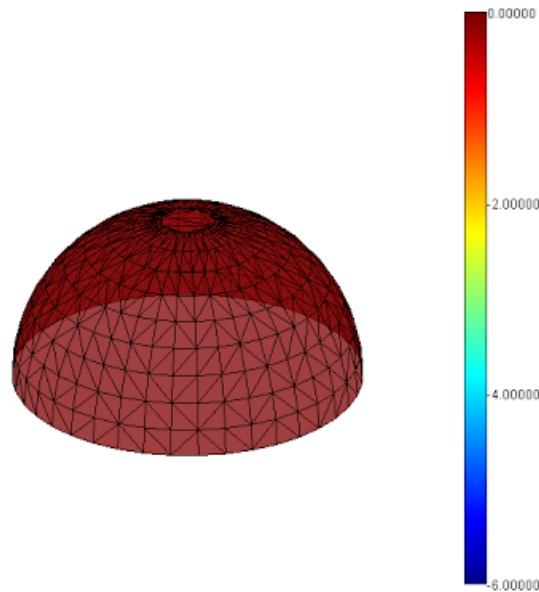
Fig. 3.3 A theoretical radiation pattern for an isotropic omni-directional antenna: 0 dB gain

3.5   Parabolic Antenna

As a part of our study, we assume to equip CubeSats with a parabolic antenna to study cross-link and down-link performances.

The placement of parabolic antenna on CubeSats is an open problem in the research field, sometimes addressed with different solutions [35]. However, placing a parabolic antenna is a complicated solution, hard to realize in terms of available space on-board and launch problems. Moreover, the pointing action to optimize the communication scheme requires an additional attitude control scheme of CubeSats, consequently, an increasing of the total mission complexity.

In conclusion, the use parabolic antennas is in contrast with our design concept based on simplicity, modularity and low cost components requirements.

Nevertheless, the performance study on cross-link in comparison with other options is still useful to give us a reference to understand how the low-cost available technologies and the solutions that we will propose can achieve the same performances levels with respect to a situation represented by the communication trough use of parabolic antennas that we assume as ideal. For these reasons, we assume to provide CubeSats with one-meter-diameter parabolic antennas despite these dimen-

sion result unrealistic for small-Sats applications.

Inflatable antennas should be mentioned, an explanation of their functionalities and potential can be found in [36]. Inflatable parabolic antennas represent a valid solution to accommodate antennas on CubeSat given available surface problems, however we prefer to maintain the focus on data volume regardless of antenna structure, by considering a certain range of performances as a function of the selected dimension

3.6   Phased Array

Phased Arrays represent the most interesting part of our research in terms of antenna performances.
As we will address in next sections, the cross-link data rate is a fraction when compared with down-link data rate. Therefore, establishing inter-satellite link (ISL) results generally useless in terms of data volumes and result more efficient to download data directly toward ground station. Hence, cross-link between CubeSat without adequate performances can be useless or harmful for the mission.
As we will address, use of phased arrays reduces differences between cross-link and down-link data rates. Thus, making possible to adopt communication strategies that include cross-link to move significant amount of data and sensibly increase the average access timing between satellites and GS with the purpose to make the system more reactive and efficient.
Several techniques have been proposed to place phased arrays on CubeSats, some of them suggest to place elements of array on deployable structures that are usually unfolded after the launch phase and are used to increase the useful surface for solar panels.
In our project we adopt a similar solution: in chapter 6 we will explain how our deployable structure can increase the available surface, and how this space will be used to host a greater number of solar panels and the proposed phased array system. By exploiting deployable structures the phased array form factor results forced to be a cross configuration: therefore only the extension and the number of elements represent discriminating factor on which is possible to act to increment the performances.

In next sections we introduce four phased array configurations were a variable number of elements are introduced respectinc the cross-configuration due to the deployable structure adopted.

The building block of all the presented phased arrays is the patch antenna introduced in section 3.3: as declared from the constructor the best antenna gain is 2dBi, therefore the theoretical array results to be 2dBi times the number of elements of the phased array. However, the radiation pattern shows a gain degradation in function of the inclination of the antenna with the received/transmitted plane wave, therefore the expected gain of phased arrays will be lower that the theoretical.

We consider a constant dimensions of phased arrays of 66 cm x 66 cm, arrays will differ from each other for the number of elements and inter-space distance between them as presented in next sub-sections.

The cross disposition of arrays is forced from CubeSat form factor: supposing a 1U CubeSat with deployable solar panels, elements of phased arrays can be placed on the deployable structures in order to maximize the arrays extension as shown in figure 3.4.
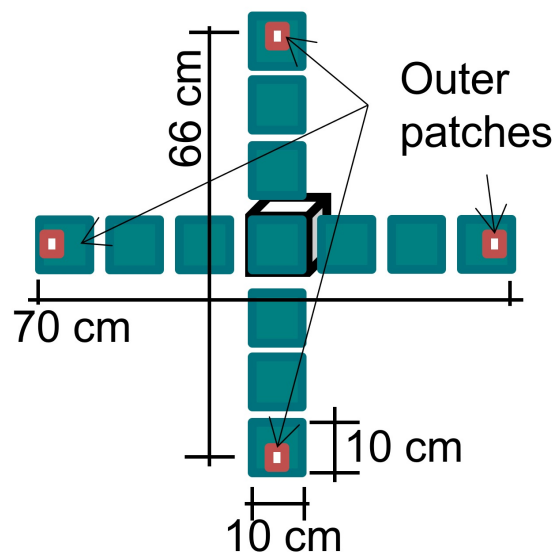

Fig. 3.4 CubeSat and Phased Array displacement concept.

Phased arrays can be seen as a composition of by two (or many) set of arrays: inner(s) and outer(s). The alternate use of this two set allows to create two or more beam width therefore is possible to exploit them to perform the estimation of the direction of arrival of the signal by combining the sensibility related to beam

apertures. In transmission, array sets allow to module the beam aperture to optimize the communication.

3.6.1   Reflect Array

Reflect arrays are a relatively new technology for CubeSats applications, they provide a significant reduction in volume occupation when compared to inflatable antennas with similar performances because the panels can be stowed in the "free space" between the bus and the canister launcher such as the P-POD. For small antenna size is possible to achieve 30 /35 dB gain. Reflect arrays are mechanically simple, presents low mass and low development costs. The tolerance accumulation of multiple panels and limits on thickness limit the maximum number of panels that can be used to develop phased arrays. ISARA [37], an innovative project leas by *NASA - Jet Propulsion Laboratory* propose to integrate reflect array with solar array in the same deployable structure. MarCo mission [38] exploited these concepts to create the first CubeSat to have flown in deep space. This technology provide CubeSat the ability to communicate thanks to the high gain reflect array, capable of transmitting 8 kbps from Mars to the Deep Space Network's 70m dish in Madrid, Spain.

Reflect arrays will be not argument of this dissertation: our analysis shows that a phased array with a gain between 9 and 15 dB is sufficient to achieve satisfactory levels of communication link performance, phased arrays better fits on the deployable structures designed and represents a good starting point for out network analysis on CubeSat constellations. Nevertheless, reflect arrays represent a valid solution to establish interlinks between CubeSats and should be considered in future projects where wider constellations extension require higher gain performances.

3.6.2   Phased Array Management System

The management of phased arrays consists of a beamforming based control strategy. To each antenna of phased array corresponds a signal conditioning channel composed by a low noise amplifier, variable gain amplifier, phase shifter and other conditioning circuitry. Channels converge in a power combiner that converge signals to the transceiver, equipped with and integrated microprocessor which analyze the received signal, estimate the direction of arrival of the signal and process the informations. In transmission mode each channel is properly conditioned in order to electronically

steer the beam and point it toward a specific direction. Signals are sent to the power amplifier than conditioned to shape the beam. Figure 3.5 shows the block diagram of the phased array management system. The detailed hardware description is presented in the hardware chapter.

The configurations that we are going to introduce consist of two main sub-arrays with a variable number of antennas depending on the configuration considered. These sub-arrays are arranged to form a cross that is is related to the structure on which the arrays are arranged.
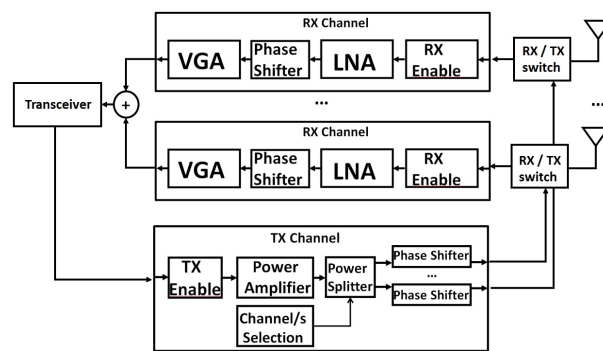
Fig. 3.5 Phased Array Management - Block Diagram.

As described before and as we will address in next sections, our phase array configurations consist in two phased array placed in a cross-configuration composed by a variable number of elements. Each sub-arrays present a linear polarization, the superimposition of them contribute to the beam shaping, the phase shifting control manage the beam pointing action as shown in figure 3.6. In figure 3.7 is shown the polarization of a couple of element of a sub-array with inter-element spacing of 0.1 m and 0.6 m.
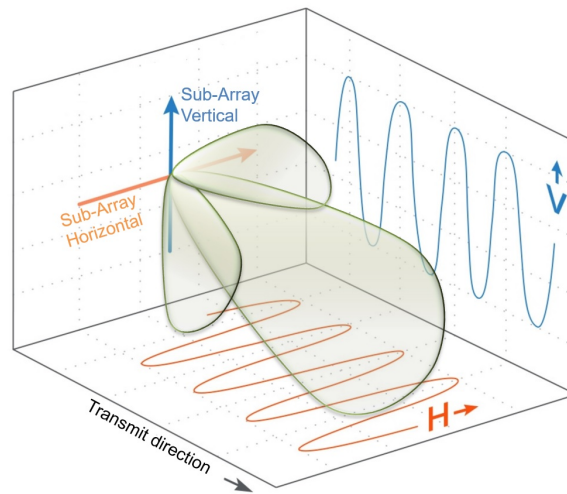
Fig. 3.6 Phased Array - PA1 Polarization.
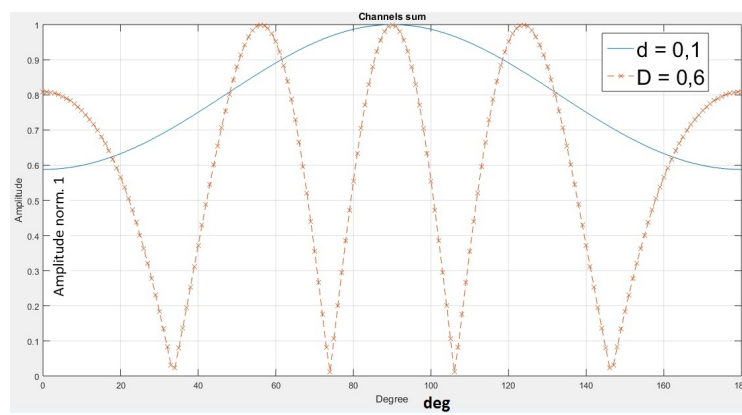
Fig. 3.7 Phased Array sub-array polarizzation. Spacing d=0.1m / d=0.6m

3.6.3   Phased Array *PA1*

Figure 3.8 shows the element placement of phased arrays *PA1*. Arrays are placed in cross-configuration, eight elements will contribute to shape the Tx/Rx beam. Inner elements are 6 cm distant from the center. While outer elements are 33 cm distant from the center.
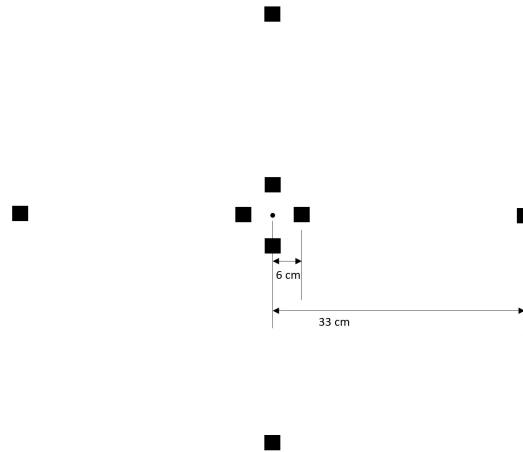
Fig. 3.8 Element displacement of Phased Array PA1.

This phased array pair has been designed and simulated, maximum gain is achieved in correspondence of the center of the main lobe and reach 9 dB. Table 3.2 resumes the minimum antenna gain levels guaranteed and its related main lobe apertures. Main lobe aperture is the central lobe used for to establish communication, secondary lobes must be reduced as much as possible.

The performances of this phased array result strongly affected by the power dispersion introduced from secondary lobes: considering a parabolic antenna with an equivalent dish dimension (66cm diameter) the gain results to be $\sim$22 dBi. With with a transmission power of 0.512mW the total EIRP results $\sim$49 dBm. Considering the best achievable performances in terms of gain of this phased array configuration, maximum achievable EIRP is $\sim$36 dBm. Therefore 13 dB results disperse on secondary lobes, moreover the main lobe aperture results too narrow, making this configuration not suitable for our purposes.

Table 3.2 Phased array PA1 - Gain vs. Main lobe aperture

Antenna Gain [dB].	Main Lobe Aperture [deg.].
@ 4dB	9
@ 5dB	6
@ 9dB	2

3.6.4   Phased Array *PA2*

Figure 3.9 shows the element placement phased array *PA2*. Arrays are placed in a cross configuration, twelve elements will contribute to shape the Tx/Rx beam. Configuration is the same as phased array pair N1 with the addition of four elements in line with the cross placed 12 cm away from the center.
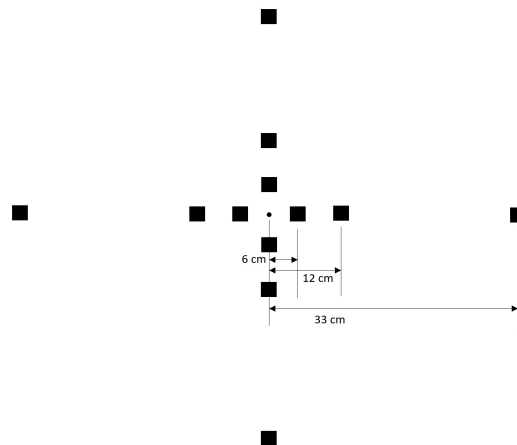
Fig. 3.9 Element displacement of Phased Array PA2.

This phased array pair has been designed and simulated, figure 3.10 shows the gain matrix, the beam of the phased array pair results "compressed" (and elongated) in a 2D image, this picture is used to provide a relationship between the achievable antenna gain and the maximum main lobe aperture. Maximum gain is achieved in correspondence of the center of the main lobe: 7,6255 dB. Table 3.3 resumes minimum antenna gain levels guaranteed and the related maximum lobe aperture.

Fig. 3.10 Pair of Phased Array PA2 - Gain Matrix.

Table 3.3 Phased array PA2 - Gain vs. Main lobe aperture

Antenna Gain [dB].	Main Lobe Aperture [deg.].
@4dB	24
@5dB	20
@6dB	16
@7dB	10

Figures 3.11 and 3.12 show the 3D model of the two phased array N2 placed in cross configuration. Main lobe gain reaches up to 7 dB, the aperture results to be about 10° degree, thus contribute to make more flexible the beam shaping action required to steer the beam.
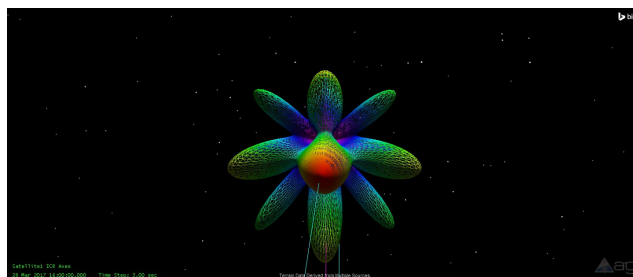
Fig. 3.11 Couple of Phase Array PA2 - Beam Front view.
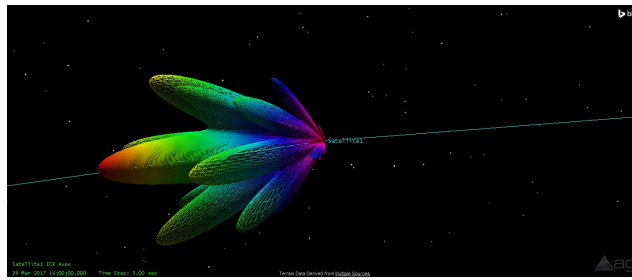
Fig. 3.12 Couple of Phase Array PA2 - Beam Side view.

3.6.5   Phased Array *PA3*

Figure 3.13 shows the element placement of phased array *PA3*. Arrays are placed in a cross configuration, sixteen elements will contribute to shape the Tx/Rx beam. Four additional elements in line with the cross of array pair N2 are placed at 18 cm away from the center to form the N3 configuration.
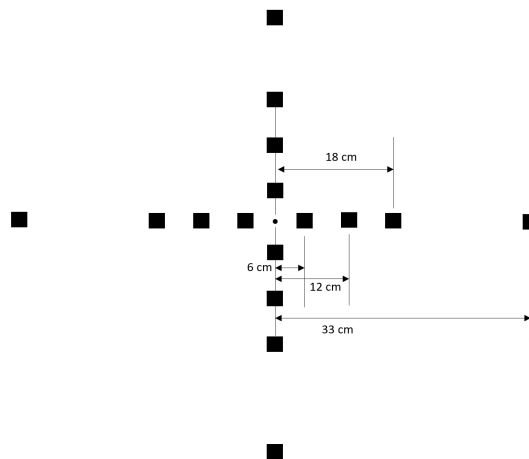
Fig. 3.13 Element displacement of Phased Array N3 couple.

This phased array pair has been designed and simulated, figure 3.14 shows the gain matrix, the beam of phased array pair results "compressed" (and elongated) in a 2D image, this picture is used to provide a relationship between the achievable antenna gain and the maximum main lobe aperture. Maximum gain is achieved in correspondence of the center of main lobe and reaches 10,645 dB. Table 3.4

resumes minimum antenna gain levels guaranteed and the related maximum main lobe aperture.
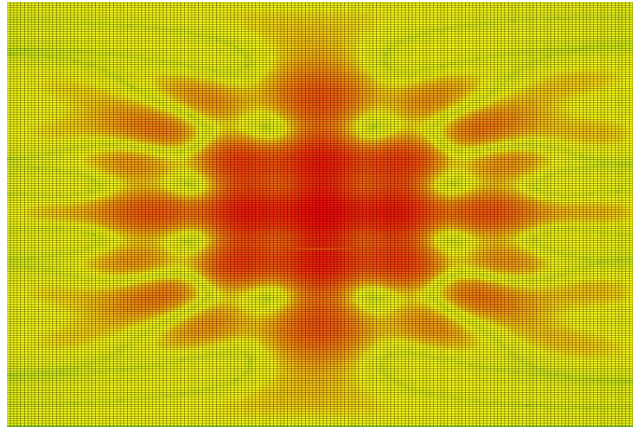
Fig. 3.14 Pair of Phased Array PA3 - Gain Matrix.

Table 3.4 Phased array PA3 - Gain vs. Main lobe aperture.

Antenna Gain Guaranteed [dB]	Max. Main Lobe Aperture [deg.]
@4dB	56
@5dB	55
@6dB	51
@7dB	48
@8dB	16
@9dB	12
@10dB	6

Figures 3.15 and 3.16 show the 3D model of the two phased array N2 placed in cross configuration. Main lobe beam aperture results to be more wide than previous, providing better performances in terms of communications flexibility.
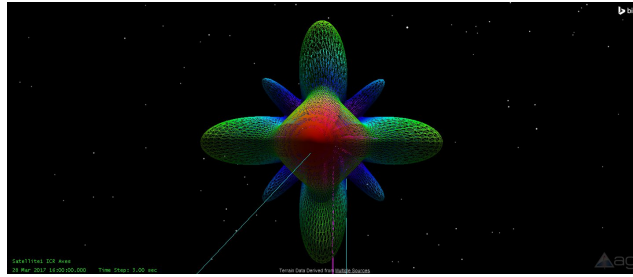
Fig. 3.15 Couple of Phase Array PA3 - Beam Front view.
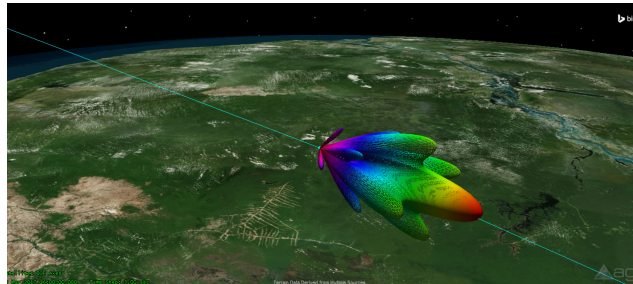
Fig. 3.16 Couple of Phase Array PA3 - Beam Side view.

3.6.6   Phased Array *PA4*

Figure 3.17 shows the element placement of phased array *PA4*. Four additional elements in line with the cross of array pair N3 are placed at 6 cm away from the center to form a square of elements in correspondence of the center of the cross.
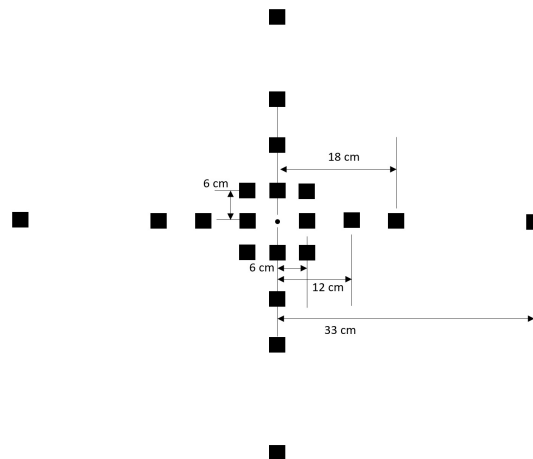
Fig. 3.17 Element displacement of Phased Array PA4 couple.

This phased array pair has been designed and simulated, figure 3.18 shows the gain matrix, the beam of the phased array pair results "compressed" (and elongated) in a 2D image, this picture is used to provide a relationship between the achievable antenna gain and maximum main lobe aperture. Maximum gain is achieved in correspondence of the center of the main lobe and reaches 11,641 dB. Table 3.5 resumes minimum antenna gain levels guaranteed and the related maximum main lobe aperture.
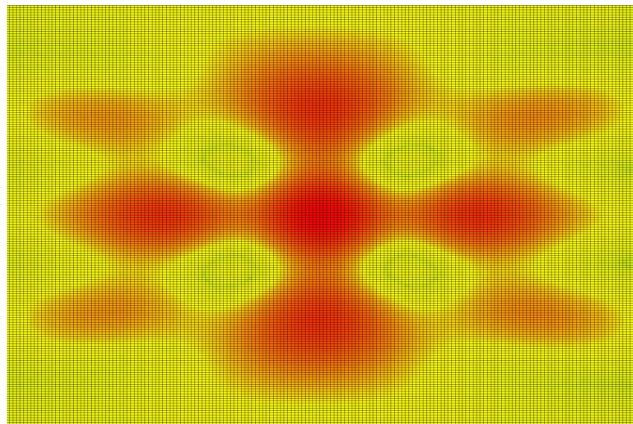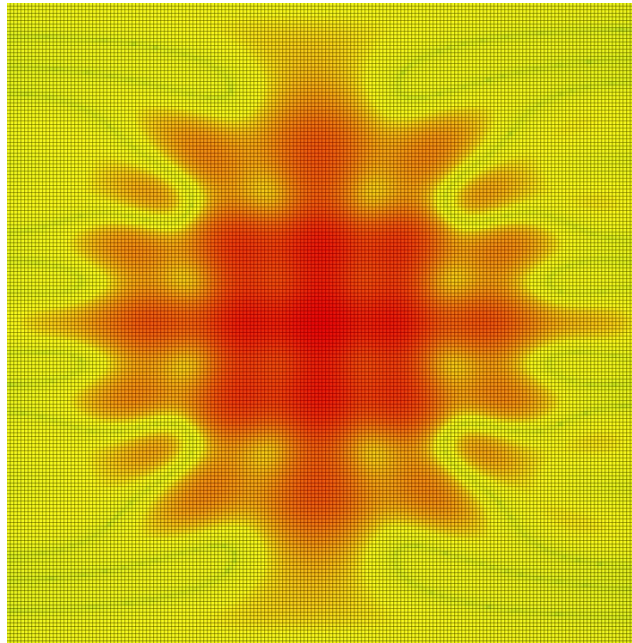

Fig. 3.18 Pair of Phased Array PA4 - Gain Matrix.

Table 3.5 Phased array PA4 - Gain vs. Main lobe aperture.

Antenna Gain Guaranteed [dB]	Max. Main Lobe Aperture [deg.]
@4dB	63
@5dB	60
@6dB	56
@7dB	54
@8dB	50
@9dB	18
@10dB	12
@11dB	7

Figures 3.19 and 3.20 show the 3D model of the two phased array N4 placed in cross configuration. Main lobe gain results to be higher than N3 configuration, number of elements results to be too much in relation to the available space on a CubeSat, beam results to be wide if compared to previous configurations and able to receive signals from 7°,12°,18°, etc. depending on the minimum antenna gain requirements.
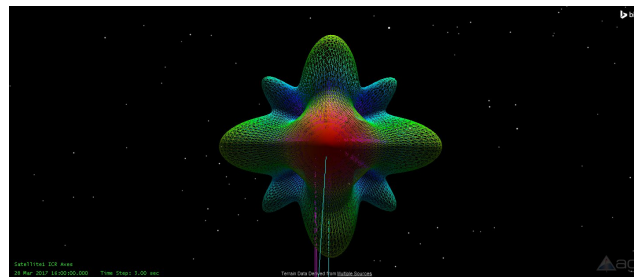
Fig. 3.19 Couple of Phase Array PA4 - Beam Front view.
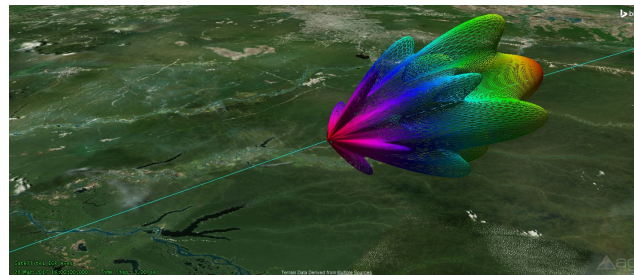
Fig. 3.20 Couple of Phase Array PA4 - Beam Side view.

3.7   Phase Array: Comparison

Table 3.6 resumes the phased array apertures *PA1...PA4* and their corresponding minimum gain levels guaranteed. With the increasing of elements composing arrays the main beam acquire larger aperture, with greater gain. On the other hand, large number of elements affect on the mechanical complexity and the available space on CubeSats especially on the power supply of the system because we suppose to place phased arrays on the deployable structures for solar panels.
The relationship between phased array performances and available space must be

defined to understand the feasibility of this communication system: we suppose to consider a deployable structure on four side of CubeSat, this triple the available surface of each side as shown in figure 3.21 for an 1U CubeSat. This surface is reserved for solar panels or for phased array elements, in table 3.7 we resume the percentage occupied surface of phased arrays configuration on the deployable structures considering 1U,3U, 6U and 12U CubeSat.
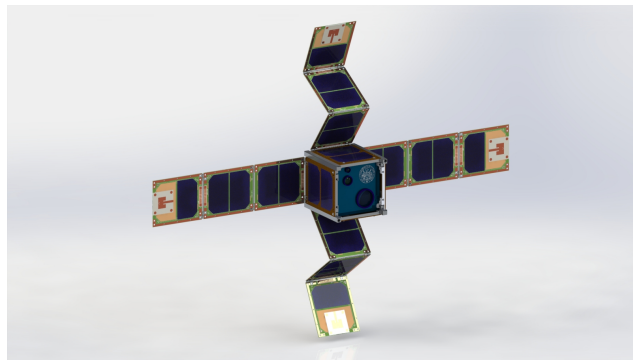
Fig. 3.21 Deployable structure example on CubeSat 1U.

As table 3.7 shows, the surface occupation of arrays involve acceptable solar panel area reduction levels. For CubeSat 1U the surface occupation reach critical values, from 8 to ∼20% of the total area reserved for solar panels, therefore additional considerations must be done in terms of mission energy budget to define if our communication system can be an acceptable solution or not. We sacrifice a small percentage of surface to obtain a great improvement in communication system in other cases. We select a 3U CubeSat with *PA4* configuration having a minimum guaranteed gain of 10,63 dB to perform next data volume analysis

Table 3.6 Phased arrays - Gain vs. Main lobe aperture.

Phased Array	Antenna Gain Guaranteed [dB]	Max. Main Lobe Aperture [deg.]
PA1	@4dB	9
PA1	@5dB	6
PA1	@9dB	2
PA2	@5dB	20
PA2	@6dB	16
PA2	@7dB	10
PA3	@8dB	16
PA3	@9dB	12
PA3	@10dB	6
PA4	@8dB	50
PA4	@9dB	18
PA4	@10dB	12
PA4	@11dB	7

Table 3.7 Phased arrays Surface Occupation.

CubeSat	Available Surface [cm^2]	Ph. Array	Ph.Array Surf.[cm^2]	Surface Occupation [%]
1U	1300	PA1	101.16	7.78%
		PA2	151.74	11.67%
		PA3	202.32	15.56%
		PA4	252.9	19.45%
3U	3700	PA1	101.16	2.73%
		PA2	151.74	4.1%
		PA3	202.32	5.46%
		PA4	252.9	6.8%
6U	5600	PA1	101.16	1.8%
		PA2	151.74	2.7%
		PA3	202.32	3.6%
		PA4	252.9	4.5%
12U	14800	PA1	101.16	0.68%
		PA2	151.74	1.02%
		PA3	202.32	1.36%
		PA4	252.9	1.7%

Chapter 4

Antenna Performances

In this chapter we present the performances of the communication links established by using the antenna types previously introduced.

Performances will vary depending on transmission power, distances and transmit and receive antennas, a deep study of the link budget will be carried out in order to understand the strength of the communications link and define boundaries in which inter satellite links can a concrete solution in CubeSat constellation management and data volume movements.

4.1 Link Budget

In next sections we calculate and evaluate link budgets related to ground-link and cross-links between CubeSats using different scenario configurations. Considering the possibilities of creating and constructing an antenna formed by phased arrays, we assume to use a the phased array *PA4* configuration with and antenna gain of $\sim$10dB. Space-links and Gound-links are studied to work at same frequency (*S-band*). Table 4.1 summarizes all parameters involved in the link budget analysis. Some of them are fixed while other are variables and used to study the constellation performances. To satisfy NASA requirements the modulation scheme is *QPSK* with the possibility to switch the coding scheme: *LDPC 1/2*, *LDPC 4/5* or *LDPC 7/8* depending on the link margin availability. *Bit Error Rate* is fixed at 10^{-6} while the considered transmission power goes from 2mW to 2W, this can be a realistic range considering the usual power supply availability of CubeSats 1U to 12U.

Link Budgets consider also positions of the ground station/s and orbit settings of CubeSats to define communication links potentiality, in next sections we study the link budget in relation to the position of satellites and we set boundaries to define mission characteristics to obtain minimum levels of moved data volume. Parameters related to the atmosphere are obtained thanks to the attenuations by atmospheric gases recommendation of *International Telecommunication Union* ITU-R P.676 [**?**] with the assumption of non-optimal weather condition, dry air at 95%. Link Budget analysis start from equation 4.1:

$$\frac{E_b}{N_0} = \frac{PL_lG_tL_SL_aG_r}{kT_sD_R}$$

(4.1)

where:

E_b/N_0 Energy per bit to noise power spectral density ratio.

P(Watt) Transmitter output power.

L_l Antenna supply line loss.

G_t Gain of the transmitting antenna.

L_s Free space loss.

L_a Additional attenuation on the link.

G_r Gain of the receiving antenna.

k Boltzmann constant (1.38×10^{-23} J K^{-1}).

T_s Noise temperature of the receiving system.

D_R Transmission Data Rate.

4.1.1   Coding Schemes

Low-Density Parity-Check Codes (LDPC) are forward error-correction codes, a method of transmitting a message over a noisy transmission channel first introduced in PhD thesis of Gallager at M.I.T. [39]. The names comes from the characteristic of their parity-check matrix which contain only a few 1's in comparison to the amount of 0's. LDPC Codes provide near-Shannon capacity performance, they are "*an excellent tools in optimizing telemetry data integrity within the limited space to ground RF spectrum available for current satellite systems* [40]".

The transmission power, antenna configuration of transmitter and receiver and, more in general, the orbital parameters of CubeSats will affect the link performances, in

Table 4.1 Link Budget Parameters Involved.

Parameter	Ground-Link	Space-Link
Modulation Scheme	QPSK	QPSK
Coding	LDPC 1/2 - 4/5 - 7/8	LDPC 1/2 - 4/5 - 7/8
Bit Error Rate (BER)	$\leq 10^{-6}$	$\leq 10^{-6}$
GS Postion	lat. 45.063396 Lon. 7.66	-
Transmit Frequency	2.4 GHz	2.4 GHz
Transmitter Power	2mW to 2W	2mW to 2W
Antenna Dimension	Patch	Phase Array 4 *PA4*
Antenna Efficiency	55%	99%
Antenna Gain	Dep. on Config.	Dep. on Config.
S/C Passive Loss	2dB	0dB
S/C Pointing Loss	Aligned mismatching 0,20 dB	0,20 dB
Transmitter EIRP	Dep. on Config.	Dep. on Config.
Altitude	400-2000km	-
Min. Elevation Angle	fixed at 5° deg	fixed at 5° deg
Range	-	50 - 3000km
Free Space Loss	-152 to -166 dB	-134 to -170 dB
Polarization Loss	0 - 3 dB	0 - 3 dB
Atmospheric Loss	0,464 dB ITU-R P.676 @ 95%	-
Rain Attenuation	0,001 dB ITU-R P.676 @ 95%	-
Scintillation / Multipath Loss	0,377dB ITU-R P.676 @ 95%	-
Cloud Attenuation	0,032 dB ITU-R P.676 @ 95%	-
Total Propagation Effects	0,874 dB ITU-R P.676 @ 95%	-
System Noise (Atmosph.)	2 dB G/T adjustment	-
Link Margin	3 dB	3 dB

particular from the link margin availability. The optimal coding scheme depends on this link margin characteristics, coding schemes differ from the various code rates and block sizes as described in the *Orange Book* of the Consultative Committee for Space Data System (CCSDS) [41]. Depending on the transmission power we use a different coding scheme to optimize the communication, in some case, where the EIRP is high we notice that a coding scheme is not necessary, therefore we do not encode the transmission in order to maximize the data rate.

The performed analysis on the coding done can be interpreted in two different ways: fist, the optimal coding scheme on the link budget can be a limit point, that is, depending on the constellation topology and on the communication requirements of the mission, it's possible to select a fixed coding scheme and define a maximum constellation extension where the selected coding scheme works. Second, an effective coding scheme switch is needed and the coding scheme switch problem must be addressed.

From the performed analysis on the coding schemes turns out that, the coding scheme performances are related to the distance between transmitter and receiver. Therefore is possible to design the communication of the constellations in two different ways: first, the optimal coding scheme on the link budget can be a limit point, that is, depending on the constellation topology and on the communication requirements of the mission, it's possible to select a fixed coding scheme (LDPC 1/2 or 4/5 or 7/8) and define a maximum constellation extension where the selected coding scheme works.

Second scenario: as we will address in the link(s) budget analysis, depending on the communication distances considered there is a variation on the coding scheme that must be used to optimize the communication, i.e. the coding scheme must change and relative switching problems must be addressed. In this case, LDPC could not be considered as optimal solution because of the quite different implementation of the encoders for different code rates. In the CCSDS Blue Book [42] a flexible advanced coding and modulation scheme for high data rate telemetry apllications is proposed: a serial concatenated convolution code that could solve our problems related to the coding switch changes.

However, the following data rate analysis has been performed considering the following coding schemes: Uncoded, LDPC 1/2, LDPC 4/5, LDPC 7/8.

The coding scheme selection remain an open problem that must be addressed if the constellation topology present significant distance variation among constellation's elements, a good starting point for future works.

All the links budgets and the analyzes that will be made in next sections are related to the LDPC coding scheme that optimizes communication. All data and results refer to the higher data rates that can be reached by considering the relationship between transmission power, distances (altitudes) and LDPC coding schemes.

4.1.2   BER vs. Eb/N0 Curves

Figure 4.1 [43] [44] show the BER vs. E_b/N0 curves for different modulations and coding schemes, we extrapolate informations regarding the interested coding schemes despite they provide information on other possible combinations. To performs our link budget analysis we obtain from this graphics the E_b/N0 values in correspondence of BER of 10^-6 for the selected coding schemes. The selected modulation scheme is QPSK, we focus on four different coding scheme, they are: UNCODED, LDPC Rate 1/2, LDPC Rate 4/5, and LDPC Rate 7/8.

E_b/N0 values are:

<div align="center">Table 4.2</div>

QPSK Coding Scheme	E_b/N0 (BER 10^-6) [dB]
UNCODED	10.5
LDPC 1/2	1.89
LDPC 4/5	3.04
LDPC 7/8	3.9

Once the E_b/N0 values have been defined is possible to calculate the Data Rate as a function of the physical distance from equation 4.1. Figure 4.10 shows an example of link budget analysis. A space-link between two parabolic antennas of one meter diameter is reported. Distance between antennas vary from 50 to 6000km. The data rate is optimized, thus indicates that most perfostudyrmance coding scheme has been selected for each distance. Curves vary depending on transmission power, values selected goes from 16mW to 2W. In case of high transmission power or low distances a bit rate limitation to 5 Mbps occur therefore the data rate remain constant until an exponentially decay occurs.

Fig. 4.1 BER vs. Eb/N0

SpaceLink - Parab.(1m) to Parab.(1m)
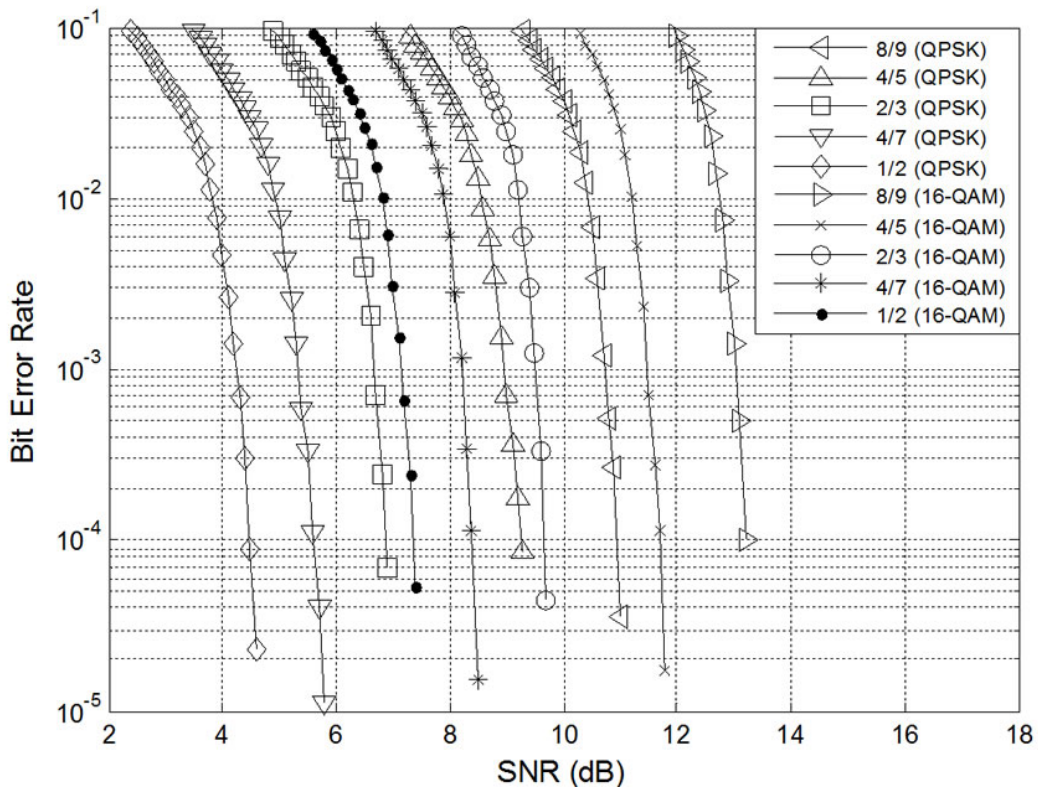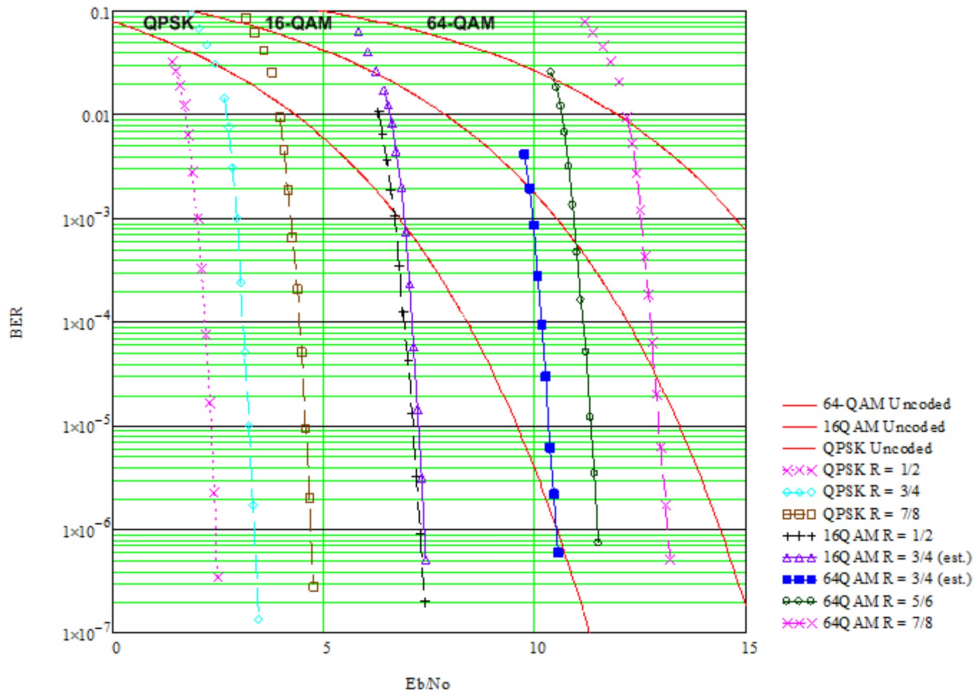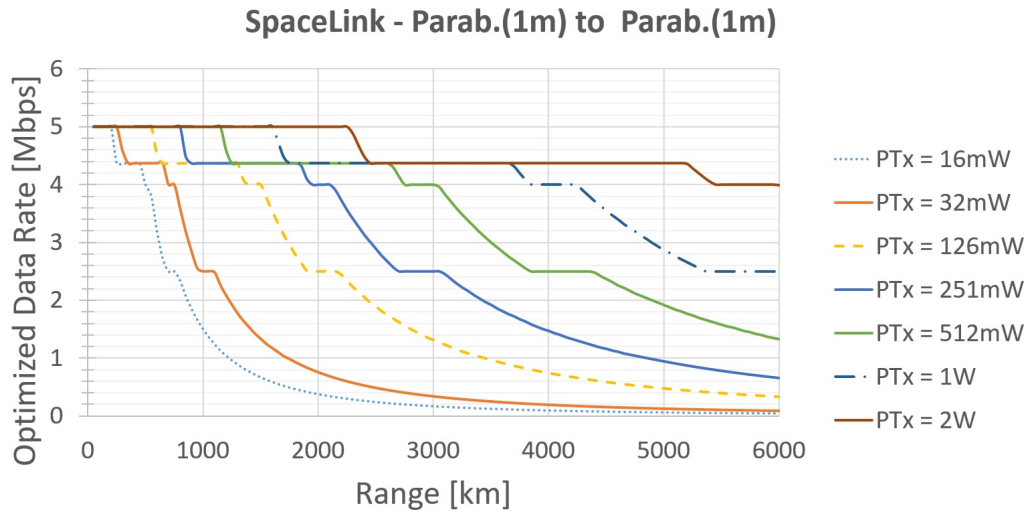
Fig. 4.2 Space Link Budget for different transmission power levels. Calculation based on formula 4.1. Max. data rate achievable 5 Mbps.

4.2   Groundlink Analysis

In this section we analyze ground-links considering different antenna configurations on CubeSats. Ground-links analysis consider range from 450km to 6000km, link configurations are:

- GL1: Omni-directional Antenna (CubeSat) -to- 5m-diameter Parabolic (GS)

- GL2: Patch Antenna (CubeSat) -to- 5m-diameter Parabolic (GS)

- GL3: Phased Array 10.63 dB (CubeSat) -to- 5m-diameter Parabolic (GS)

For each configuration we analyze the up-link and down-link budget.

4.2.1   Up-link

As described in previous sections, omni-directional antenna provide flexibility in terms of signal irradiation, they limit additional strategies in terms of attitude control to establish the link, however they present lower gain and some problems in terms of realization and accommodation on CubeSats.

Figure 4.3 shows the data rate curves relative to the up-link between a 5-meter diameter parabolic antenna on ground station transmitting at 1W. Depending on the receiver antenna and from distance between CubeSat and GS data rate level considerably vary. The Up-link represent the least problematic part of the data volume analysis; the high EIRP on ground station allows to move an exhaustive data volume toward constellation that can be ulteriorly increased by increasing the transmission power, that not represent a critical problem as the down-link. Particular attention must be given to curve *Patch(80°)*, it indicate the data rate levels achieved when the patch antenna results misaligned and signal is received at 80° respect to the patch's perpendicular. Patch antenna misalignments comports strong degradation of link capabilities and must be kept under control through CubeSat attitude strategies.
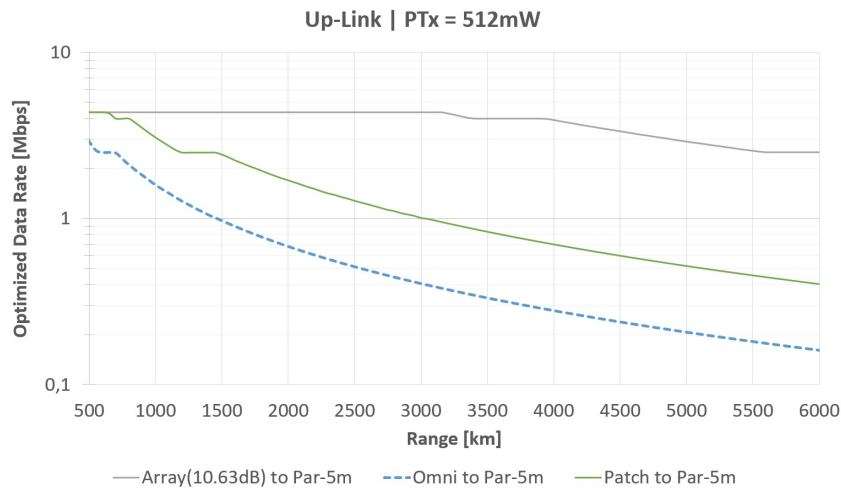
Fig. 4.3 Up-link: GL1,GL2,GL3 @ 1W.

4.2.2 Down-link

Figure 4.4 shows the optimized data rate values achievable when the selected antenna configuration transmit toward the 5-meter parabolic antenna on the ground for a fixed transmission power of 512mW. Unlike up-link, the available transmission power results reduced due to the available power supply on CubeSats. As for up-link patch antenna inclination strongly affect the link reliability, therefore patch must be kept pointed to GS to optimize link during transmission. Next data volume analysis will compare achievable data rate levels of down-links with data volume that are moved along the constellation to define if down-link capabilities are able to support the

data throughput. We assume to use omni-directional antenna as reference for next considerations, at 512mW it provides 80 kbps to 2 Mbps in considering a range from 500 to 6000 km from the ground station. This curve will represent the down-link reference to define the condition under which space-links can bring advantages in constellations.
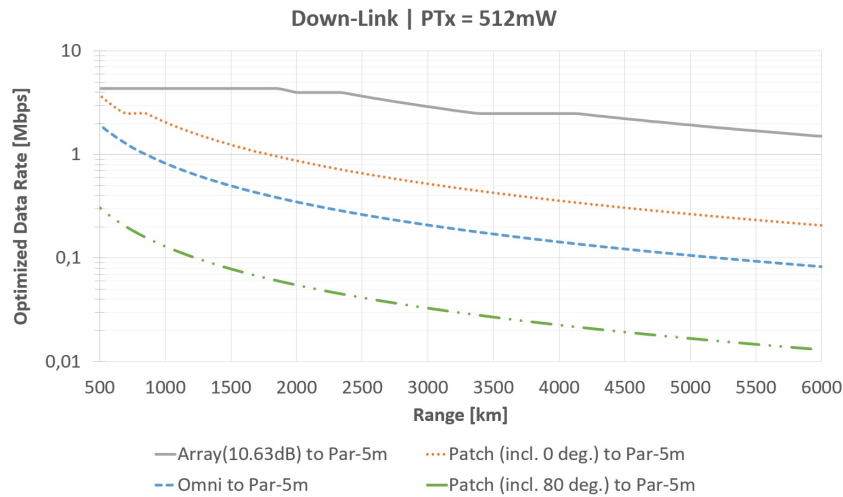
Fig. 4.4 Down-link: GL1,GL2,GL3 @ 512mW.

Note

Up-Link and Down-Link budget has been performed for a range from 0 km to 6000 km to take into account the maximum ideal distance (slant-range) between a CubeSat in LEO orbit and a ground station. The Low-Earth-Orbit is between the atmosphere and the van Allen bands, between 160 and 2000 km. If we consider a CubeSat orbiting at 2000 km the maximum slant range between the CubeSat and the ground station will be 5430 km (tangent to the Earth passing through the ground station) . This distance do not take into account the 5° minimum elevation angle usually imposed for up/down link communication.

4.3   Space-link Analysis

The space-link analysis performed include six antenna configurations, they are:

- SL1: Patch -to- Patch

- SL2: Array -to- Patch

- SL3: Array -to- Array

- SL4: Patch -to- Parabolic (1m-diameter)

- SL5: Array -to- Parabolic (1m-diameter)

- SL6: Parabolic -to- Parabolic (1m-diameter)

Patch antennas and phased arrays has been already introduced to study up/down-links, they represent the most realistic solution to perform space-links in terms of antennas accommodation on CubeSats. The use of omni-directional antennas to establish ISLs is not reported because during the fist phase of our analysis we measured that the data rate levels they provide is not sufficient to support the throughput that meets our requirements. Parabolic antenna of 1-meter diameter introduced in configurations SL4,SL5 and SL6 is principally used as a benchmark for the performance of previous configurations. Despite some techniques has been proposed to fit parabolic antennas on CubeSats we do not propose them as valid solution for our constellation.

The purpose of Space-link analysis is to collect data regarding maximum data rate achievable with all the proposed antenna configurations in relation to PTx and distances.

The final goal is to define if establishing ISLs can bring advantages to the constellation, to do that we must consider the down-link data rate previously studied to understand if the space-link achievable data rate levels can play a role in overall data movement system.

4.3.1   Space-link 1: Patch-to-Patch

Figure 4.5 shows optimized data rate achievable when PTx is respectively 126mW, 251mW, 512mW, 1W and 2W for the Patch-to-Patch cross-link configuration. Analysis with lower PTx levels are not reported because of low data rate performances. Curves present an instant drop in correspondence of 500 km of satellites mutual spacing due to the optimal LDPC coding scheme switch. Analysis range is 50 km to 3000 km: Supposing a constellation with element separation from 250km to 1000km the guaranteed DR is 1 kbps when PTx is 512mW ($\sim$27 dBm). Information reported

in this graph define the maximum achievable radius of the constellation in relation to data volume that designer want to move. Just like the ground-link, misalignments of patch antennas brings to a quick degradation of the communication. To avoid this problem multiple patch antennas can be placed on each face of CubeSats (e.g. [45]).

Fig. 4.5 Spacelink 1 - Data Rate vs. Satellite distance and Transmission Power.

4.3.2 Space-link 2: Array-to-Patch

Figure 4.6 shows the Phased Array-to-Patch configuration cross-link that considers optimized data rate achievable when PTx is respectively 126mW, 251mW, 512mW, 1W and 2W. Given the gain of phased array (10,63 dB), data rates curves reach higher values when compared to Patch-to-Patch configuration. However, to obtain this gain with a phased array, issues in terms of accommodation on CubeSats must be addressed. Compared to previous example, phased array guarantees better performances in terms of PTx required and maximum allowed distances between elements of the constellation.
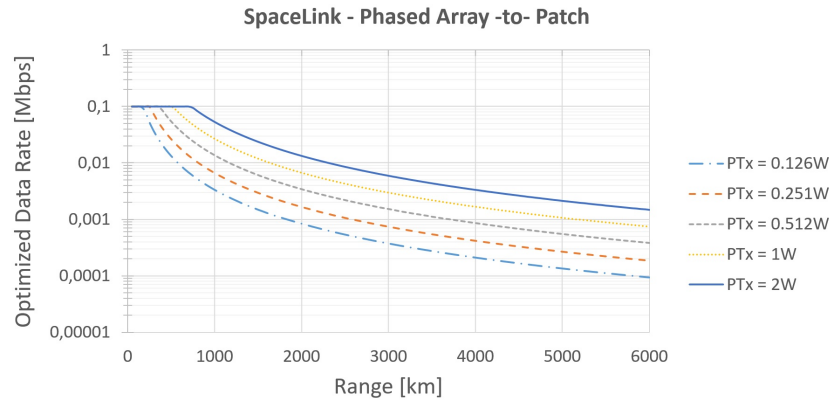
Fig. 4.6 Spacelink 2 - Data Rate vs. Satellite distance and Transmission Power.

4.3.3   Space-link 3: Phased Array -to- Phased Array

Figure 4.7 shows Phased Array-to-P.Array configuration cross-link that considers optimized data rate achievable when PTx is respectively 126mW, 251mW, 512mW, 1W and 2W. Since phased arrays result valid solution to establish communication links on CubeSat, we expect to use them to set up space-links with the purpose of reaching higher distances and higher data rate levels. Array -to- Array allows constellation elements to be separated by a distance up to 3000 km and communicate each other at 25 kbps up to 40 kbps, depending on PTx. Thanks to the electronic steerable feature of phased array, mutual pointing action increases the possibility to maintain a stable communication link.
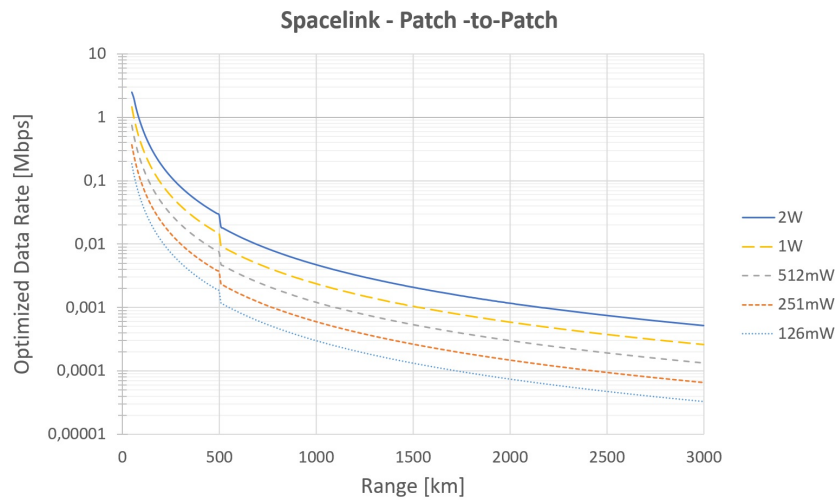
Fig. 4.7 Spacelink 3 - Data Rate vs. Satellite distance and Transmission Power.

4.3.4   Space-link 4: Patch-to-Parabolic

Figure 4.8 shows the Patch-to-Parabolic cross-link configuration. Use of parabolic antennas is not proposed as valid solution for CubeSat communications, anyway we analyze link performances to define a sort of "ideal" case, where communication reaches high values in terms of EIRP. However, despite the use of a 1-meter diameter parabolic antenna, patch antenna strongly reduces performances. Performances reported in this graph results to be better than the P.Array-to-Patch configuration but unrealistic to develop in terms feasibility.
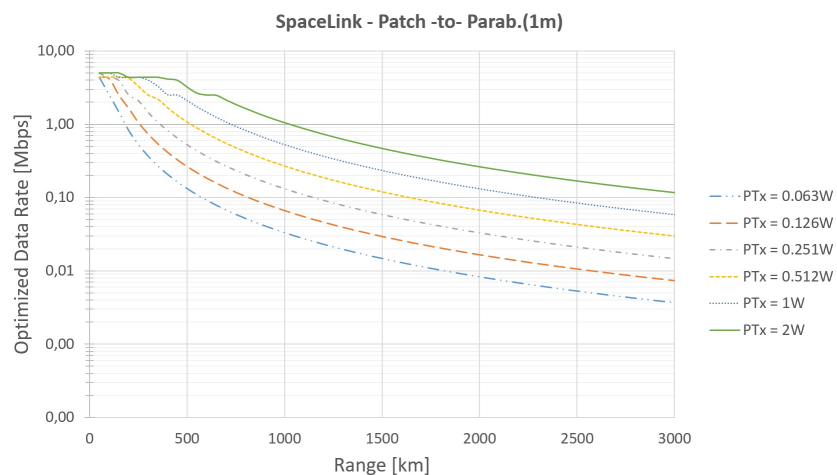
Fig. 4.8 Spacelink 4 - Data Rate vs. Satellite distance and Transmission Power.

4.3.5   Space-link 5 and 6: P.Array-to-Parabolic and Parabolic-to-Parabolic

Figures 4.9 and 4.10 show Phased Array-to-Parabolic and Parabolic-to-Parabolic cross-link configurations.

Previous constellation analysis, not reported in this dissertation, propose parabolic antennas as solution in cluster configurations involving bigger satellites utilized as relay placed in an equatorial orbit to behave as walker constellation, a sort of mother-ships float that provide constant access to the daughter-ships CubeSat constellation. This configuration has been adopted to multi-hop space communication, nevertheless our intention is to report performances of SL5 and SL6 just to give an ideal realistic "best case" performances reachable for ISL communication. SL5 and SL6 present the best data rate levels of all configuration proposed, we consider them as upper boundaries confront levels.
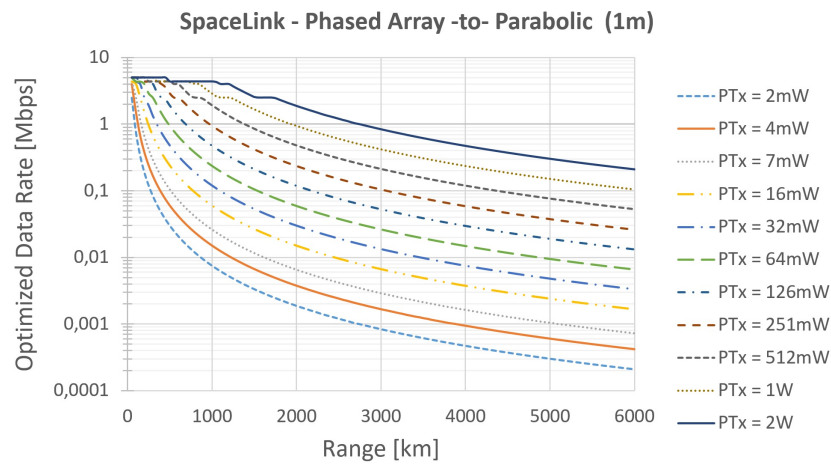
Fig. 4.9 Spacelink 5 - Data Rate vs. Satellite distance and Transmission Power.

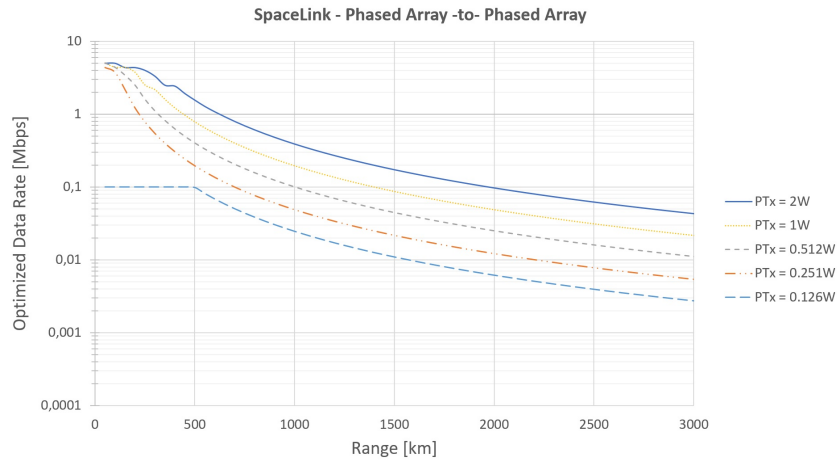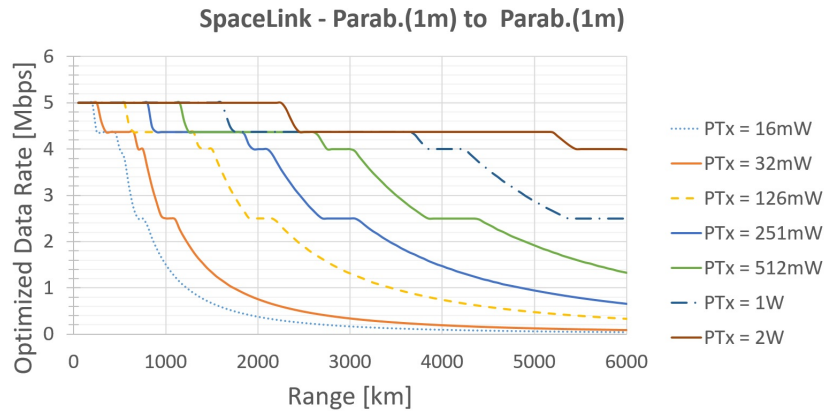Fig. 4.10 Spacelink 6 - Data Rate vs. Satellite distance and Transmission Power.

4.3.6   Space-link Comparison

Figure 4.11 shows the configurations comparison when PTx = 512mW.

As expected, Phased Array-to-Patch configuration presents better performances than patch-patch: SL2 results ten times more performing than SL1 considering at the same distance condition between satellites.

Better performances than SL2 are reached when P.Array-to-P.Array (SL3) configuration is considered: SL3 curve (gray) is almost one decade above SL2 and presents similar performances to SL4. In SL4 a parabolic antenna is involved: at 1000 km range distance DR difference between SL3 and SL4 is 0,2 kbps. Thus, confirms that Phased array provides a positive ratio between performances and feasibility for CubeSat application.

As we will address in next sections, the relationship between maximum settable constellation's radius and guaranteed minimum data rate is the fundamental parameter that justify cross-link and bring advantages to the accessibility and maximum transferable data volume.

The relationship between constellation extension, data rate levels and mechanical development requirements of configurations SL2 and SL3 offer a valid starting point for CubeSat constellation performances analysis in LEO orbit.

SpaceLink Communication Comparison | PTx = 512 mW
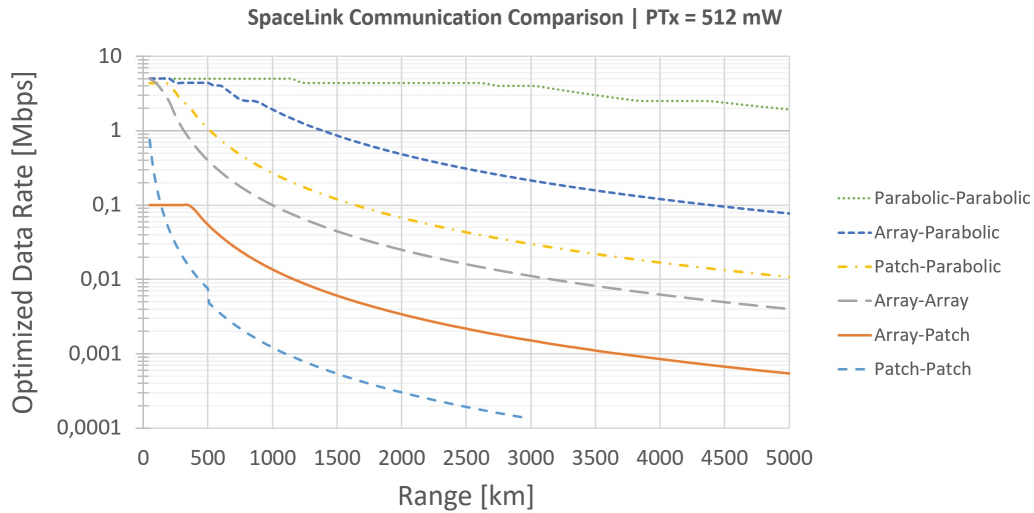
Fig. 4.11 Spacelink Communication Comparison @512 mW.

4.4   Ground-link Space-link Ratio Analysis

Analysis on ground-link and space-link provide indications in absolute values about maximum achievable performances depending on configuration in use, distances with ground station, mutual satellites spacing and transmission power.

PTx goes from 2mW to 2W because we consider a realistic range available depending on CubeSat typology: from 1U to 12U. Furthermore, we suppose CubeSat dispose variable power supply to establish the communication, depending on tasks required during the orbit .

To perform a clear study on constellation feasibility conditions we classify communication links in two subcategories: *data links* and *command links*. *Data links* supports high data rate, principally used to move a consistent data volume.

Command links are characterized by low data rate, used to transfer simple commands that dynamically adjust the behavior of CubeSats. *Command links* are characterized by low data rate and used to transfer simple commands and emergency information. Therefore, the gap between *data links* and *command links* depends from a data rates line of demarcation value and its strictly related to the mission requirements. In our study we consider *command links* all communication channel with data rate under ~30 kbps while greater data rates values can be considered as *command links*.

Data rates analysis shows that only space-links can assume one of these two link

subcategories, ground-link can be considered always as *data links* even if commands are passed over it. When space-link results able to move a significant amount of data (*data links*) it will be exploited to transfer data trough the constellation or toward the ground station in order to exponentially increase the overall data volume moved during the entire lifetime of CubeSats.

To understand the advantages of ISLs we consider which conditions in terms of power levels, orbital parameters, mutual position of CubeSats, etc.. make cross-link efficient in term of CubeSat's mutual accessibility, daily GS visibility and in total data movement.

4.5   Packet Delivery Time & Antenna Selection

We select four different antenna combination to study the algorithm performances in relation to hardware and transmission power availability. These antenna combination are:

- Omni-directional antenna -to- Omni-directional antenna

- Patch antenna -to- Omni-directional antenna

- Patch antenna -to- Patch antenna

- Phased Array -to- Omni-directional antenna

The antenna characteristics and the performances of links that they can establish will be better presented and analyzed in next chapter. In this section our focus is to underline how the communication hardware can affect the execution time of our algorithm. Given the optimized data rate achievable between these antenna combinations is possible to calculate the packet delivery time as:

$$T_d = \frac{Pd}{DR_c} + \frac{SL}{c} \tag{4.2}$$

where:

T_d is the Total Packet Delivery Time, P_d is the packet dimension (46 Byte), DR_c is the data rate relative to the antenna combination selected, SL is the slant range between antennas and c is the light speed. The flight time can be ignored considering

the relative short distance involved in this study. Considering [46] we can assume that the LDPC decoding latency vary from 10 to 500 μs, therefore we can ignore it in the total packet transmission time budget.

Figure 4.12 shows the data rate values of the selected antenna combinations and the packet delivery time in function of the distance between satellites with a transmission power of 512mW.
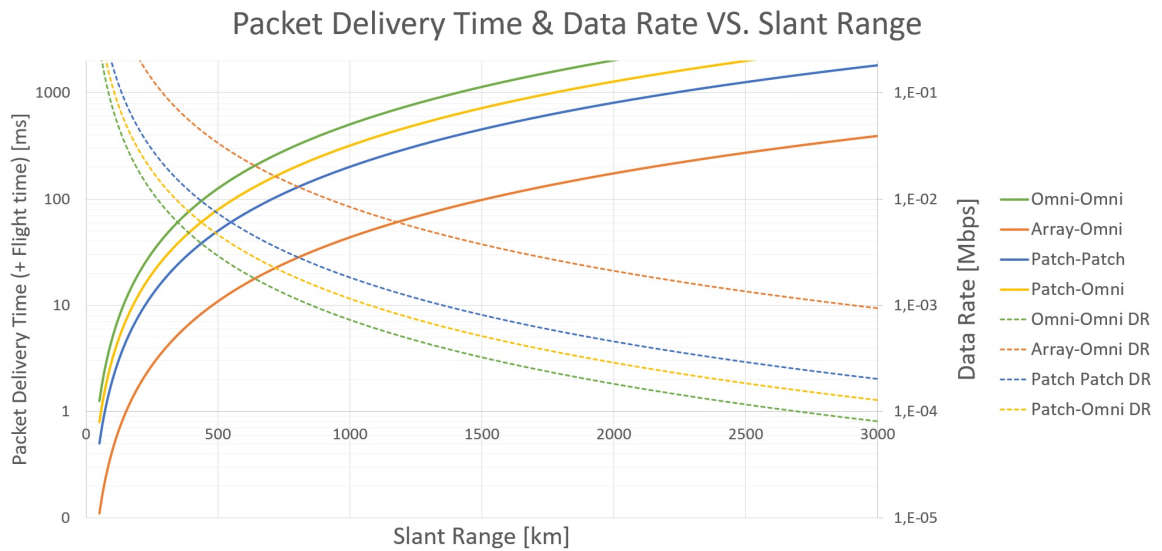
Fig. 4.12 Packet delivery time.

4.5.1 Antennas Performances Considerations

Particular attention must be given to phased array and patch antenna. The performances of these two configurations vary depending on physical displacement of satellites.

Phased Array

Despite best performances in terms of single packet delivery time, phased array results not applicable to our algorithm: the reduced main lobe aperture of phased arrays influence the total broadcast time of a single packet. Omni-directional antennas can irradiate in all directions while phased array must steer their beam in order to cover all the directions in function of their main lobe aperture. The broadcast time of a single packet for phased array results:

$$T_{Bpa} = \left(\frac{A}{L_{pa}} \right) \left(\frac{Pd}{DR_{pa}} + \frac{SL}{c} \right) \tag{4.3}$$

where A is the field of view that phased array must cover to broadcast and L_a is the lobe aperture that guarantees the data rate DR_{pa} level considered. Considering negligible the contribution of packet flight time, is possible to compare the broadcast time of omni-directional antennas with phased arrays:

$$\left(\frac{A}{L_{pa}} \right) \left(\frac{Pd}{DR_{pa}} \right) = \left(\frac{Pd}{DR_{omni}} \right) \tag{4.4}$$

Therefore, the minimum lobe aperture of phased array to equal the efficency of omni-directional antennas in terms of broadcast time must be:

$$L_a \geq A \left(\frac{DR_{omni}}{DR_{pa}} \right) \tag{4.5}$$

Otherwise, omni-directional antennas guarantees better performances for clustering formation.

Patch Antenna

Considering the constant motion of satellites, by using patch antennas to establish communication links is immediate to conclude that if the transmitter is not pointing the main lobe of its patch antenna toward the receiver, the communication link will be affected by a degradation due to the non-linear radiation pattern that characterize these type of antennas.

Supposing two satellites on same or similar orbit with transmitter antenna pointing toward Earth and receiver antenna pointing to transmitter, the total EIRP of transmitter depends on the relative position of the receiver (and/or vice versa). Therefore, communication link suffers of important degradation depending on antenna's misalignments. Figure 4.13 shows an example of communication link trends as function of satellites relative position. Satellite are placed on the same orbit, dotted curves represent the Tx antenna gain variation depending on slant range for 500km and 2000km altitudes, data rate levels vary depending on the slant range between satellites. Green curve represent the maximum data rate achievable without antennas misalignments.
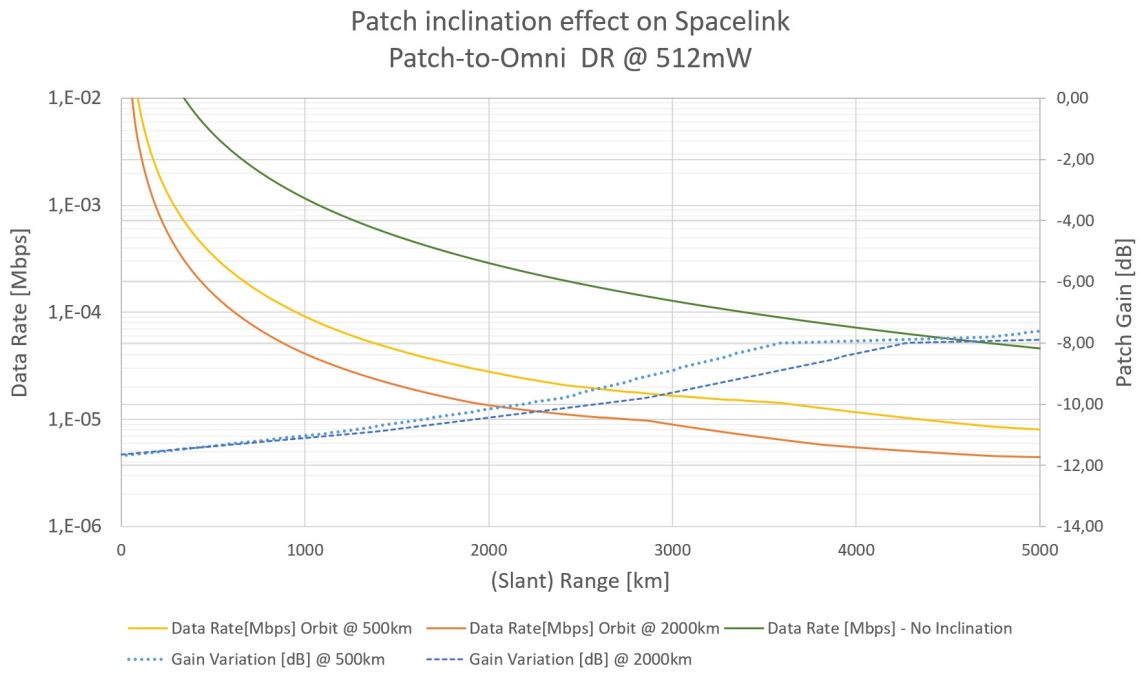
Fig. 4.13 Patch inclination effect on space-link.

Chapter 5

Constellations Topologies

In this chapter we present three constellation topologies that we use to test the improvements in terms of total data volume by applying our proposed antenna configuration communication system for CubeSat in constellations. We introduce the constellation topologies, their orbital parameter and analyze their access to the ground station.

5.1 Ground Station Settings

Ground station position is common and fixed for Flower and SSRGT constellations, a parabolic antenna of 5 meter diameter is placed on the rooftop of Dept. of Electronic and Telecommunication of Politecnico di Torino as shown in figure 5.1. Coordinates and GS informations are resumed in table 5.1. Equatorial constellation communicates with the same antenna placed on the equator.

Table 5.1 Ground Station position.

Ground Station Parameter	Value
GS Latitude	45,063396
GS Longitude	7,660017
GS Altitude	0,24 km
Antenna Type	Parabolic
Diameter	5 m
Frequency	2.4 GHz
TX Power	2mW to 2W
Main Lobe Gain	47.693 dB
Back Lobe Gain	-30 dB
Efficiency	55 %
Aperture	0,5665° deg.
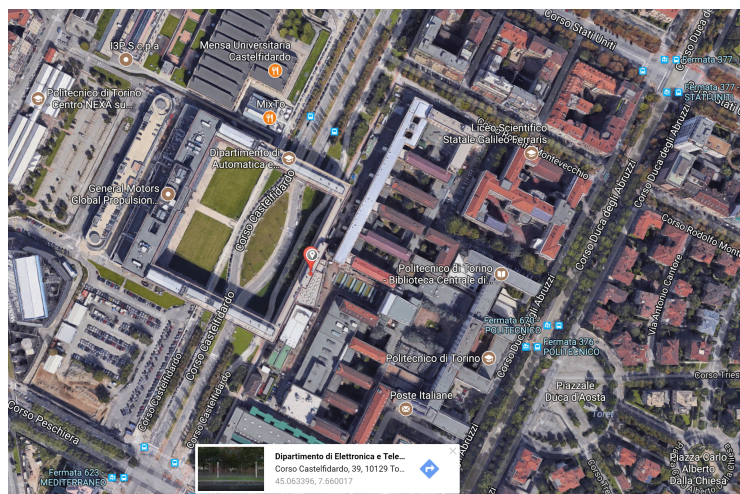
Fig. 5.1 Ground Station position - DET - Polito.

The ground station has been created with *STK* in order to be simulated, is provided with a sensor able orientate the antenna, performing pointing action toward the desired satellite. Figures 5.2 show the ground station simulation performed using *STK*.

(a) GS to Spacecraft link.

(b) GS to Spacecraft link.

Fig. 5.2 GS Polito Simulation: link with a CubeSat.

Azimuth-Elevation mask has been added to the simulation to consider the terrain conformation impact on communication link, the 5° degree minimum elevation angle considered as field-of-view limit for the ground station excludes any possibility from the territory to interact with measurements. Figure 5.3 shows the point of view from the Ground Station. In 5.3, the light blue cone pointing toward a satellites represents the automatic pointing view cone performed by the ground station, the aperture of the cone is proportional with the bandwidth of the parabolic antenna on GS. Figure 5.4 shows the ground station antenna beam simulation during communication with CubeSats. These simulations has been performed to study the access timing of satellites to the ground station for each constellation topology and to confirm mathematical analysis performed during the link budget analysis.
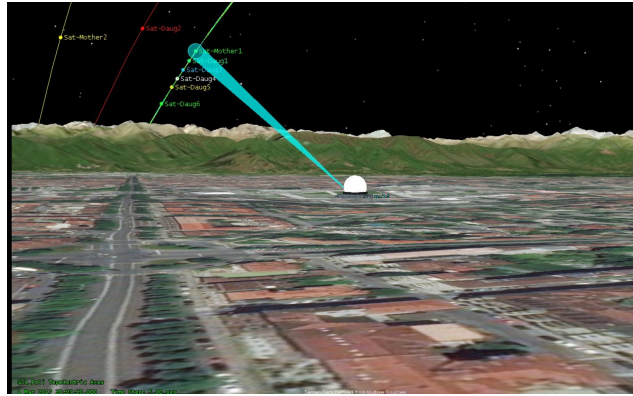
Fig. 5.3 Ground Station point of view.
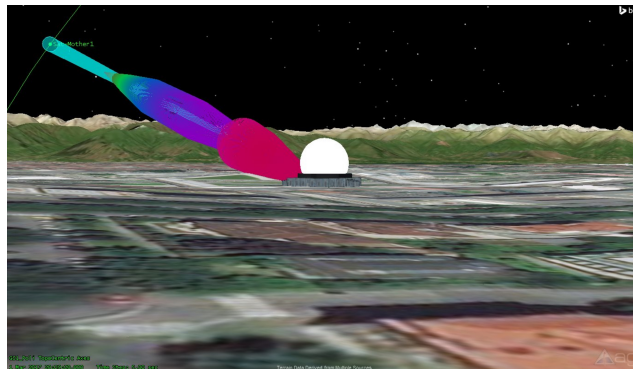
Fig. 5.4 Ground Station Beam.

5.2   Access Types

The simulations we are going to introduce and analyze has been performed thanks to *STK* and refers to a simulation period of one month: April 2017. We measured the mutual access time between satellites and the access from satellite to the Ground Station supposing two access conditions: long and short range.

Long range refers to a maximum line of sight of 3000 km. This access can be related to *command links*: considering cross-link data rates values calculated in previous sections, with space-link SL3 we can achieve data rates level between 3 and 30 kbps depending on PTx. Long range access refers to a useful visibility of satellites, where small amount of data can be transmitted for the constellation coordination purposes or to establish an emergency channel.

Short range access refers to a 60° degree ideal sensor placed on satellites. Considering

the basic local configuration mother-daughters we select as module to form and analyze constellations, we suppose to place on each mother a 60° sensor pointing toward the daughter-ship plane.

In constellation topologies presented daughters altitude is always lower than mothers, daughters move over their orbit quickly than mothers, the visibility/access between mothers and daughters is limited in time and the distance between them is variable. By imposing a window cone access view from mothers thanks to a 60° cone sensor we implicitly impose a maximum distance at which mothers and daughters can communicate on *Data Link*. Consequently a minimum data rate level is guaranteed. The cone aperture depends from the mission designer and its related to the constraint on minimum data rate desired for *Data Link*.

This maximum distance depends from the altitude difference according to:

Maximum communication distance (Md)

$$Md = \frac{Am - Ad}{cos(30)} \qquad (5.1)$$

Where Am is the Mother-ship altitude and Ad is the daughter altitude (approximation which does not consider the orbit curvature).
Out from the 60° degree cone we assume a growing deterioration of the link quality due to pointing and distances problems. We do not consider measurements and access despite is still possible to communicate outside the 60° view cone. Figures 5.5 and 5.6 refer to the Equatorial Topology, they provide a graphic example of the 60° cone view communication limit introduced.

5.3 Constellation Topologies

In this section we introduce three constellations topologies to study the impact of the proposed communication system on the inter-satellite links, satellite accessibility and improvements in the data volume transfer among the element of the constellation and from/to the ground station.
The goal is to apply our proposed configuration for communication to realistic constellation scenarios to understand the advantages of cross-link communication in

LEO orbit.

Testing scenarios are:

- Equatorial Constellation

- Flower / Sink Constellation

- Sun-synchronous Repeating Ground Track (SSRGT) / Sink Constellation

The SSRGT and the Flower constellations presents several problems in term of constellation topology maintenance, in particular, SSRGT satellites require a propulsion system to remain Sun-synchronous while Flower's satellites require continuous corrections to respect the spacing among elements of the constellation. In addiction, the altitude for the proposed constellations will not respect the 25-years lifetimes unless propulsion is used to de-orbit.
Orbit maintenance problems strongly affect the mission requirements and the lifetime of the entire constellations, in particular, the ΔV parameter must be considered to define the costs in term of orbit maintenance. The ΔV parameter is a measure of an impulsive variation of the velocity, that is needed to perform orbital maneuvers.
Nevertheless, the orbital maintenance problems related to the selected constellations will not be part of this dissertation: the proposed constellation topologies are used to shows the improvements in terms of data volume that our communication system can brings and how the topology, not its maintenance, can affects this improvements. Flower and SSRGT represent an already used solution for Earth observation missions and perfectly fit to the *store & forward* data transmission concept, on which we rely to increase the mission total data volume. However, we do not exclude that other constellation topologies could bring further advantage in terms of connectivity and communication performances, a proper constellation topology study must be dressed to understand our communication system performances.

5.4   Equatorial Constellation Topology

The equatorial constellation topology is introduced as a simplified case study scenario. We assume this configuration as a module, a local part of a bigger constellation.

This scenario represents a specific case in which a Cluster-Head has been elected and, for different reasons, maintain its role during all simulation time. This configuration reduces the dependences from orbital characteristics of satellites and represents the first approach to study performances in realistic constellation.

Four daughter-ships and one mother-ship form the constellation. The mother-ship is called D1, is placed at 1100 km altitude and is provided with the 60° degree cone sensor. Sensor simulates a cone-shaped down-facing area in which cross-link communication performances are guaranteed. Daughter-ships are are named respectively D6, D3, D7 and D8 at ∼500 km altitude, on the same equatorial orbit. D6 and D7 separation (*true anomaly* difference) corresponds to the maximum view of D1 cone sensor at 500km altitude. D8 and D3 separation is smaller, between D7 and D8. To perform this analysis we select a ground station placed on the equatorial latitude in order to maximize the access between ground station and satellites.

Figures 5.5 and 5.6 show the equatorial constellation.
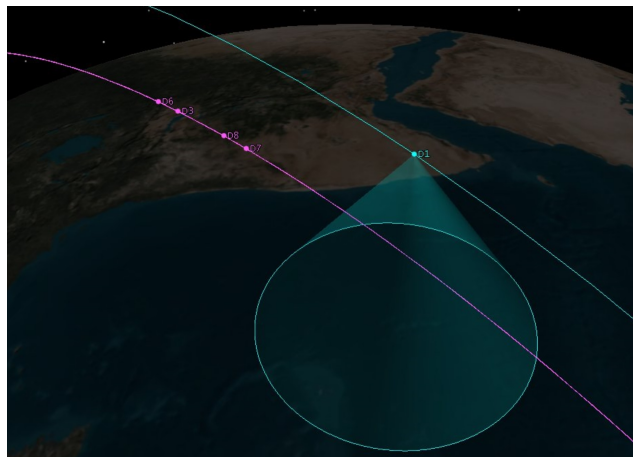
Fig. 5.5 Equatorial Constellation satellite placement.
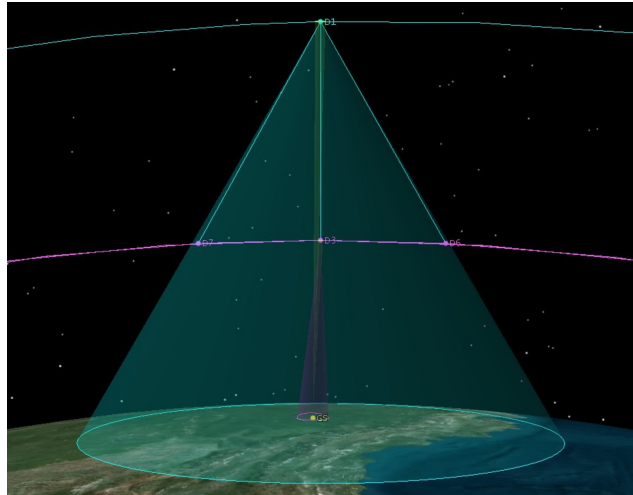
Fig. 5.6 Equatorial Constellation satellite placement.

5.4.1 Equatorial Constellation Access

Access analysis considers 30 days of April, 2017. Table 5.2 refers to the access between Satellites and Ground Station.

Table 5.2 Equatorial Constellation - Access to Ground Station.

Satellite	Link Type	Monthly Access (s)	Monthly Access(h)	Average Daily Access(s)	Average Daily Access(h)
D3	to GS	245041,787	68,067	8168,059	2,269
D6	to GS	245041,787	68,067	8168,059	2,269
D7	to GS	245041,787	68,067	8168,059	2,269
D8	to GS	245041,787	68,067	8168,059	2,269
D1 (Moth.)	to GS (no Daugh.)	374457,287	104,016	12481,9	3,467

Note

Access D1 (mother-ship) -to- GS (no Daugh.) refers to the total access time from D1 to GS when any daughter-ship is in view with GS.

Table 5.3 refers to access from D3, D6, D7, D8 to mother-ship (60° cone sensor) **when all satellites are not in view with the ground station**.

Table 5.3 Equatorial Constellation - Access to Mother-ship.

Satellite	Link Type	Monthly Access (s)	Monthly Access(h)	Average Daily Access(s)	Average Daily Access(h)
D3	to D1	41623,293	11,562	1435,286	0,399
D6	to D1	41623,29	11,562	1435,286	0,399
D7	to D1	1623,286	11,562	1435,286	0,399
D8	to D1	41623,288	11,562	1435,286	0,399
Total	-	166493,157	46,248	5741,143	1,59476

5.5   Flower/Sinks - SSRGT/Sinks

We introduce the other constellation topologies for our case study: Flower / Sink and SSRGT / Sink. As presented in [47], two candidate constellations for a hypothetical Earth observing mission has been designed.

In order to reduce the complexity of the constellation design process, both candidate constellations have been designed to have a small spatial coverage, which is the area of the target a constellation observes. Even with a smaller spatial coverage, however, CubeSats often have limited access to ground stations. To mitigate the effects of limited CubeSat access to ground stations the "data mule" methodology proposed by [48] has been employed.

The "data mule" methodology consists of using a set of source satellites to collect data, and a set of sink satellites to transport the collected data to a ground station. The sink satellites are larger, more powerful satellites with more access time to ground stations than source satellites, but less access time to target areas than source satellites. In order to maintain relevancy between the two candidate constellations, each candidate constellation to contain six sink satellites and nine source satellites has been designed.

Our concept is to maintain the topologies but avoid the use of larger satellite exploited as "sinks" and use the same CubeSats, with the same communication hardware and the same communication configuration.

Our goal is to study the average daily and monthly data volume that can be moved among the constellation.

5.6 Flower Constellation Topology

The flower constellation is a repeating ground track orbit with an axis of symmetry that coincides with the spin axis of the Earth. Flower constellations are well suited for Earth observation because each source satellite in a flower constellation has the same orbit shape and all the satellite node lines are displaced equally along the equatorial plane [47][49]. Table 5.4 resumes the orbit characteristics of the flower / sink constellation.

Table 5.4 Flower Constellation - Orbit Parameters.

Orbital Properties	Flower Sens	Flower Sinks
Apogee Altitude	500 km	1100 km
Perigee Altitude	500 km	1100 km
Inclination	165°	35° km
RAAN	Satellite 1-9: 0, 40, 80, 120, 160, 200, 240, 280, 320°	0°
True Anomaly	Satellite 1-9: 0, 53.54, 98.12, 134.1, 165.2, 194.8, 225.9, 261.88, 306.46°	Satellite 1-6: 0, 60, 120, 180, 240, 300°

Figure 5.7 shows a picture of the Flower / Sink constellation during a simulation.
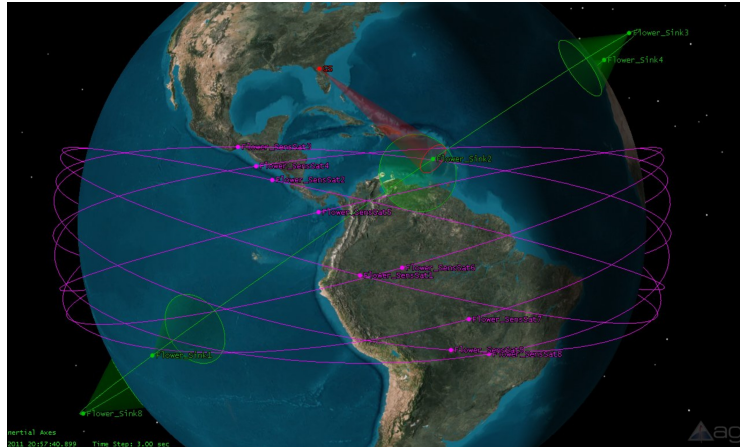
Fig. 5.7 Flower / Sink Constellation.

5.6.1   Flower Constellation Access

Figure 5.8 shows the graph relative to the average monthly access to ground station of Flower Sensors. Despite sinks are used to communicate with the GS also Sensors can be exploited for it, in most of the cases they presents better channel performances due to their lower altitude. Total data transfer to the ground station is a combination between Sensor and Sink data down/up-load with the GS.
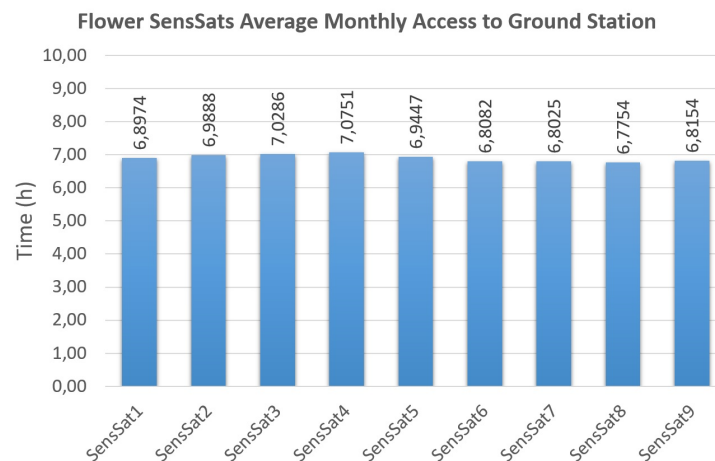
Fig. 5.8 Flower Sensors access to GS.

Flower Sensors have similar access timing to GS. Differences relative on the RAAN (right ascension of the ascending node) orbit parameter are detected. Graph

in figure 5.9 shows the average monthly access of Flower Sensor satellites to Flower Sink satellites considering the 60° degree visibility cone sensor on Sink satellites. The effect of the RAAN differences is more accentuate in this graph. Flower Sensors 5 and 6 access for a longer time to Sinks during the simulation.

**Flower SensSats Average Monthly Access to SinkSats 60°
deg Sensor
(when SensSat are not in view with GS)**
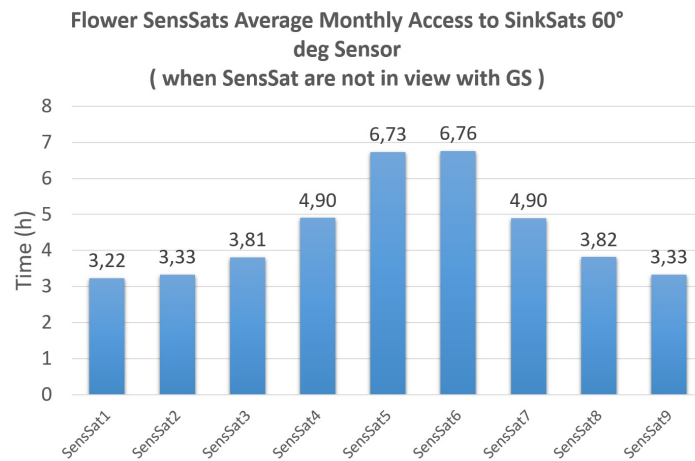
Fig. 5.9 Flower Sensors access to Sink (sensor 60°).

The average access time of Flower Sink satellite to GS is resumed in table 5.5.

Table 5.5 Flower sinks to GS average access.

| Flower Sink Satellite Access to Ground station	Time
Monthly Access (s)	1468055,828
Monthly Access (h)	407,7932
Average Daily Access (s)	48935,194
Average Daily Access (h)	13,593

Flower Sensor Mutual Access

To optimize communications and improve data flow and satellite access we collect data on mutual access time between Flower Sensor satellites. Access are reported in table 5.6, these links can be used as constellation sync channels, emergency channels or to perform hop-to-hop communication with the ground station if possible. Mutual access result constant during simulation time. During constellation design this ability

must be considered to exploit all the constellation potential. These access are not considered in our performance budget.

Table 5.6 Flower Sens to Sens Access.

Satellite	Monthly Access to other Sensors (h)
Flower Sens1	5760
Flower Sens2	5760
Flower Sens3	5504,789
Flower Sens4	5760
Flower Sens5	5760
Flower Sens6	5760
Flower Sens7	5760
Flower Sens8	5504,704
Flower Sens9	5760

Figure 10.4 shows the access between Flower Sensors and Sinks and between Sensors during the simulation. Red lines indicate the connections between Sensors and Sink. Green lines indicates connections between Sensors.
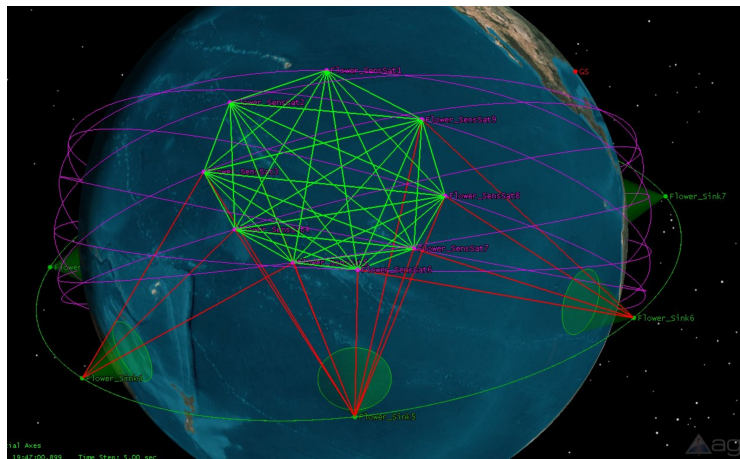

Fig. 5.10 Access in Flower Constellation.

Flower / Sink 6000km Access

Figure 5.11 shows the average daily access at a maximum distance of 6000km between Flower Sensors and Flower Sinks satellites when Sensors are not in view with the ground station. Depending on satellite, each Sensors can be connected to a sink for an average daily time between 4,38h and 6,31 h per day. These measures refers to a line of sight access, the ISL performances must be analyzed to define if *command link* can be established.

Flower SensSats Average Daily Access to a SinkSat at 6000km
(when SensSat not in view with GS)
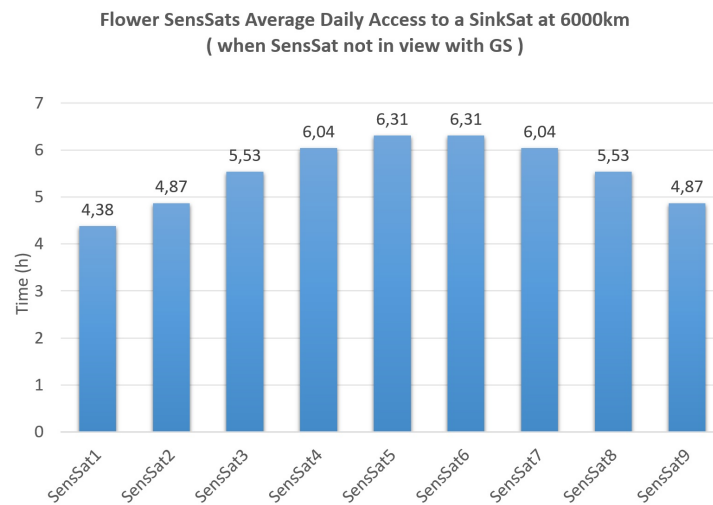
Fig. 5.11 6000km line of sight Access in Flower Constellation.

5.7 Sun-synchronous Repeating Ground Track (SS-RGT) Constellation

SSRGT orbits have desirable features for remote sensing and Earth observation applications, since these orbits have near constant illumination angles and approach targets with identical viewing angles up to twelve times per day [50]. These characteristics are amenable to Earth observation missions in both the visible and infrared spectrum. Satellite systems such as the LANDSAT program [51], and imaging and remote sensing satellites and constellations, such as Spot satellites [52], and RapidEye [53] leverage the SSRGT orbit.

To maximize the access time between the source satellites and the target, source satellites in has been equally about a polar orbit at an altitude of 500 km. Sink

satellites has been equally distributed on a circular orbit at a 70° inclination and an altitude of 1100 km.

Table 5.7 resumes the orbit characteristics of the flower / sink constellation.

Table 5.7 SSRGT Constellation - Orbit Parameters.

Orbital Properties	SSRGT Sens	SSRGT Sinks
Apogee Altitude	500 km	1100 km
Perigee Altitude	500 km	1100 km
Inclination	165°	35° km
RAAN	0°	0°
True Anomaly	Satellite 1-9: 0,40, 80, 120, 160, 200, 2409, 280, 320°	Satellite 1-6: 0, 60, 120, 180, 240, 300°

Figure 5.12 shows a picture of the SSRGT / Sink constellation during a simulation.
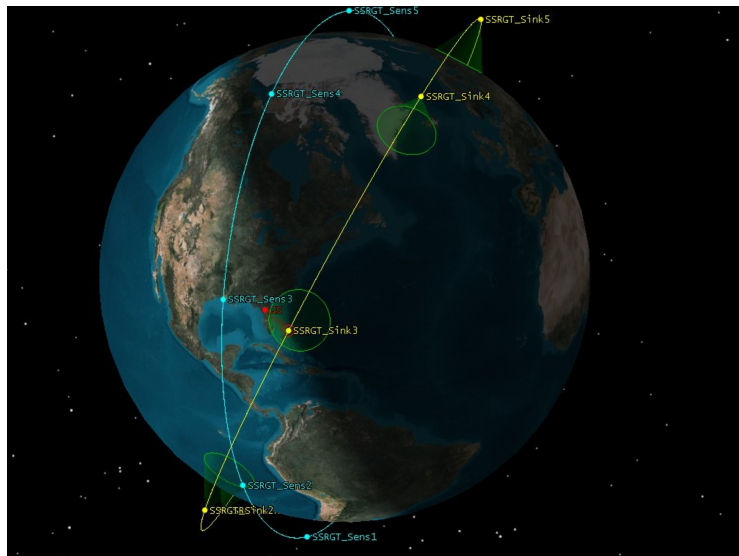

Fig. 5.12 SSRGT / Sink Constellation.

5.7.1 SSRGT Constellation Access

Graph 5.13 resumes the average monthly access from SSRGT Sensors to GS. Timing results very similar to each other, the constellation topology provide a uniform access

for each sensor, differences shown are related to the short simulation time (1 month). Average monthly access to GS results higher than Flower/Sensor topology due to the orbit inclination features of SSRGT constellation. The daily average access is $\sim$ 25,5 min per day.

SSRGT SensSats Average Monthly Access to Ground Station
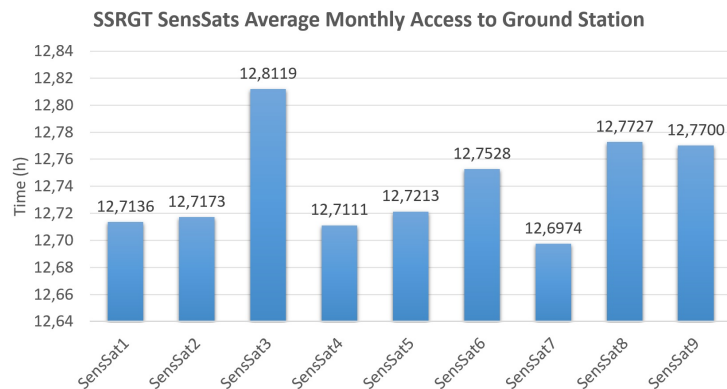
Fig. 5.13 SSRGT Sensor access to GS.

Graph 5.14 shows the average monthly access of SSRGT Sensors to the 60° cone sensor of Sink Satellites when SSRGT sensors are not in view with GS. Similar access values are measured for each satellite, SSRGT configuration results to be more "linear" compared to Flower / Sens constellation: SSRGT satellites are placed in the same orbit with different true anomaly values, they are equally spaced on the same orbit, therefore similar access values are the expected results. Access from Sensors to Sinks is 5,3 hour per month in average, corresponding to $\sim$ 10,6 min per day.

SSRGT SensSats Average Monthly Access to SinkSats 60° deg Sensor
(when SensSat are not in view with GS)
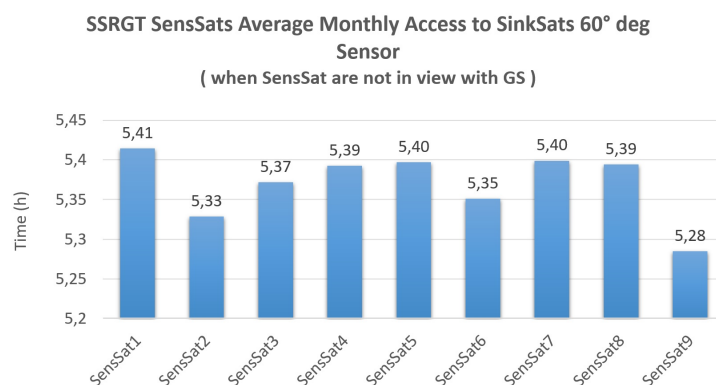
Fig. 5.14 SSRGT Sensor access to 60° Sensor on Sinks.

The average access time of SSRGT Sink satellite to GS is resumed in table 5.8.

Table 5.8 Flower sinks to GS average access.

SSRGT Sink Satellite Access to Ground station	Time
Monthly Access (s)	956934,802
Monthly Access (h)	265,815
Average Daily Access (s)	31897,826
Average Daily Access (h)	8,86
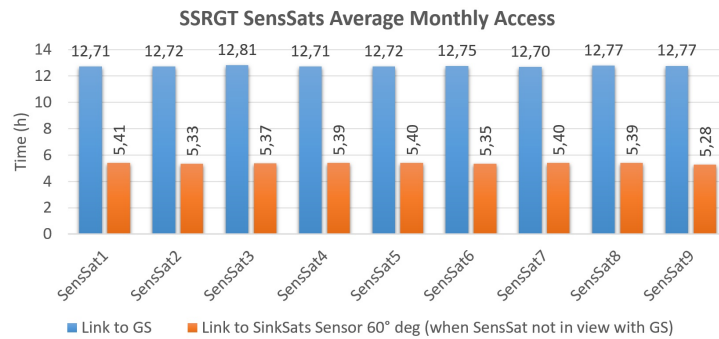
Fig. 5.15 SSRGT Sensor access to GS and Sinks (sensor 60°).

Figure 5.16 shows the orbits of SSRGT Sensors (light blue), orbit of SSRGT Sinks and their relative 60° cone sensors (yellow) and the 6000km line of sight between Sensors and Sinks (light blue). Picture detail shows *data links* established between SSRGT-Sink-8 with SSRGT-Sens-5 as shown in the detail picture.
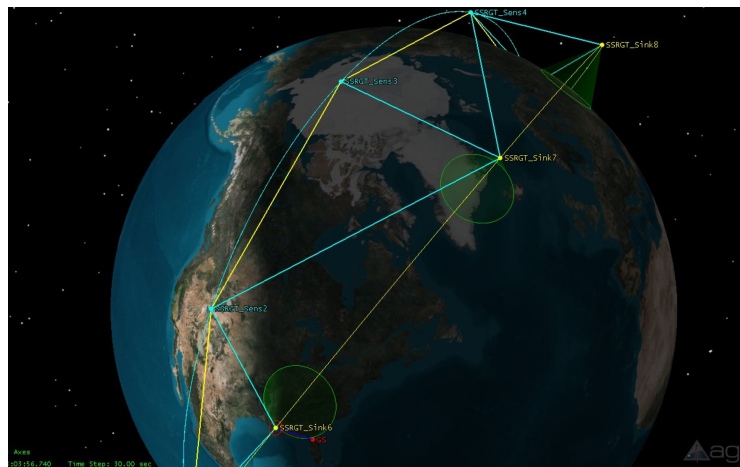
(a) SSRGT access picture.

(b) SSRGT access picture detail.

Fig. 5.16 SSRGT Access Types.

SSRGT / Sink 6000km Access

Figure 5.17 shows the average daily access at a maximum distance of 6000km between SSRGT Sensors and SSRGT Sinks. Depending on satellite, each Sensors can be connected to a sink for an average daily time of 5,41 h per day. ISL performances must be analyzed to define if *command link* can be established.
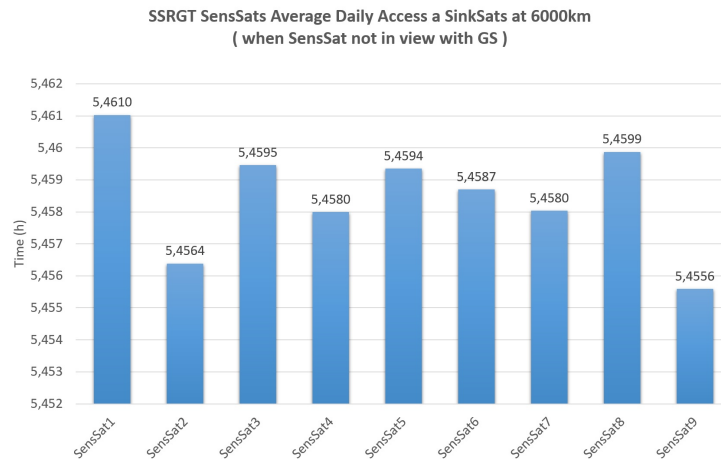
Fig. 5.17 6000km line of sight Access in SSRGT Constellation.

Chapter 6

Hardware Design and Implementation

In previous chapters we introduced the phased arrays as reliable solution to establish inter-satellite communication links between CubeSats. We defined how clusters can be formed and which advantages can be obtained in term of daily data volume by thanks to phased arrays. In this chapter we explain how the hardware of the phased array system has been designed and developed.

Establish communication link represent the basic function of phased array, however is also possible to establish the mutual physical position of satellites. Thanks to an appropriate algorithm we manage phased array in order to estimate the position of the received signal when phased array is in receive mode, thus allow to track the transmitter and adopt beamforming techniques to maintain the link at its maximum capabilities. Moreover, the position estimation allows to obtain additional information about the physical position and evolution of the elements participating to cluster, these informations can be used from clustering algorithm to manage node status with more precision.

We defined the relation between the phased array structures introduced, their number of elements and spacing with the corresponding beam shapes and gain levels. Thanks a beamforming strategy every antenna of phased array can be managed to establish the communication and estimate the physical position of the received signals. Same strategy can be also applied during the transmission phase: every

channel of phased array is managed in order to contribute to the creation of the beam and shaping it to point the main lobe toward a specific direction. The array result electronically steerable, therefore is possible to point the beam without any attitude modification of CubeSat.

A deployable structure that fits to four CubeSats sides able to triple the available surface of each side has been considered as base to accommodate phased arrays and solar panels and the ratio between surface occupied as been analyzed as critical factor for the feasibility. Besides the hardware of the communication system, this chapter presents the deployable structure that increases the external surface of CubeSats, fully developed at Department of Electronic and Telecommunication of Politecnico di Torino.

In this chapter we focus on the phased array management hardware system, we present main blocks and their functioning. Then we present how the system can be accommodated on a CubeSat 1U.

6.1   General System Description

Figure 6.1 shows how the entire system works. The *clustering algorithm* contributes to the cluster formation and maintenance phase, its main goal is to complete the clustering process in order to define a specific role of the satellite and define connections with other elements of the cluster.

The *general management system* is responsible for switch from cluster to data transfer operations: once the cluster formation process is completed and the satellite results stable in its cluster and can transmit/receive data from other CubeSats. The *general management system* receives information from the clustering algorithm regarding the satellite status inside its cluster and information about the available time windows that will be use for data transfer phase. Moreover, receives information from the data transfer sub-system regarding the data transfer status. The combination of this information are processed to define how to alternate from cluster to data transfer operations. Cluster operations have the priority.

The *data transfer and array pointing management* is responsible for managing the data transfer and establish high data rate communication links between cluster's elements by sending high level commands regarding antenna pointing actions required

to the hardware management sub-system. It defines which and how many data must be passed during the available data communication slot (or data transfer window) at his disposition.

The *Communication Sub-System* represents the hardware of the entire system, the working principle, the hardware design and the direction of arrival estimation algorithm utilized will be introduced in next sections or chapters.
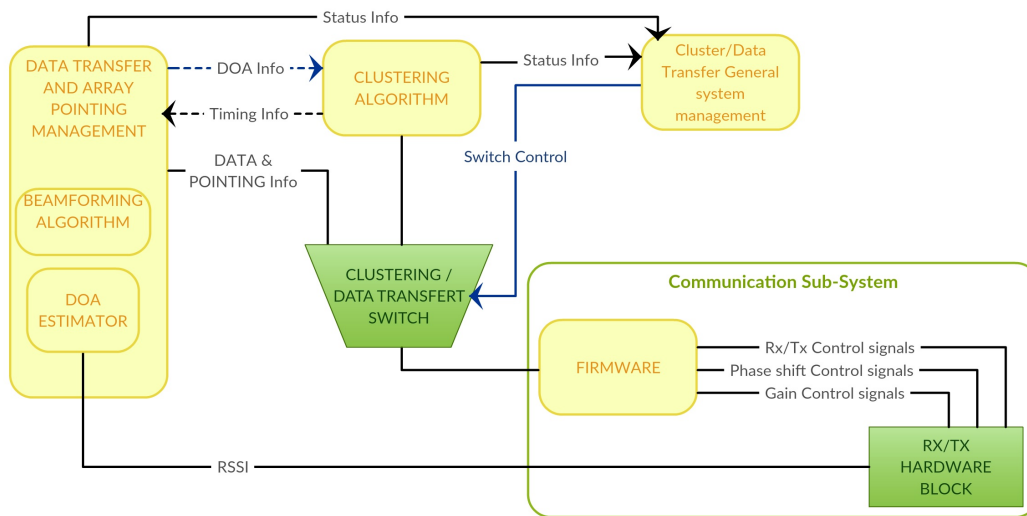
Fig. 6.1 System block diagram.

6.2 Hardware Design

We create the prototype of phased array number one *PA1* presented in chapter three. The developed hardware is shown in figure 6.3. As previously described *PA1* is formed by two sub-arrays composed by four elements each, placed in a cross-configuration. Each sub-array contributes to the creation/shaping of the beam and to the physical position estimation of the received signal along its x and y axes. We have developed four of the eight expected channels to test the physical position estimation system along one axes, x or y.

To simplify the system in terms of signals conditioning and design process and to reduce realization cost of the prototype we decide to develop the system in order to operate in a bandwidth from 800MHz to 960MHz instead 2,4 GHz. Moreover, ITAR restrictions and problems on the availability of phase-shifters and power combiner

forced us to work in sub-1GHz bandwidth.

The system can be considered as a rudimental prototype useful as proof of concept of the communication and postion estimation system: advanced phased arrays systems usually work at higher frequencies and execute analog to digital conversion of signal before analyze and modify signals.

Our prototype performs the analog signals conditioning before sending the combination of channels to the transceiver, thus allowing to reduce the costs and the complexity of the system. By performing analog signal conditioning at low frequencies we reduce synchronization problems, signal conditioning complexity issues and transmission power requirements. However, components like the analog phase shifter, introduce errors due to lower sensibility, non-linear shifting characteristic, higher insertion and line loss and noise.

Figure 6.2 shows the block scheme of the phased array management system hardware.
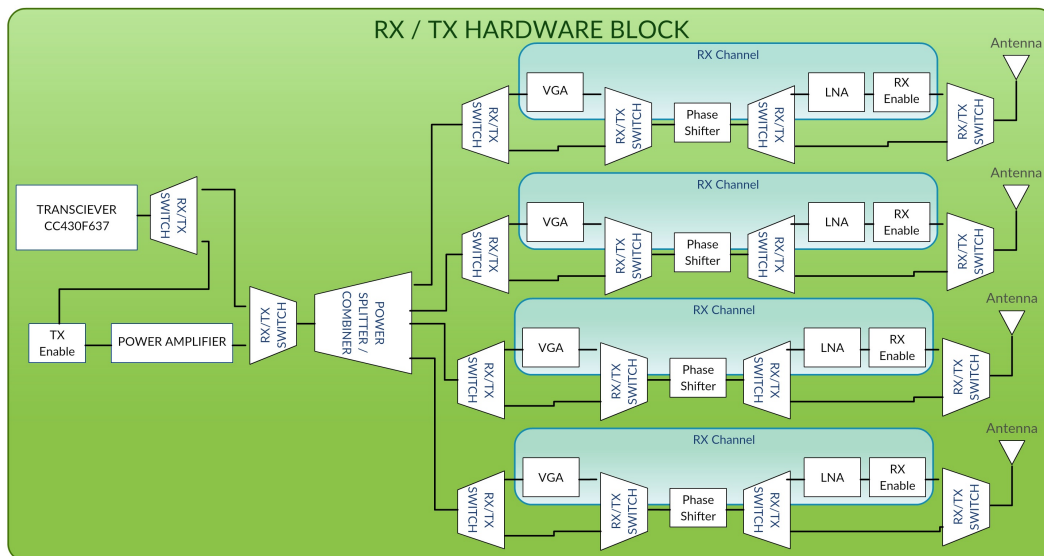

Fig. 6.2 Phased Array Management - Hardware block diagram.
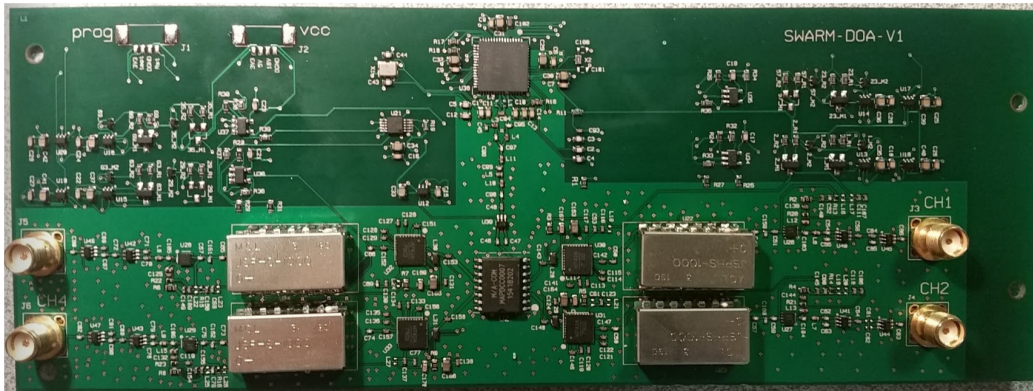
Fig. 6.3 The developed hardware: four channel phased array.

The transceiver selected is the *CC430F6137* from Texas instruments, an ultra low-power micro-controller from *MSP430* family system-on-chip (SoC) with integrated RF transceiver cores that consists of several devices featuring different sets of peripherals targeted for a wide range of applications. A network of RF switches are introduced on several part of the circuitry to set the system as transmitter (Tx) or receiver (Rx). Schematic is shown in figure 6.4.

On *receive* mode to each antenna is connected its correspondent Rx channel, composed by: Enable Switches, Low Noise Amplifier (LNA), Variable Gain Amplifier (VGA), RX/TX Switches.

All the receive channels flows into the *Power Combiner* which perform perform the channel combination and send the resulting signal to the transceiver.

On *transmit* mode every antenna is connected to its Tx-channel by setting Rx/Tx switches. The TX-Channel performs the conditioning of the transmitted signal, Tx channel is so composed: RX/TX Switches, Enable switches,Power Amplifier, Power Splitter, Channel selection Block, Phase shifter, Enable Switches.

Note

All lines has been adapted at 50Ω
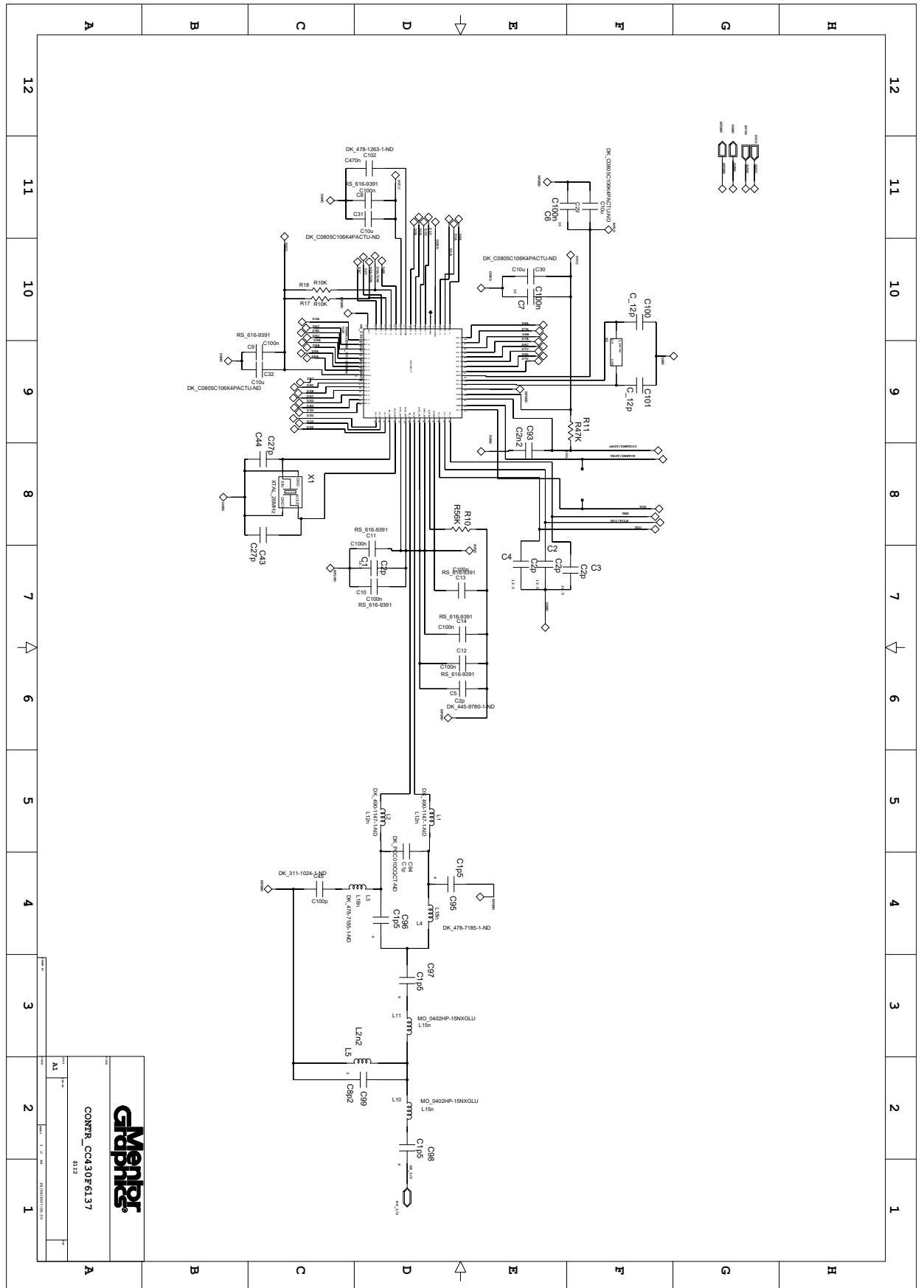
Fig. 6.4 Transceiver Schematic.

6.2.1   Enable Switch / RX/TX Switch

This block allows to switch from transmit to receive mode or to enable/disable a transmit/receive channel. Schematics is shown in figure 6.5, the selected switch is the AS179-92LF from SKYWORKS:it support up to 6W input power in a frequency range from 20MHz to 4GHz. A single switch control signal managed by the CC430xx is sent to the two logic gate (not) connected with the two switch control port, control voltage is 0-5V.
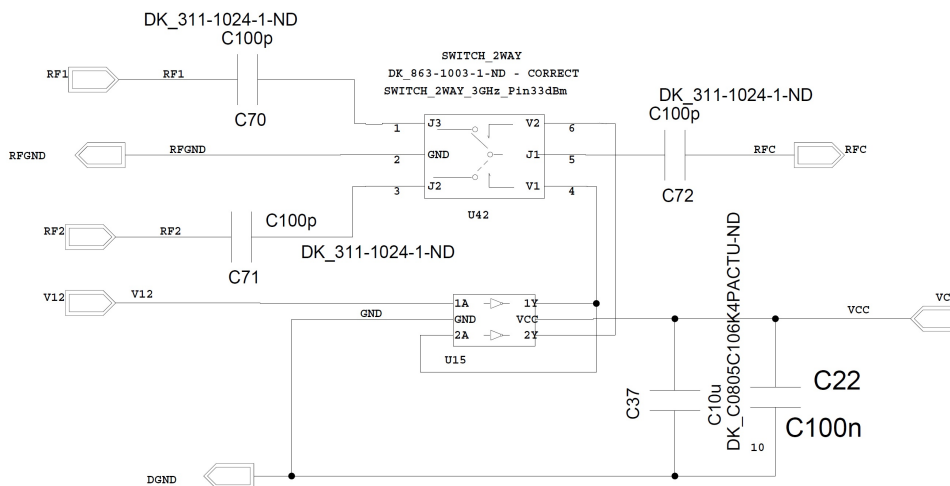
Fig. 6.5 Rx/Tx Switch.

6.2.2   Low noise amplifier (LNA)

The selected component is the *SKY67151-396LF* from SKYWORKS. This LNA presents an integrated active bias and very low noise figure (<0.5 dB) over a 2 GHz BW. It operates over the broad frequency range of 0.7 to 3.8 GHz. Conditioning circuitry has been designed to provide a small signal gain of 26 dBm over a bandwidth from 700M Hz to 1 GHz. Schematic is shown in figure 6.6.
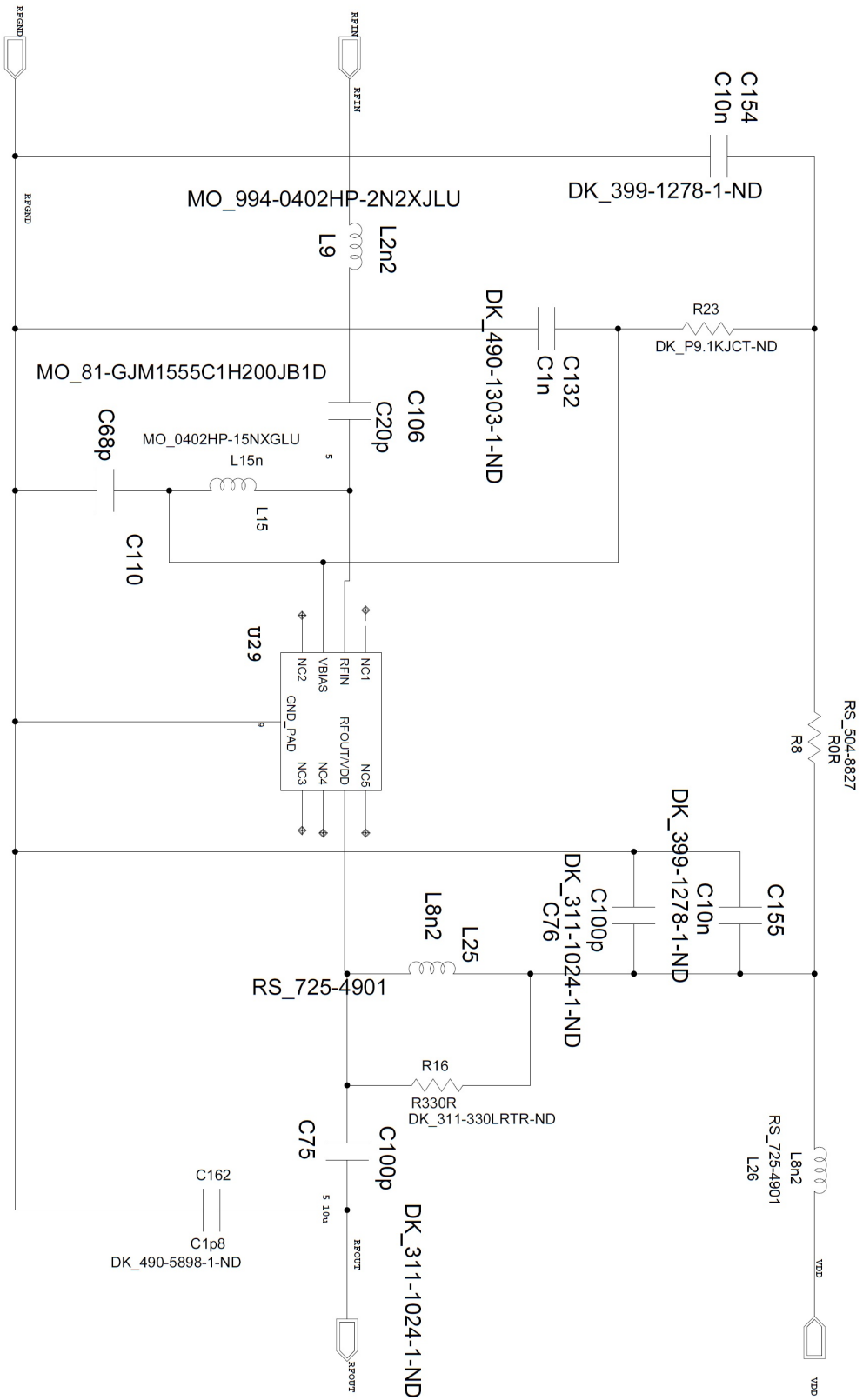
Fig. 6.6 Low noise amplifier schematic.

6.2.3 Variable Gain Amplifier (VGA)

The selected component is the *HMC742ALP5E* From *Analog Devices*, it represent the second signal amplifier stage. It can be used to develop more advanced beamforming techniques or to introduce signal offsets. Programmable gain range is -12 to +19.5 dBm controlled by SPI interface connected with CC430xx. Operating range is from 70MHz to 4GHz. Schematic is shown in figure 6.7.
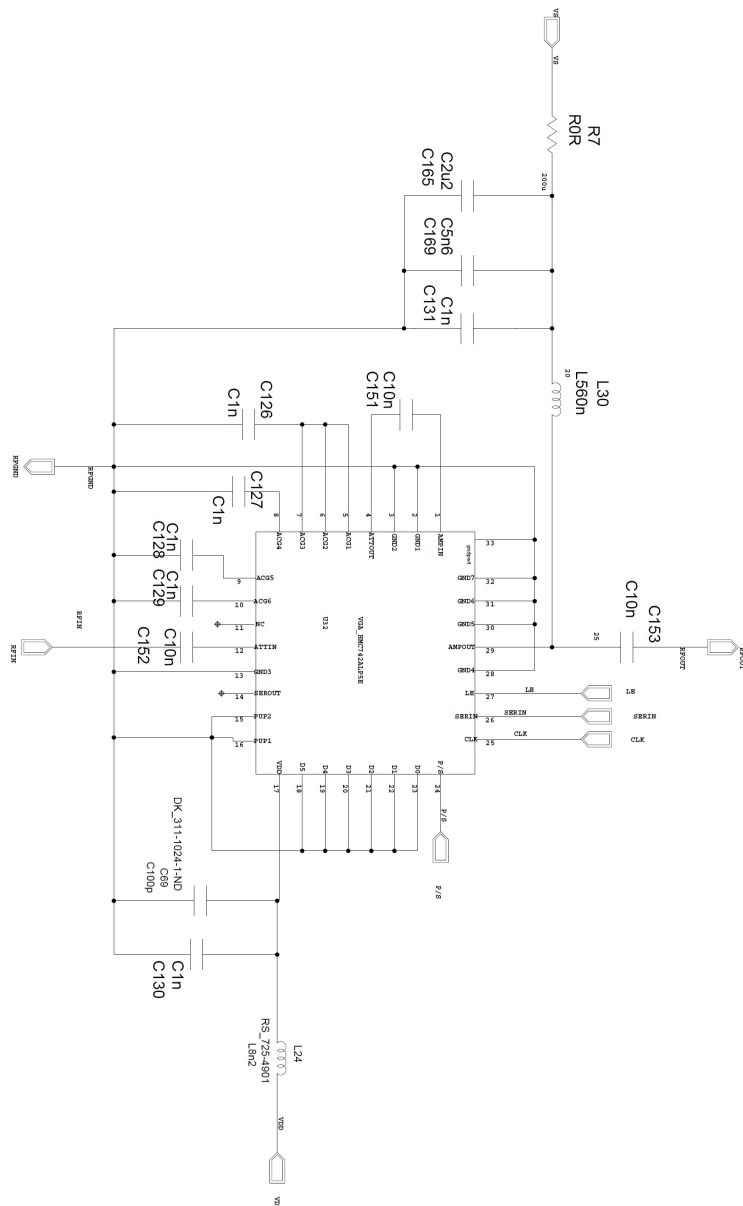
Fig. 6.7 Variable Gain Amplifier schematic.

6.2.4   Phase Shifter

The selected phase shifter is the *JSPHS-1000+* from *Mini Circuits*. It represents the
key component to perform beamforming techniques, phase shifting range is 0°/180°
deg. over a bandwidth from 700 MHz to 1 GHz. Schematic is shown in figure 6.9.
Shifting characteristic is shown in figure 6.8; we decided to reduce the voltage
control range from 0V to 14.5V to avoid undefined shifting values due to the flat-like
trend in proximity of 15V voltage control. Therefore the shift ranges is results 0°
to ~170°. This do not represent a problem as the whole system capabilities, DOA
estimation and beamforming communication, are performed in field of view from
40° to 140° of the phased array.
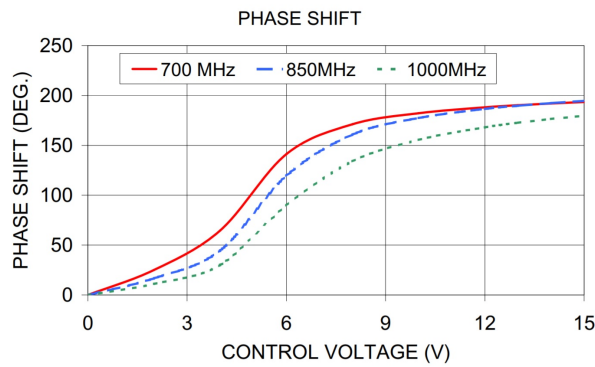
Fig. 6.8 Phase Shifter characteristic.
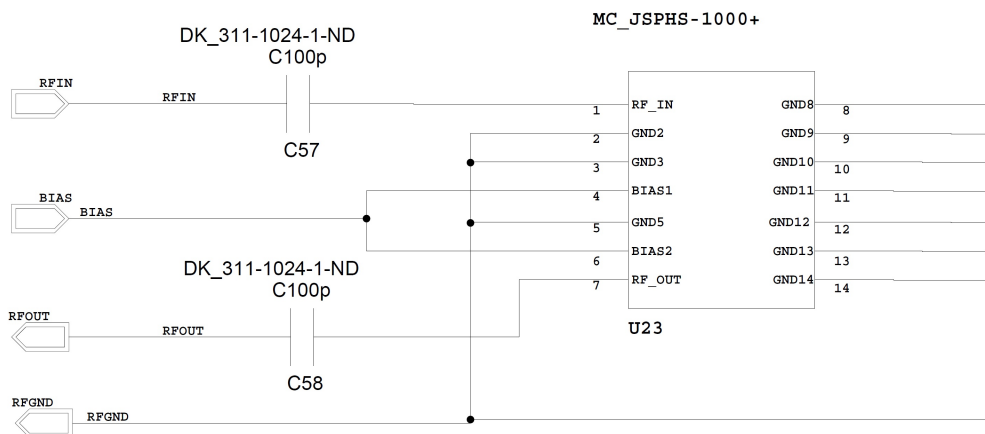
Fig. 6.9 Phase Shifter schematic.

6.2.5 Power Splitter/Combiner

The selected components is *MAPDCC0007* from *Macom*. It combines received signals from each Rx-Block and send the results to the transceiver in order to be analyzed. Allowed bandwidth is 824 to 960 MHz. Schematic is shown in figure 6.10. *MAPDCC0007* is bi-directional, therefore, during the Transmit mode signal is sent to PIN7 and is equally splitted in four equal signal with same power levels.
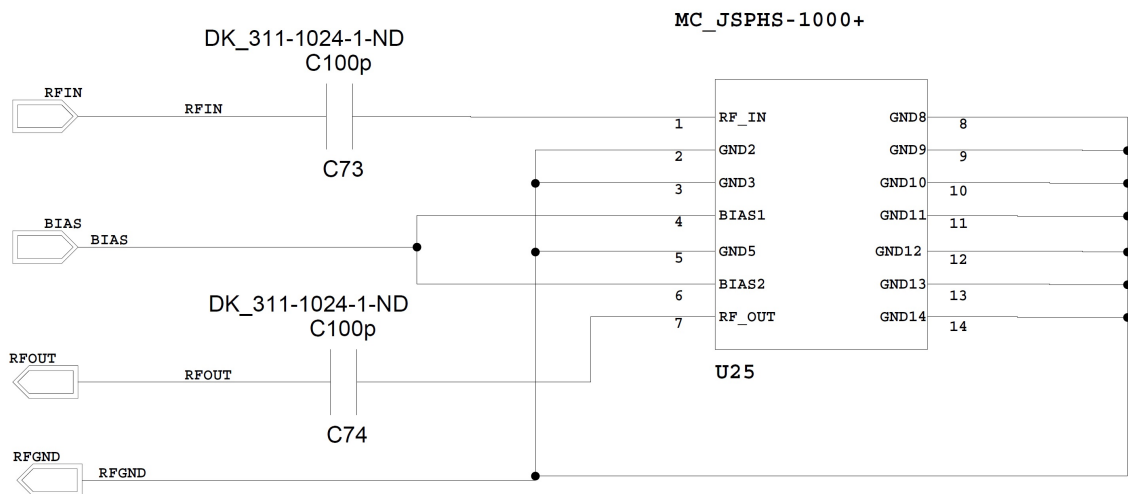
Fig. 6.10 Power Combiner/Splitter.

6.2.6 Power Amplifier and Channel Selection

The selected component is the *RF6886* from *RF Micro devices*. It amplify the transmitted signal from CC430F6137 up to 34dBm. Allowed frequency range is 100 MHz to 1GHz. The channel selection has been designed and created by using an appropriate configuration of RF switches used to design also the Rx/Tx switches. These two blocks has been designed but not developed in the PCB presented in figure 6.3,therefore schematics are not reported.

6.3   The Deployable structure

The deployable structure [54] has been completely designed at Dept. of Electronic and Telecommunication of Politecnico di Torino. it consists in a modular structure composed by *tiles* [33] that can be mounted on CubeSat faces. The structure deployment is based on a system of hinges equipped with torsion springs without need of mechanical guides. The opening follows an accordion-like movement in a perpendicular way with respect the face of CubeSat on which is fixed. The opening is performed in less than 5 seconds with a settling time less than 10 seconds. The tile dimension is equal to the CubeSat face, considering a 1U CubeSat (10x10x10 cm), each deployable structure is composed by three tiles of 10x10cm; four structures can be mounted on a single 1U CubeSat. For each side the surface increase to 10x10x30 cm. According to this, for a 3U CubeSat 10x10x30 cm, the structure increases to 10x10x90 cm each face and so on. Figure 6.11 shows the opening sequence of one structure designed to fit on 1U CubeSat. The deployable structure has designed for a CubeSat 1U, its the working principle can be extended to every CubeSat standard structure.
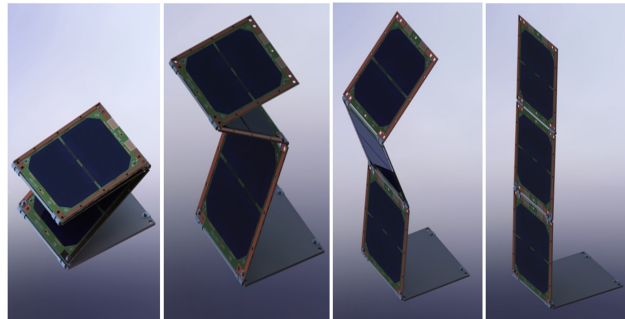
Fig. 6.11 Single structure - deployment sequence.

Deployable structure tiles do not require support structures as they are made by PCB boards. Hence, they can host functional systems like the antennas, solar panels and/or flat components. Therefore, Every PCB tile of the structure can be used to perform different tasks independently. A small part of tile side is used to create electronic connections between tiles thanks to flat cables or flexible PBC segments. These connections are exploited to connect solar panels to the power management system of CubeSat, to transport signals to/from antennas, etc..A preliminary thermal

analysis has been performed during the design process of AraMiS [33] process, calculations can be found in [55] and [56] and considers several cases, main considerations are made on: Thermal equilibrium, no generation or accumulation inside; thermal balance, color uniform, with internal heat generation; system not in thermal equilibrium, transient analysis and realistic case.

To reduce the physical occupation and respect thickness (6 mm max) and volume allowed for the standard of the P-POD launcher all mechanical components are miniaturized as shown in figure 6.13. Sealing wires keep closed the structure during the launch phase and the accommodation of CubeSat inside the P-POD. Side blocks has been designed to avoid folded tiles to hit each other when folded and stowed in the P-POD. An extrusion have been created close to the corners of each tile and its used to aligning and interlock tiles each other as shown in figure 6.12. The extrusion fits in the standard holes of the upper tiles, its wedge shape avoid to block the deployment of the structure due to thermal expansion.
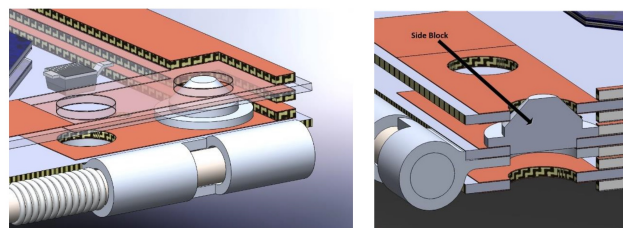
Fig. 6.12 Side Block used when tiles are folded.

Sealing wires can be detached using less than 450 J with a current of 800 mA. Wire resistance is oversizes, it can withstand a force greater than 500 N, despite they must counterbalance forces less than 25 N of the torsion springs that deploy the structure. The release technology for the deployment structure is based on an innovative thermal fuse that works at low energy consumption. When enabled, thermal fuses heat up until they reach the proper temperature to melt the latch and release the deployable structure.
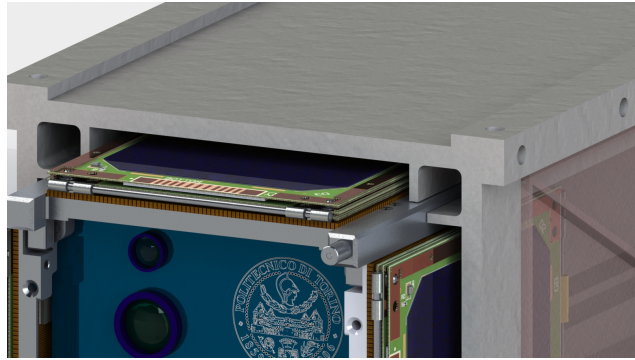
Fig. 6.13 Deployable structures and CubeSat accommodation inside P-POD.

Chapter 7

Direction of Arrival (DOA) Estimation

Direction of arrival (DOA) estimation or *direction finding* has been an active area of research that found application in the field of radar technology, electronic surveillance, sonar and in several application for position location and tracking system. The estimation of the direction of arrival of one or multiple signals and their multi path components is important in systems employing adaptive antenna arrays. These antenna systems are capable of automatically forming beams in the desired direction and steering nulls in the direction of the interfering signals. Direction finding techniques can be used to estimate the direction of arrival (DOA) of received signal/s.

This part of our project focus on the DOA estimation of the received signal/s among CubeSats. After the cluster formation phase CubeSats have sufficient information about the relative positions of other components of their cluster; the communication can be improved by switching from the use of the isotropic omnidirectional antennas to the use of phased arrays, proposed antenna configurations to establish links are array-to-array/ omni-to-array and array-to-omni. The DOA estimation supports the communication link maintenance, helping to point the beam towards a specific direction and dynamically optimizing the link status. Moreover, DOA and Range estimations are send back to the clustering algorithm, these information will be integrated with other collected during the cluster formation phase in order to refine the knowledge of the mutual physical position.

7.1   An overview on beamforming algorithms

The array-based DOA estimation techniques can be cataloged in four different types: *conventional*, *subspace based*, *maximum likehood*, *integrated*. *Conventional* methods are based on classical beamforming techniques and requires large number of elements to achieve high resolution. The *Delay-and-Sum* [57] conventional method consists in applying a (or not) phase delay to each channel of the phased array in order to electronically steer the beam in all possible directions and analyze the sum of channels to find peak in the output power estimate DOA.

Subspace based techniques are high resolution sub-optimal techniques which exploit the eigenvalues structure of te input data matrix. MUSIC [58] and ESPRIT [59] are an example of subspace based beamforming algorithm. MUSIC provides informations about the number of incident signals on the array, direction of arrival, strength and cross-correlation between incident signals, noi, power, etc. Despite MUSIC provides very high resolution, it requires a very precise and accurate array calibration. Other variants of MUSIC have been prosed, we do not report them in this dissertation. The Estimation test of signal parameters via Rotational Invariance Techniques (ESPRIT) algorithm introduces the concept of sub-array division to perform measurements and strongly reduces the computational and storage requirements of MUSIC, making it a good candidate to manage our phased array.

Maximum likehood were one of the first techniques to be investigated for DOA estimation, they are superior to the suboptimal techniques. However, *Maximum likehood* and *integrated* result computationally intensive, therefore we decided to do not use them as solution to manage our phased array system.

We choose *Delay-and-Sum* technique for our project: due to its low requirements in terms of computational costs and development time and difficulties, it represent a perfect solution to manage our phased array communication system.

7.2   Delay-and-Sum DOA estimation working principle

The beamforming algorithm used to manage the phased array and estimate the direction of arrival (DOA) is the *Delay-and-Sum*: figure 7.1 shows a two-antennas array separated by distance *d*. Supposing that a plane wave arrives from direction θ

the induced signal s_1 on the first element is equal to *s(t)* while on the second element the plane wave arrives after a time delay τ, proportional to the distance between the antennas and to the direction of the source θ. The signal on the second element results to be:

$$s_2 = s(t - \tau) \tag{7.1}$$

where:

$$\tau = \frac{d}{c} cos(\theta) \tag{7.2}$$

Therefore, signals s_1 and s_2 result at different phase unless the plane wave arrives orthogonally respect to the array, this happen only when $\theta = 90° + k\pi$, $k = [0,1,2,..N]$.
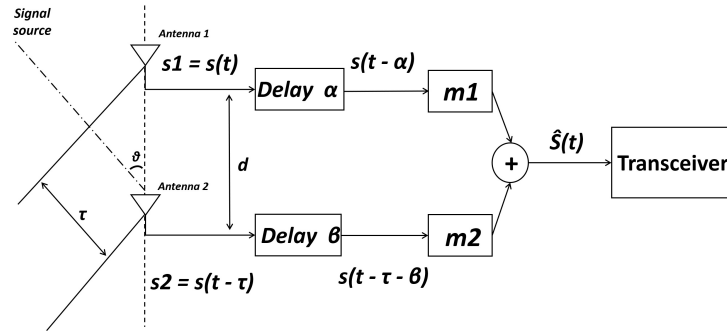
Fig. 7.1 Phased Array - Working Principle.

To measure the plane wave reception delay between antenna*1* and antenna*2* delay elements α and β are introduced. The goal is to null the phase difference between signals by introducing a further phase shift, thus allows to put the array in the condition as if looking orthogonally the plane wave. Then, by measuring the phase shifting introduced is possible to estimate the direction of arrival (DOA) of the plane wave. Moreover, we introduce elements m_1 and m_2 to give a specific "weight" of each channel, thus provide more flexibility to the estimator algorithm and reduce noise.

The output signal is the sum of signals received on each array channel modified by the signal conditioning block chains. $\tilde{S}(t - \tau)$ results maximized when $s(t - \alpha)$ is in phase with $s(t - \tau - \beta)$, therefore, the output is proportional to the angle of incidence

θ of the plane wave. By identifying values of α, β, m_1 and m_2 that maximize the output is possible to estimate θ.

Supposing to set $m_1 = m_2$, the phase shifting of α and β can be programmed to steer the array in a particular direction, known as the look direction. This process is similar to steering the array mechanically except that is done electronically.

Referring to figure 7.1, by setting $\alpha = \tau + k\pi$, and $\beta = k\pi$, $k = [0,1,2,..N]$, then s(t – α) results in phase with s(t – τ – β), therefore the output is maximized.

7.3   Control Strategy and Simulations

Figure 7.2 shows a schematic of the phased array configuration selected *PA1* placed on the deployable structure designed for CubeSat 1U. Every array is used in pair of two element depending on the inter-element separation, couples are 2-3 / 7-6, are used to estimate an approximate direction of arrival of signal (θ) while antenna couple separated by a distance of 0.6 m (1-4 / 5-8) are used to give more sensitivity to the estimation.
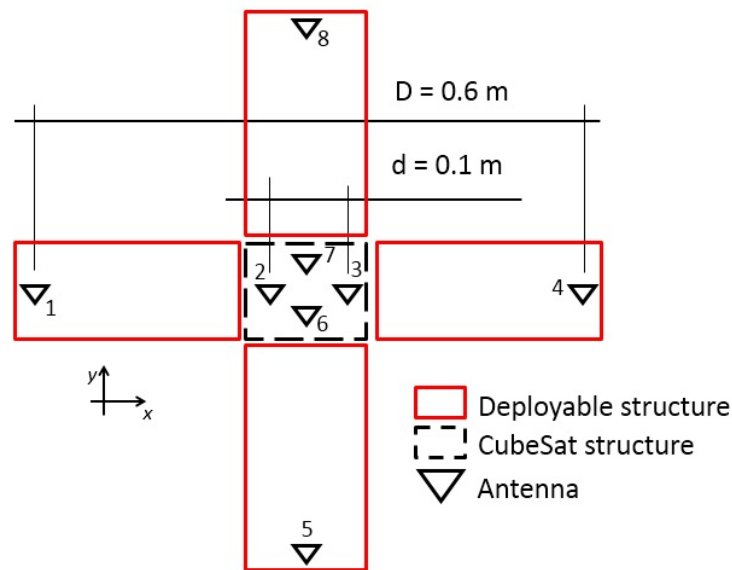

Fig. 7.2 Phased array configuration 1 on deployable structure.

We refer to array 1-2-3-4 in further considerations. By imposing $m_1 = m_2 = 1$ and $\alpha = \beta = 0$ and simulate the behavior of the system by varying θ from 0° to 180° deg. (refer to figure 7.1).

When element couple 2-3 separated by $d = 0.1$ are active, $\tilde{S}(t - \tau)$ result maximized only when the plane wave arrives orthogonally on the array ($\theta = 0°$ deg.). We obtain a wide operating rage, 0° to 180° degree, however the amplitude measure results strongly affected in case of noise on transmission, therefore DOA estimation can be inaccurate.

To respect limits imposed by components we assume to work at 900 MHz / 1GHz , wavelength results $\lambda = 0.33$ to 0.315 m: by comparing λ with the inter-element spacing of couple 1-4 ($d = 0.6$ m) multiple phase cancellations occur, as a consequence multiple maximization point of $\tilde{S}(t - \tau)$ are reported while varying θ from 0° to 180° deg. These multiple peaks represents the secondary lobes created by this phased array couple (1-4) and affects the direction of arrival estimation process. By performing phase measurements with wider inter-element spacing we earn greater accuracy on amplitude variation of $\tilde{S}(t - \tau)$ but results impossible to establish θ because we are unable to establish which lobe is receiving.

Figure 7.3 show the 2D simulation, signals $\tilde{S}(t)$ when couples 1-4 and 2-3 are reported on same graph, multiple peak (secondary lobes) are registered when d=0.6 m due to phase cancellation. Single maximization point when inter-element spacing $d = 0.1$ m is involved.
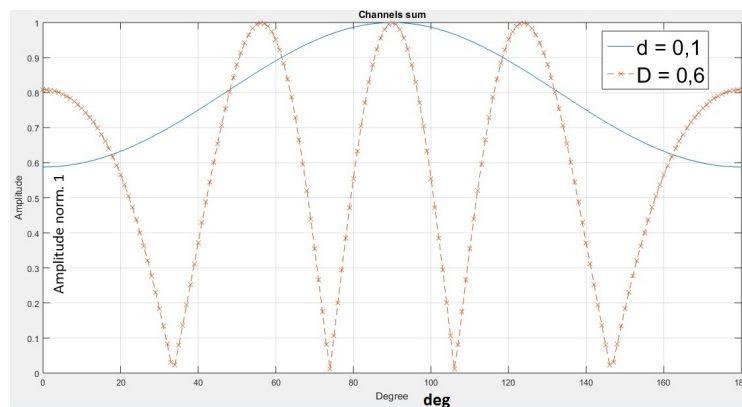

Fig. 7.3 Beam shape of Couple 1-4(left) vs. Couple 2-3(right)

Thanks to the combined action of phased array couples 1-4 and 2-3 then to couples 5-8 and 6-7, the phased array *PA1* will be able to estimate with accuracy the DOA (θ) of the received signal with respect to its observation plane.

7.3.1   On-Board Hardware Calibration

A calibration system represent a fundamental factor for the correct functioning of the phased arrays. Several factors such as, the imperfections in the structure deployment, vibrations during the launch that causes mechanical distortions, modifications in the electrical length of cables due to temperature differences, aging, etc.. causes mal-function on the pointing system. An on-board calibration method must be foreseen in order to guarantee the correct functionality of the system. Several calibration methods have been developed, we propose the REV method [60]. In On-Board REV, the electric field of mutual coupling of antennas is measured and compared with values obtained from factory tests to adjust phase mismatching (figure 7.4). We leave the calibration process, comprehensive of the software development and measurements on the developed hardware as future works.
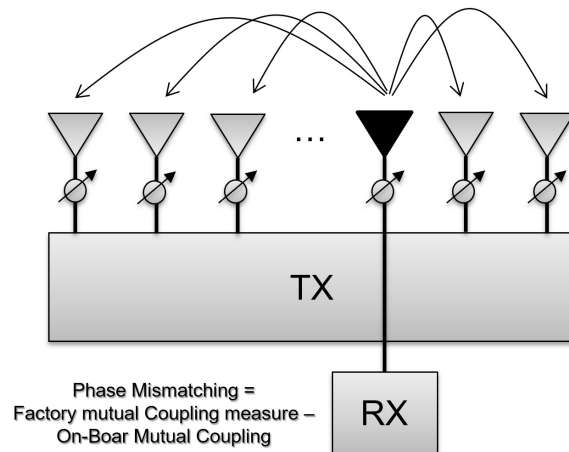
Fig. 7.4 Phased Array Antenna On-Board Calibration REV Method.

7.4   Simulations Results

Our Direction-of-Arrival (DOA) estimation algorithm has been developed and simulated considering specific simulation conditions. The most realistic configuration to establish an inter satellite communication is between one of the proposed phased array configuration and a patch antenna. To be in line with all the measurement and considerations made and with next analysis, we consider a phased array configuration

with $\sim$10 dB gain receiving a signal from a patch antenna with 2dB gain, the transmission power is fixed at 512mW. Figure 7.5 reports the link budget information calculated in section 4.3.

SpaceLink - Phased Array -to- Patch
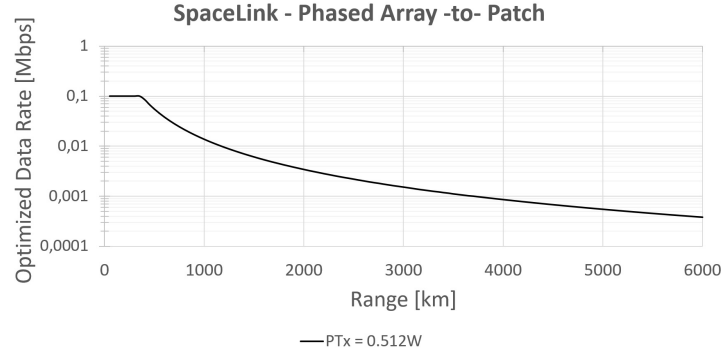
Fig. 7.5 Phased Array / Patch Space-link Data rate. Transmission Power 512mW.

As described before, the *Omptimized Data Rate [Mbps]* refers to the LDPC coding scheme that optimized the data rate performances, therefore we are assuming to transmit at the highest possible speed considering EIRP and distances.
The DOA algorithm developed requires $\sim$60 steps to perform a complete sweep over 180° and estimate the direction of arrival of the received signal: supposing that each satellite is equipped with our transmission system equipped with the *CC430F6137* we have the possibility to set the bandwidth *B* of the receiver filter between 906 Hz and 81,25 kHz.
Considering the packet transmission time and the DOA algorithm required steps we decide to fix the channel bandwidth *B* at 6kHz and 60kHz in order to obtain a sweep timing of the phased array of 1 ms and 10 ms respectively.

In table 7.1 we report the simulation distances considered with the consequent optimal LDPC code that must be used in order to obtain an estimation the $\frac{S}{N}$ levels on the receivers.

As shown in table 7.1, LDPC $\frac{1}{2}$ is the coding scheme that optimize the ISL for the selected configuration, the $\frac{Eb}{N0}$ considered for simulations is 1,89 dB for a BER of 10^{-6}.
Simulations were performed for each $\frac{S}{N}$ level calculated, results are shown in figures 7.7 (a-j). A plane wave has been sent to the 4-elements phased array with the angle of incidence θ from 0° to 180° to simulate each possible direction of arrival of the

Table 7.1 DOA Simulation Settings.

Range [km]	DR [kbps]	Cod. Scheme	$\frac{Eb}{N0}$[dB]	$\frac{S}{N}$|B 6kHz[dB]	$\frac{S}{N}$|B 60kHz[dB]
500	54,76	LDPC $\frac{1}{2}$	1,89	14,1	1,41
1000	13,69	LDPC $\frac{1}{2}$	1,89	3,525	0,35
1500	6,08	LDPC $\frac{1}{2}$	1,89	1,565	0,156
2000	3,42	LDPC $\frac{1}{2}$	1,89	0,88	0,088
2500	2,19	LDPC $\frac{1}{2}$	1,89	0,56	0,056

signal.

Without noise, DOA estimation error result 0,5 x 10^{-3} on average as shown in figure 7.6: this error is directly related to the DOA estimation algorithm sensitivity of 1 x 10^{-3} degree. As shown in all simulation results, in bands 0-40° and 140-180° there is an estimation error increase; this is related to the limited phase shifting capabilities of phase shifters of 0-180°. Therefore, when signal arrives from a very narrow angle, phased array performances decreases, limiting the effective field of view of the system. We can assume a reliable estimation range for signals coming from 40° to 140°.
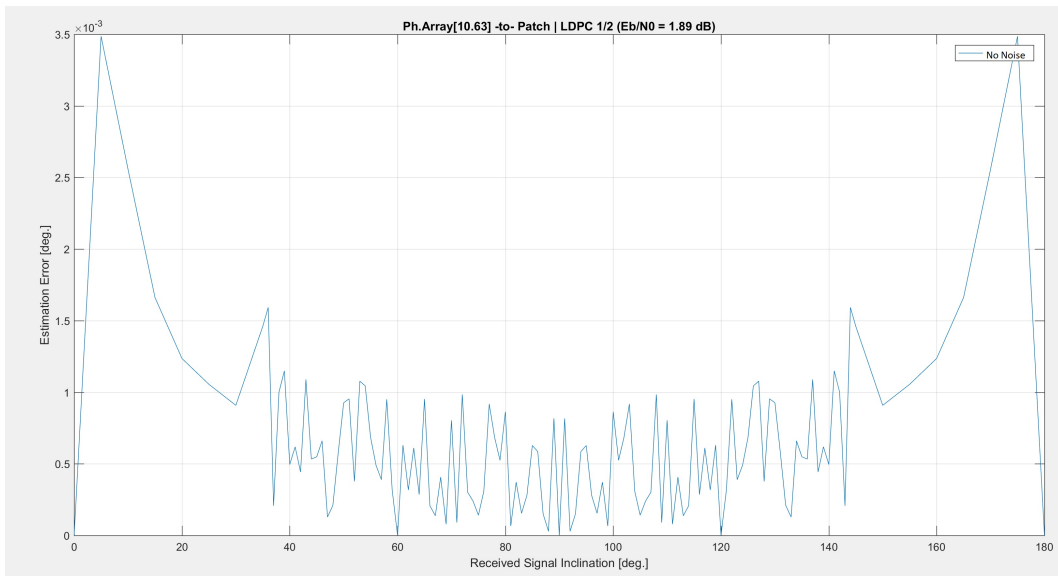

Fig. 7.6 DOA estimation error without Noise.

Fig. 7.7 DOA Estimation Errors vs. S/N levels.
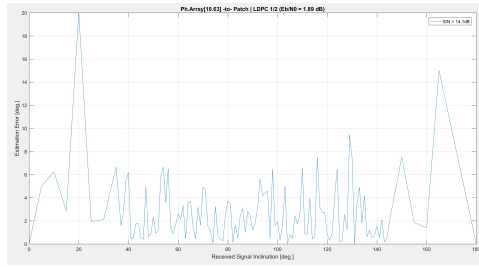
(a) S/N = 14.1 dB.
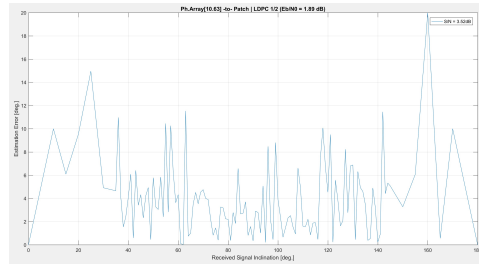
(b) S/N = 3.52 dB.
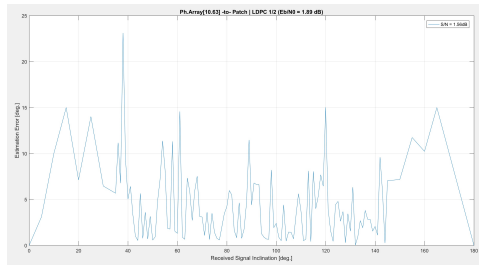
(c) S/N = 1.56 dB.
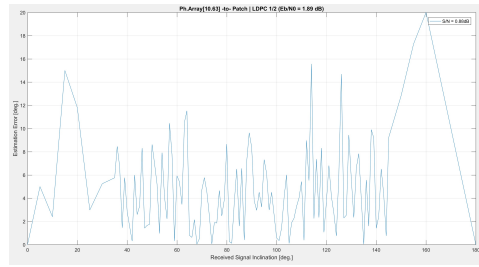
(d) S/N = 0.88 dB.
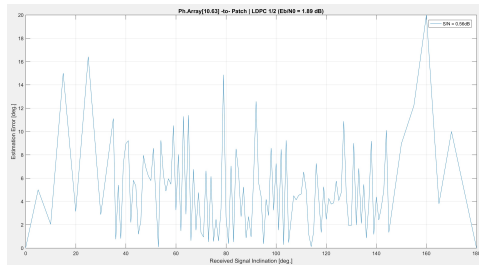
(e) S/N = 0.56 dB.
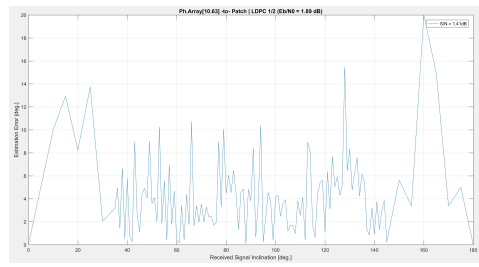
(f) S/N = 1.41 dB.
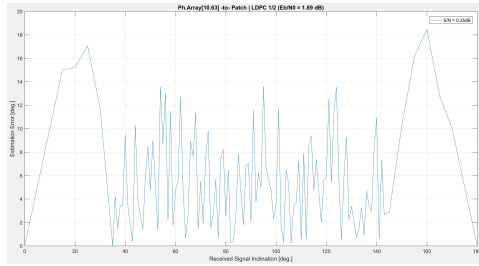
(g) S/N = 0.35 dB.
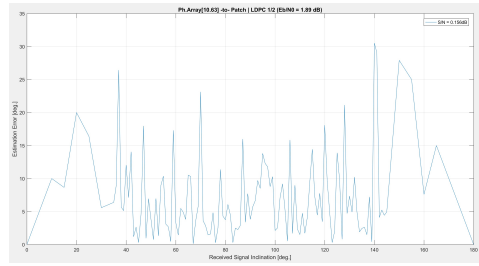
(h) S/N = 0.156 dB.
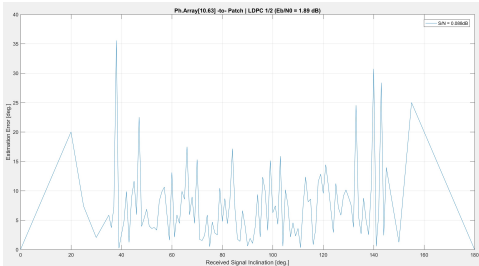
(i) S/N = 0.088 dB.
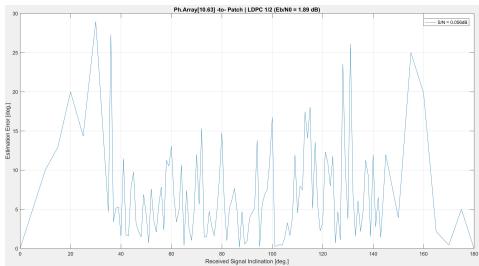
(j) S/N = 0.056 dB.
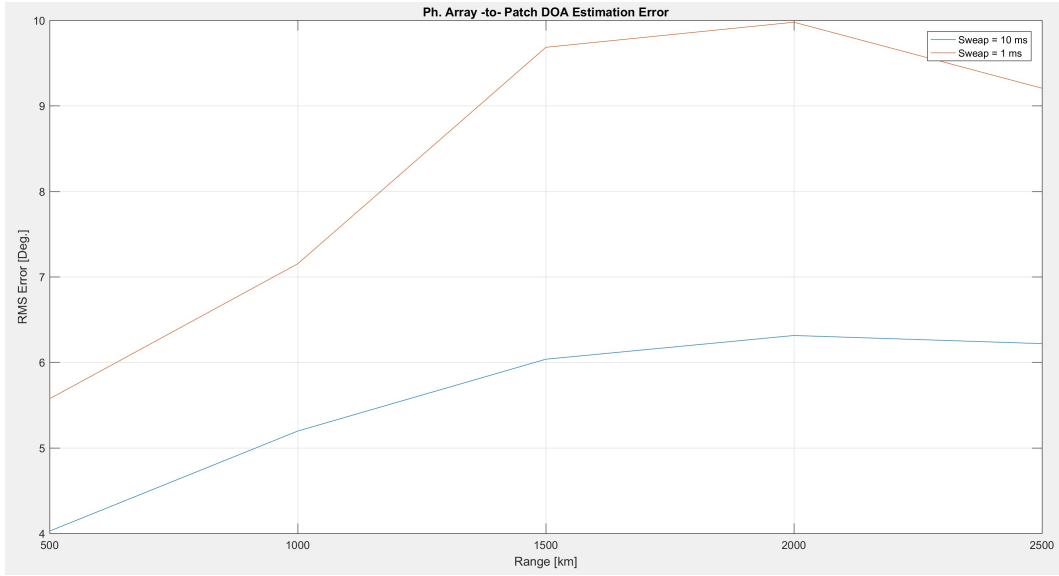
Fig. 7.8 DOA RMS Error vs. Range [km]

As shown in previous graphs, $\frac{S}{N}$ values vary depending on the distance between satellites and on the selected channel bandwidth B, therefore on the DOA estimation required time. Figure 7.8 shows the RMS error as a function of the distance between satellites and sweep time of the phased array. We assume that the acquisition time of the signal is less than a sweep step.

Considering the phased array configurations *PA3* and *PA4* we refer the to table 3.6 to define the relationship between the maximum antenna gain guaranteed at a specific lobe aperture (a summary is shown in 7.2). By using *PA3* and setting B at 6 kHz the DOA estimation average error vary from 4° to ∼6° depending on range, therefore the DOA estimation algorithm results still efficient considering the communication settings. Considering the aperture of 12° of the phased array *PA4*, we conclude that B can be 60 kHz because the maximum DOA estimation error is ∼10°. However, the error evaluation refers to RMS values therefore, in this case, the communication functionalities can be considered on the edge point.

Table 7.2 Phased Array: Gain vs. Lobe Aperture.

P.Arra Config.	Min.Gain Guaranteed [dB]	Max. Lobe aperture [deg.]
PA3	10	6°
PA4	10	12°

7.4.1   Antenna Misalignments

When unfolded, panels of the deployable structures are joined together thanks a system of hinges. Ideally the structure results straight, perpendicular to the CubeSat side on which is mounted. However, the hinge system cannot guarantee a perfect aperture of the structure, each of them can introduce a few degree error compared to a perfect horizontal deployment.
Considering a deployable structure for a 1U CubeSat composed by three tiles and the developed phased array *PA1*, we performed a sensitivity analysis to understand how the antenna misalignments due to the hinges error affect the DOA estimation process.
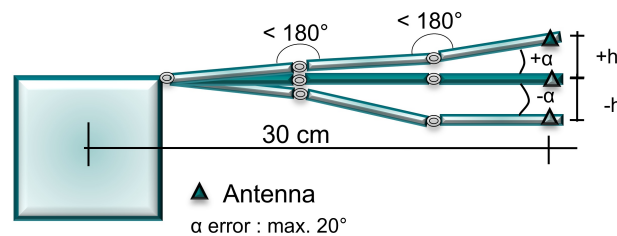
Fig. 7.9 Antenna misalignment error

Referring to figure 7.9, we suppose the worst case in which the superimposition of inclination errors of each hinge involves a total of +/- 10° of wrong inclination. The wrong inclination is more reflected on the position on the outer antennas placed at the edge of the 30 cm deployable structure, therefore the antenna is shifted of +/- $1 sim 10$ cm higher or lower if compared to the ideal structure plane's. This physical shifting can be considered as an offset on the phase shifter of the channel of the antenna.

Simulations considers 1 ms sweep time to mitigate the errors due to channel bandwidth B. Figure 7.10a shows the sensitivity of DOA estimation (without noise) of a received signal for a misalignment α= -/+ 10° degree.

Without noise, DOA estimation error increase from 0.01° deg. (DOA algorithm error) to $\sim$ +/- 1° degree when the received signals comes from an inclination between 60° and 120° and grows outside this range because the phase offset limits the operative range of the phase shifter of the antenna channel, therefore its functional operating range results reduced.

Figure 7.10b shows the impact of antenna misalignment on DOA estimation in function of distance between satellites.

Fig. 7.10 DOA Estimation Errors vs. misalignments
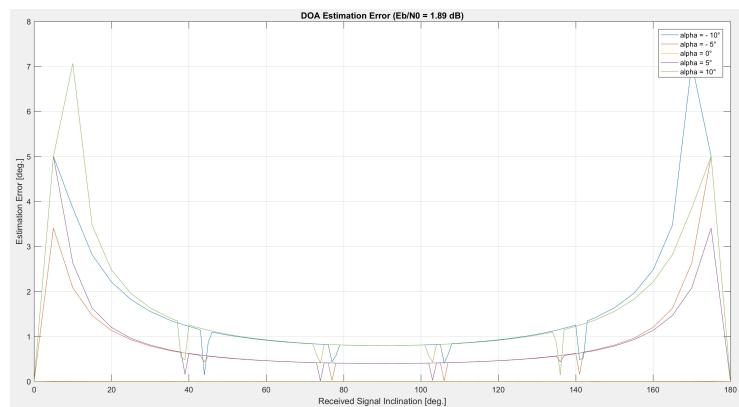
(a) Antenna misalignment: DOA estimation without noise
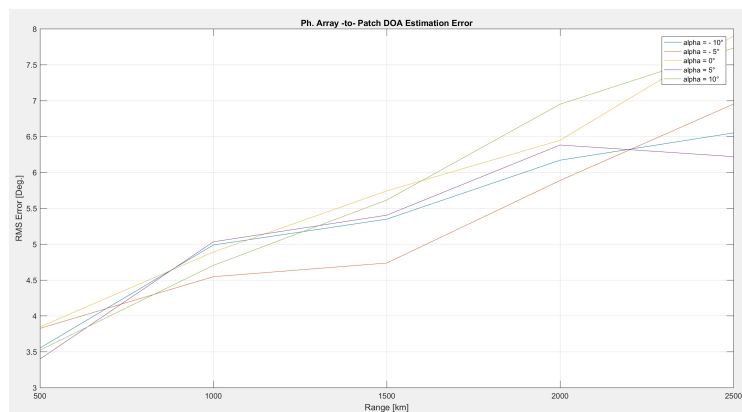
(b) Antenna misalignment: DOA estimation vs. Range[km].

Chapter 8

The Proposed Clustering Algorithm

8.1 Introduction

Algorithms introduced in previous sections represent only a part of all the algorithms developed to address MANETs management problems. However, PC, 3hBAC, MO-BIC and On-Demand WCA provide a good overview of different techniques adopted to manage networks of mobile nodes. The strategies presented focus respectively on concepts of simplicity for cluster management, on the reduction of interactions in cluster maintenance phase and on the cluster management based on mobility or a combination of many factors.

Other algorithms have not been presented as they have conceptual features very similar to algorithms described or present characteristics that make them unsuitable for our scenarios or some of their stage has not been clearly addressed.

Essentially, a unique algorithm able to manage a MANET in every situation, with every node mobility behavior, hardware and condition does not exists and is not possible to develop, each algorithm introduced presents strengths and weakness and work better under certain conditions.

As described before, our clustering algorithm for CubeSat Constellations will exploit some concepts previously introduced with some modifications: next section describes our algorithm. We comment critical stages to understand how previously exposed concepts has been integrated and which modification has been introduced to avoid their weaknesses.

In our clustering algorithm, nodes can assume six different states, figure 8.1 shows their name and the shapes used during the algorithm testing phase.
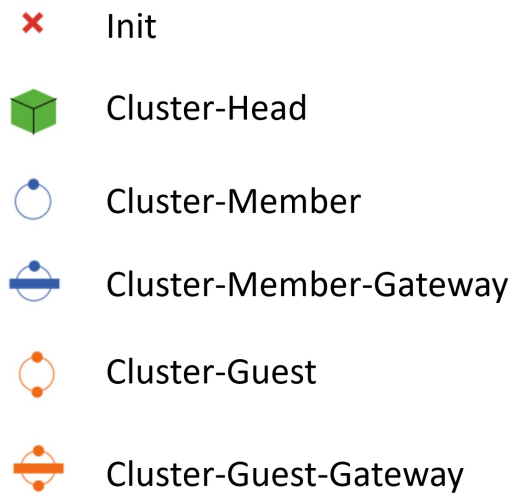
Fig. 8.1 Satellites Status Types.

8.2 Proposed Clustering Algorithm

Figure 8.2 presents the state diagram of the proposed clustering algorithm. Cluster formation (light blue) and cluster maintenance (light yellow) represent the two basic steps to create clusters of mobile nodes, common for every clustering algorithm. Next sections describe more in details the proposed algorithm and each single stage. We provide descriptions and comments of the operations that must be performed to reach clusters formation.
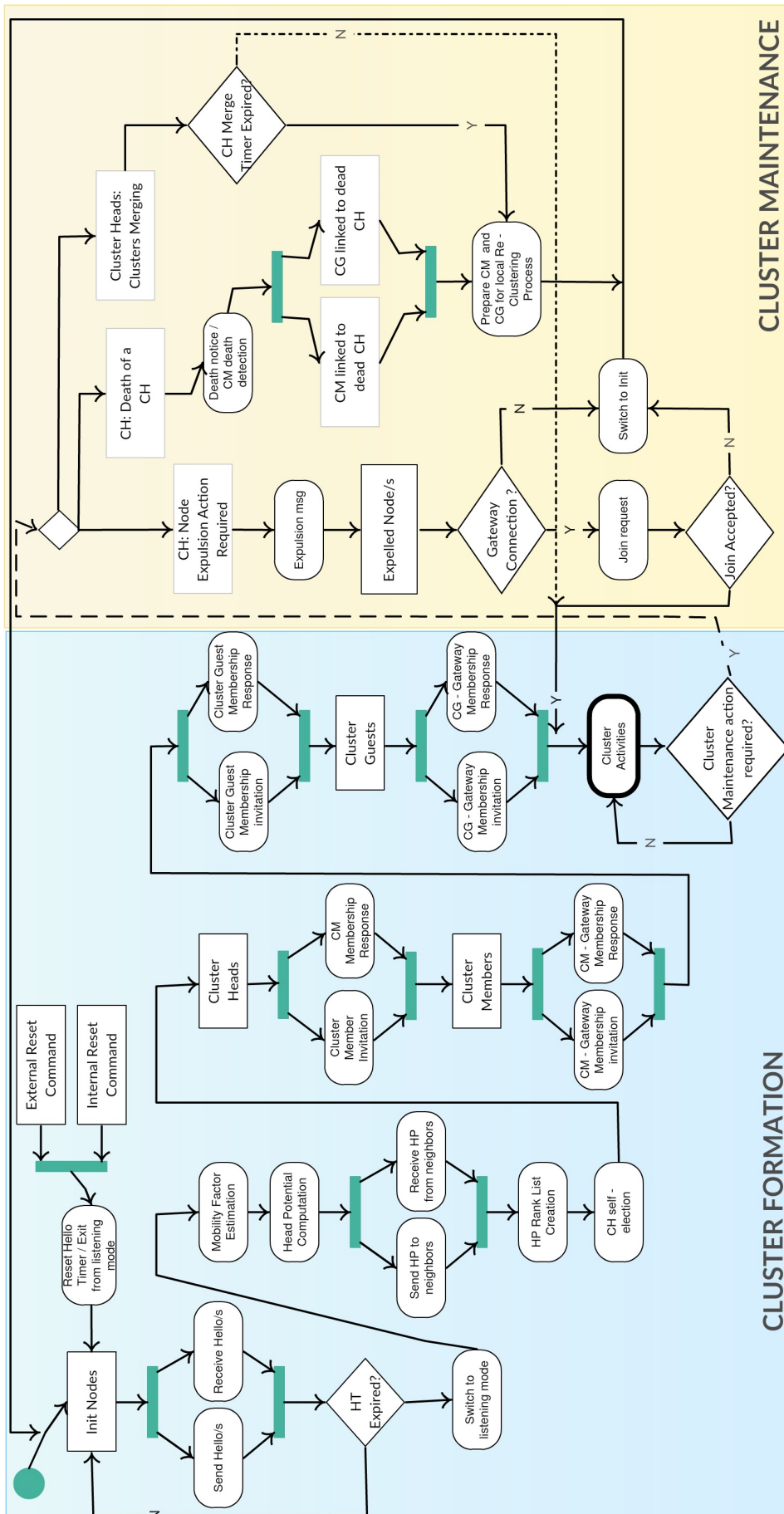
Fig. 8.2 Proposed Clustering Algorithm: State diagram.

8.2.1   Stage 1 - Neighborhood Exploration

Initially nodes are at *Init* (I) state and send/receive *Hello* messages to/from their neighbors. During the initial cluster formation phase *Hello* messages are exploited by nodes to know how many and which nodes are included in their neighborhood. The distance for which nodes consider each other as neighbors depends from the communication link and the mission preliminary analysis. We define this dimension as *Maximum Neighbors Distance (MND)*, that is the maximum distance for which other nodes can establish a communication link that guarantee a predefined performance level.

The neighborhood exploration phase can be performed during a limited time period defined by the *Hello Timer* (HT). When HT expires, *Init* node stops sending *Hello*s and put them self in listening mode.

HT is reset when one of three condition is verified:

- A *Hello* message is detected

- Cyclic Hello message phase

- An external HT reset command is sent to node

Cross-talk problems must be addressed during the design phase of the mission.

Comments

The hello message neighborhood exploration phase represents a similar behavior of the cluster formation Passive Clustering algorithm. Every node can independently participate to the cluster formation process by broadcasting *Hello* messages. With the introduction of the Hello Timer our algorithm become more efficient in terms of energy consumption. In PC network topology can affect the energy consumption in case of low density network due to the fact that hello messages are sent in any case.

8.2.2 Stage 2 - Mobility Factor Computation

Every node calculates its own Mobility Factor (MF). MF can be expressed as the number of neighbor nodes that will stay inside its Maximum Neighbors Distance (MND) for a defined time interval t.

Comments

To calculate MF each node must be aware or estimate the mutual physical position and relative speed of its neighbors, the *Hello* messages exchange phase can be exploited to obtain these informations.
A similar concept of MF can be found in *On-Demand WCA* algorithm where distance between neighbors and average moving speed represent two fundamental factors to elect a local node as leader.
In our algorithm, these two factors provide information on the cluster evolution: MF is the minimum node contact time needed to perform the local cluster formation.

8.2.3 Stage 3 - The Cluster-Head Potential

The Head Potential is used to indicate the node ability to become a cluster-head. It is calculated considering these factors:

- ID

- Mobility Factor (MF):

- Cluster Head Serving Time (CHST)

$$HP = c_1 MF + c_2 CHST + ID \tag{8.1}$$

where:

$$c_1 + c_2 = 1 \tag{8.2}$$

CHST represents the ability of nodes to behave as Cluster-Head. It consider the maximum number of node that a CH is able to manage and the total time that a node can serve as CH depending of the available on-board hardware and mission requirements. It's possible to include other factors related to the characteristics of nodes or mission design. For satellites: the charge / discharge cycles of the battery, sun exposition timing, orbit drift, orbit differences, etc.

8.2.4   Stage 4 - Cluster Head Claim

Every node broadcast its HP with the neighborhood and create a local HP ranking list based on values received.
Node on top on its HP ranking list declare itself as Cluster-Head (CH) and sends a cluster-head claim to nodes with the potential to become Cluster-Member. In case of conflict, node with lowest ID becomes the CH.

8.2.5   Stage 5 - CM Membership Response

Nodes which received the CH-claim choose to become Cluster-Member or not consider the claim. It's possible to join as effective CM to only one CH.

8.2.6   Stage 6 - CM Gateway Membership

Elected Cluster-Members send CM-Gateway Claim to nodes that think can become CM-G. If the claim is reciprocal, CM set itself as gateway of that specific CM for which he sent and received a claim. The possible links combination are shown in figure 8.3
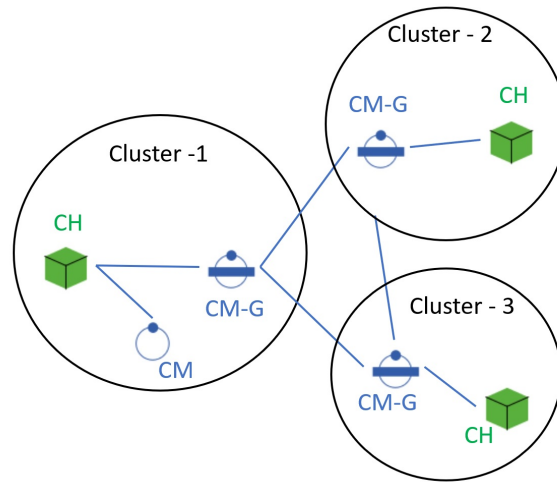
Fig. 8.3 Cluster-Members Link type.

8.2.7 Stage 7 - Cluster-Guests Membership

Elected CMs send a Cluster-Guest invitation to nodes remained in their HP list (probably *Init* state) inside the MND. This stage follows same rules of Stage 4 and 5. Nodes who received the CG invitation can choose to join to the CM as CG, CG-gateway (in case of multiple invitation) or can refuse the invitation. Figure 8.4 shows al the possible link combination that CG can assume.
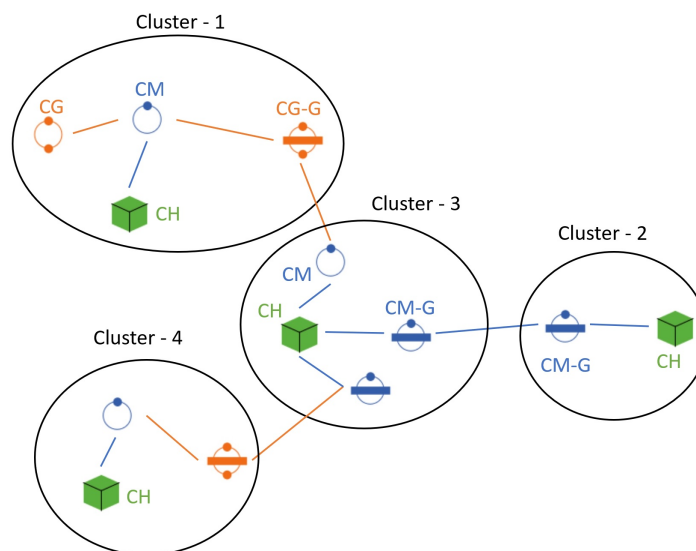
Fig. 8.4 Cluster-Guest Link type.

8.2.8   Stage 8 - Guest-Guest-Gateway (Optional)

Like CM-G, Cluster-Guest can establish links each other to make the cluster network as branched as possible. The CG-G connection follows same rules of stage 6, applied to CG.

Comments

The concept of CG-G is to provide a capillary data distribution among the cluster, however the communication between Cluster-Guests can results instable in case of significant relative mobility differences.

8.2.9   Stage 9 - Cluster Maintenance: Node Expulsion

Due to CH serving time restrictions CHs are allowed to expel nodes from local cluster to respect quantity limits on element that CH can manage.
In this case the CH will warn the interested node and interrupt the communication. The excluded node tries to join to its gateway connection,if exist. Through a join request it try to maintain or improve its status (from CG to CM) inside the new cluster, otherwise it declares itself at *Init* state and switch to listening mode.

8.2.10   Stage 10 - Cluster Maintenance: Node Inclusion / Clusters Merging

If a CH "dies", only a CM linked to the "died" CH can assume the role of new CH: therefore, the re-clustering activity is controlled/limited to local clusters.
If the new elected CH had gateway connections they are considered still valid/active. Despite it does not represent the optimal solution in terms of cluster network structure the re-clustering interactions required to stabilize the network are limited. Node previously CGs of the new CH does not become automatically CMs: they switch back at *Init* state.
If a CH gets in contact with another CH the CH-Merge-Timer prevents re-clustering effect for a certain period. This timer is inspired by the *CCI* timer of MOBIC algorithm. The CH-Merge-Timer can be fix or dynamic, related to the mobility factor

(MF). There is no need for synchronization between merge-timers, both timers must be expired to start the re-clustering process.

CMs and CGs stops to be connected to a CH when they are outside from their mutual MND: periodical update must be performed to be aware of mobility evolution of nodes.

Chapter 9

The Proposed Clustering Algorithm: Implementation, Simulations and Performances

9.1 Introduction

The algorithm has been developed with some simplifications, different setting conditions has been introduced to analyze the algorithm behavior under specific conditions. Simulations has been performed using Netlogo simulator [61].
Hello Timers has been disabled, nodes never switch to listening mode, they constantly send/receive *Hello* messages while at *Init* state to explore their neighborhood. This choice has been made to simplify the transmission synchronization process required when nodes switch from listening mode to neighborhood exploring phase.

To develop the algorithm that fit for CubeSat constellations we must consider practical issues related to the communication protocol, available hardware, scenario conditions, constellation's element setting, constellation mission, etc.
The first step to define in which condition our algorithm can be applied is to estimate the execution time required to form clusters as a function of the available hardware and orbital satellite configurations.

9.2 Communication Protocol

In order to estimate / measure the execution time we must address problems related to the communication protocol: we suppose that satellite are not aware about the status of their neighborhood, they start to communicate through *Hello* messages to explore it at stage *1* of our algorithm; moreover, most of next stages include broadcast information exchange. As a consequence, cross-talk problems occur because satellites transmission strategy does not behave according to a common communication timer that synchronize transmission priorities.

To avoid cross-talk problems we define a *communication window* within which all satellite of constellation can communicate. This window is divided in time *slot*: the duration of a slot is defined as the time required to send a *packet* along a certain distance. During each stage of the clustering algorithm each satellite that need to transmit choose randomly a slot to transmit a its packet, then remain in listening mode until a new *communication window* start. This technique do not totally eliminates cross-talk problems because one or more satellite can choose the same slot to transmit. However, the probability to cross-talk on the same slot can be studied, analyzed and addressed thanks to the repetition of broadcast communications in a new communication window. We decided to add one slot for each satellite that compiles the constellation.

To make this technique work we must synchronize transmitter during the primordial stage of the constellation, when satellites are released in orbit. Then, a synchronization adjustment action between transmitter is carried out during the constellation formation phases. Therefore, the transmitter synchronization is used to define a common start time of *communication window*. Figure 9.1 shows an example of the *communication window*, its slots and the random selection of satellites.

COMMUNICATION WINDOW						
Slot 1	Slot 2	Slot 3	Slot 4	Slot 5	...	Slot N
Satellite 2	Satellite 5	Satellite N-1 Satellite N-6	Satellite N-4		...	Satellite 7
		Crosstalk !		Empty!		

Fig. 9.1 Communication window and slot random selection.

9.2.1 Packet Dimension

Basic information about satellites orbit, address and status (CH/CM/CG) are the information that must be passed between satellites to create clusters: the packet is used to by our algorithm to create clusters and maintain them. Particular attention must be given to the *Additional Info.* slot: it is used by satellites to communicate the cluster membership agreement or cluster joint reject messages. Table 9.1 resumes all the information and their dimension enclosed in the *Hello* packet.

Table 9.1 Packet dimension.

Data Type	Dimension	Description
Sync	5 B	Tx and Rx oscillator synchronization
Address	6 B	To be in line with the amateur radio address coding
Node ID	6 B	Call Sign
Node Status	2 B	Indicate the status of Tx Satellite
Additional Info.	5 B	Variable use depending on algorithm stage
Satellite Orbit Info	12 B	Two Line Element Set
Semi Major Axis	(2 B)	
Eccentricity	(2 B)	
Inclination	(2 B)	
RAAN	(2 B)	Right Ascension of the Ascending Node
True Anomaly	(2 B)	
Apogee Longitude	(2 B)	
Attitude	8 B	Attitude of Satellite
EIRP	2B	Equivalent Isotropic Radiated Power
Total	46 B (368 b)	

9.3   Algorithm Implementation and Simulations

9.3.1   Algorithm Implementation Details

The cluster formation time is strictly related to the antennas configurations, to the transmission power and to orbit parameters of cluster. Figure 9.2 shows a general messages exchange phase of a communication window: each satellite randomly select one slot for its broadcast then switch to listen mode to collect information from others. During a communication window each satellites broadcast informations and receive all broadcast information sent from neighbors. In table 9.2 we estimate the number communication windows required by each stage of the algorithm to statistically reduce cross-talk problems and keeping them under defined levels. We decided to add 20% time more to every slot to relax constraints on communication and avoid jamming due to synchronization lags.
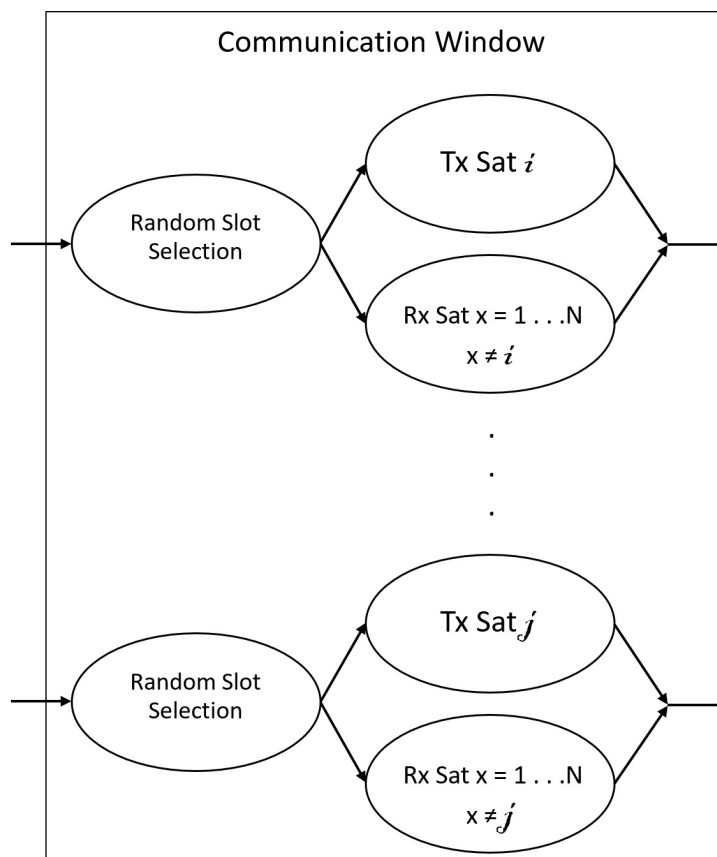
Fig. 9.2 Nodes message exchange in a communication window.

Table 9.2 Cluster formation steps.

Stage	Window Required	Description
#1 and #2	2 Window	Neighborhood exploration during Hello Timer. Collecting orbit info. Mobility Factor calculation.
#3	No Window	Head Potential Estimation
#4.a	1 or 2 windows	Head Potential Broadcast. Head Potential list creation.
#4.b	1 or 2 window*	CH Claim.
#5	1 or 2 window*	CM Claim response.
#6	1 or 2 window*	CM Gateway connection.
#7.a	1 or 2 window*	CM Guest Claim.
#7.b	1 or 2 window*	CG response.
#8	1 or 2 window*	CG Gateway connections.

* window dimensions optimized based on nodes in transmission.

9.3.2 Communication Windows & Cross-Talk Mitigation

The number of communication window necessary to complete each stage of our algorithm depends from the probability that two or more satellites select the same slot during a communication window and is given by:

$$P1_{cross-talk} = \sum_{x=2}^{n} \left[\left(\frac{1}{r}\right)^x \left(\frac{r-1}{r}\right)^{n-x} \left(\frac{n!}{x!(n-x)!}\right) \right] \qquad (9.1)$$

where:

n = number of satellites that must transmit r = number of slots x = probability that slot is selected by 2,3,4.. n at the same time

The probability that the same satellite goes in cross-talk for two consecutive times is:

$$P2_{cross-talk} = \left(\frac{N_{P1}}{n}\right)^2 \qquad (9.2)$$

where:

N_{P1} is the number of node that previously gone in cross-talk (calculated on $P1_{cross-talk}$)

We decided to repeat the transmission, that is, add a communication window to the interested stage, every time that $P2_{cross-talk}$ were $\geq 7\%$.

9.4   Simulations

All simulations were performed considering a fixed configuration as shown in table 10.1. The proposed clustering algorithm has been developed and simulated, in next section we present the performances and results.

Table 9.3 Simulation Configuration.

Description	Value
Tx Antenna	Omni-directional
Rx Antenna	Omni-directional
Tx Power	512[mW]
EIRP	27,09 dBm
Working freq.	2.4 [GHz]
Modulation Scheme	QPSK
Coding Scheme	LDPC 1/2, 4/5, 7/8

9.4.1   Cluster Formation: Timing and Distances

Considering the required communication windows from each algorithm stage we obtain the cluster formation timing. Figure 9.3 shows the cluster formation timing curves for two constellation composed respectively by 10 and 50 satellites. For each constellation we suppose that each satellite have the ability to establish a relative communication link with relative access at 4-10% (Cluster-Head peak) and 80-100% (formation flight). Space-link is performed supposing omni-directional antennas

working at 2.4 GHz and a fixed transmission power of 512mW.

Due to the relationship between between distance, max. data rate and packet flight time (negligible), with the increasing of satellite's MND increase the delivery time of every packet, consequently each communication window require more time to be transmitted. Therefore, when there is a proportional relationship between the selected MND and the algorithm execution time.

When relative access is 4-10% the constellation is divided in sub-clusters, one for each CH (20% of total) therefore the overall cluster formation time is minimized, sub-clusters are formed in in parallel and, exception for Gateway connections, they do not interact each other, as a consequence the required formation time result reduced. When access is 80-100% the constellation is managed as a single cluster coordinated by one CH, all informations about orbit position and CMs join messages will flow from/to it.
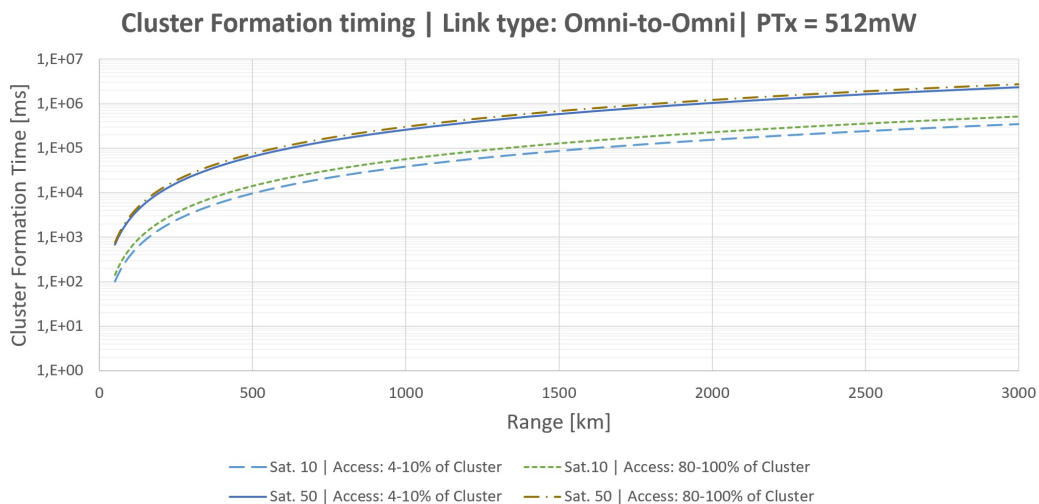
Fig. 9.3 Cluster formation time | Ptx=512mW | omni-to-omni spacelink.

After the cluster formation process we assume that a data volume must flow through the network, otherwise the cluster formation process will occupy all the spendable time for the communication making the process itself useless!
We assume that the clustering algorithm occupy at maximum the 20% of total useful contact time between satellites, therefore we consider an additional time after the

cluster formation which is used to performs data exchange phase, that is:

$$T_{Ctot} = T_{Cf}(20\%) + T_{De}(80\%) \tag{9.3}$$

where:

T_{Ctot} is the total clustering time, T_{Cf} is the required time for cluster formation and T_{De} is the available time for data exchange.

Figure 9.4 and 9.5 show respectively the cluster formation timing curves comprehensive of the additional contact time for data volume transmission with different of antenna configurations introduced for a fixed transmission power of 512mW.
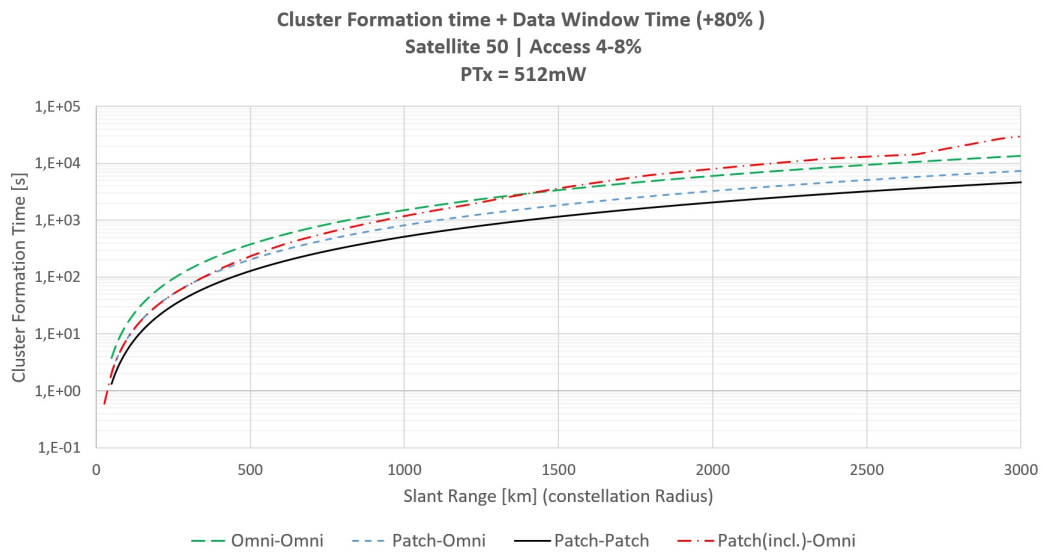
Fig. 9.4 Cluster formation time | Ptx=512mW | omni-to-omni space-link.
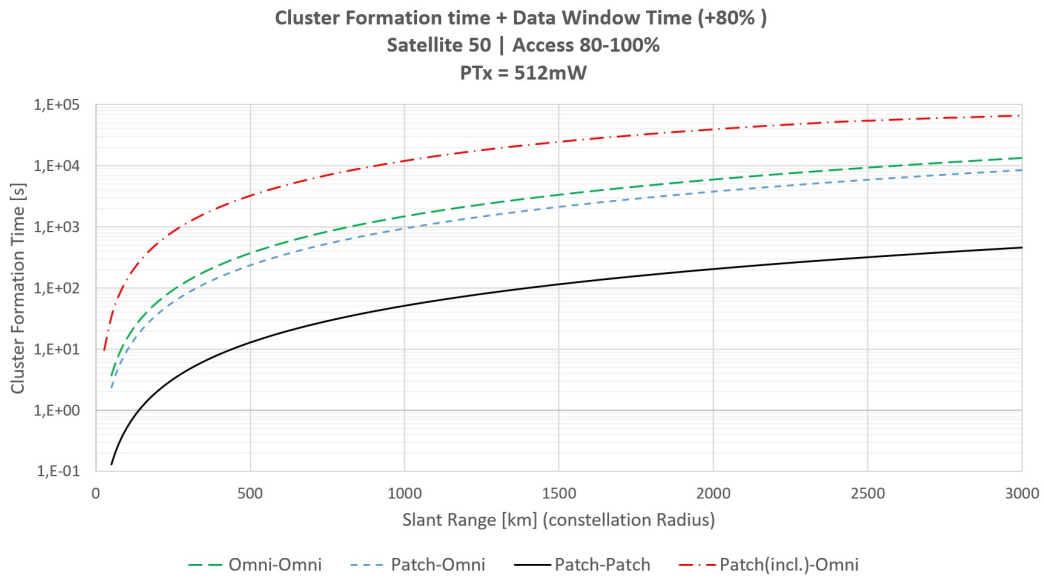
Fig. 9.5 Cluster formation time | Ptx=512mW | omni-to-omni space-link.

9.4.2 Cluster Trend

Graph 9.6 shows the cluster trend for a constellation of fifty nodes.
Considering a random homogeneous distribution of satellites in space, we simulate
our algorithm by varying the access that a single satellite can establish with others to
observe the node state variation assumed with the increasing of the relative access.
When access is 0%, satellites are unable to communicate, e.g. due to high separations
or hardware problems. When access is 100% every satellite can establish a link with
any other element of the constellation.

Cluster Trend: Node Status vs. Number of satellite in view
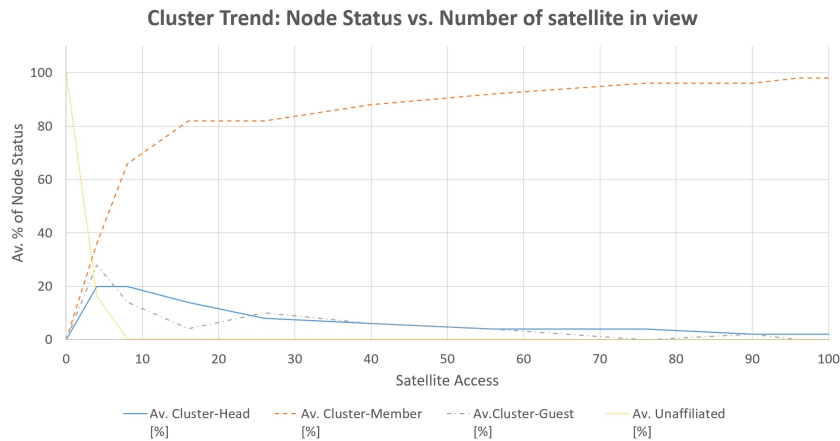
Fig. 9.6 Cluster Trend - Average Status of nodes vs. node visibility.

Initially nodes are at *Init* state, 100% of them result unaffiliated. With the increasing of satellites access, start the formation process: for low access levels, clusters are composed by a reduced number of members while others satellites assumes the role of guests. During this initial phase the constellation can reach its maximum extension, higher distances imply the impossibility of satellites to participate to the cluster formation.

Low access means that the spatial distribution makes impossible to create high number of *CH - CM* connection due to the minimum time required inside the *Maximum Neighbors Distance (MND)* from cluster-heads, therefore satellites join to clusters with as guests. Figure 9.7 show the formation process considering low access levels, small clusters composed by few satellites are created, the constellation result not connected in a concrete network, small scattered clusters are created.
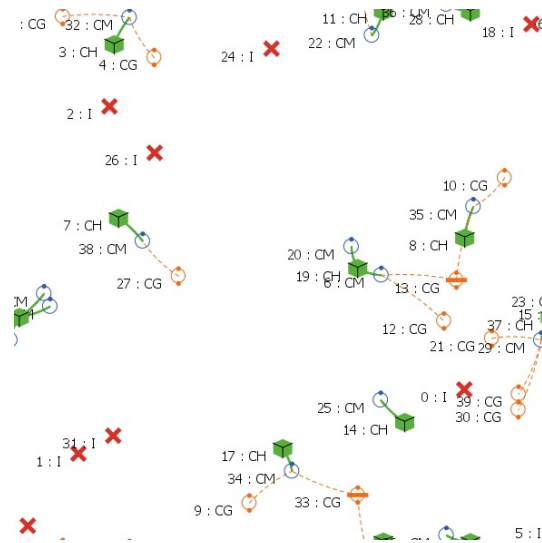
Fig. 9.7 Cluster trend - Satellite access 0-5%.

When relative access reaches levels between 4-10% a cluster-head formation peak is reported, constellation results connected in a network in which most of satellites can communicate each other by assuming role deepening on their orbital conditions and communication link performances. These mutual access levels brings to a CH election peak due to the growing number of satellites resulting in mutual view. Constellation results mostly connected as shown in figure 9.8.
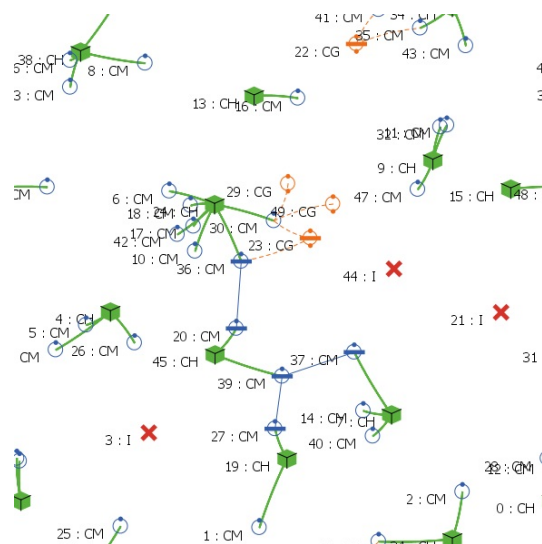
Fig. 9.8 Cluster trend - Satellite access 4-10%.

The access increasing means that satellites are getting closer and closer, the constellation extension results reduced and communication links are more reliable because satellites that in a previous situation can participate as Guest can now become an active member of the local cluster as CM. With the increasing of satellite access the cluster can be described as satellites orbiting in *formation flight*.The cluster assume a star topology where a few (or one) satellite assume the role of CH while others establish strong connection in quality of C-Members (figures 9.9 and 9.10)
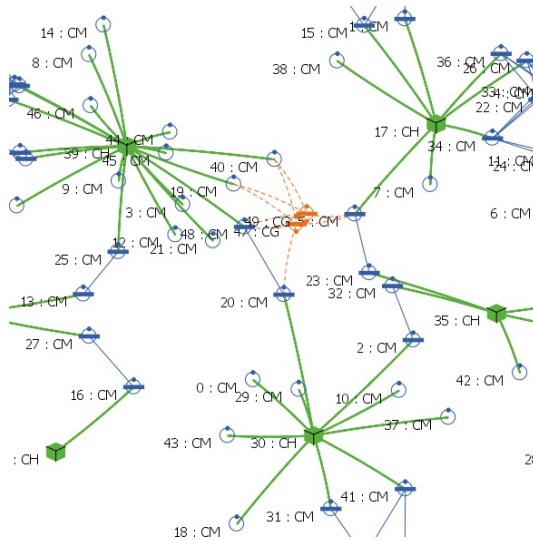
Fig. 9.9 Cluster trend - Satellite access 40-80%.
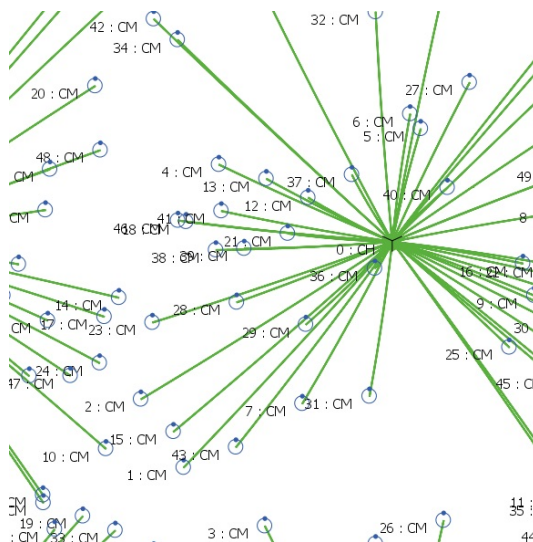
Fig. 9.10 Cluster trend - Satellite access at 100%.

9.5 Constellation Topology Considerations

Considering the algorithm execution time and the +80% additional required contact time, the constellation orbit characteristics plays the fundamental role to define if our clustering algorithm is efficient or not.

A mission analysis must performed to define which communication hardware and power levels are available on each satellite to define which clustering execution range is required. Afterwards, the informations regarding mutual access must be obtained by analyzing the mission orbit characteristics of each satellites.

By combining these information it's possible to define if the algorithm can be applied to the mission.

We calculated the relative access between satellites orbiting on same inclination and direction having different altitudes. Figure 9.11 shows the relationship between clustering algorithm execution time and maximum altitude difference possible between two satellites. Execution times refers to links performed thanks omni-directional antennas working at 2.4 GHz at 512mW.

Supposing that the highest satellites of the constellation is at 2000km altitude and the selected MND is 1000 km.The minimum altitude allowed for satellites that guarantees the required contact time results ~1044km.
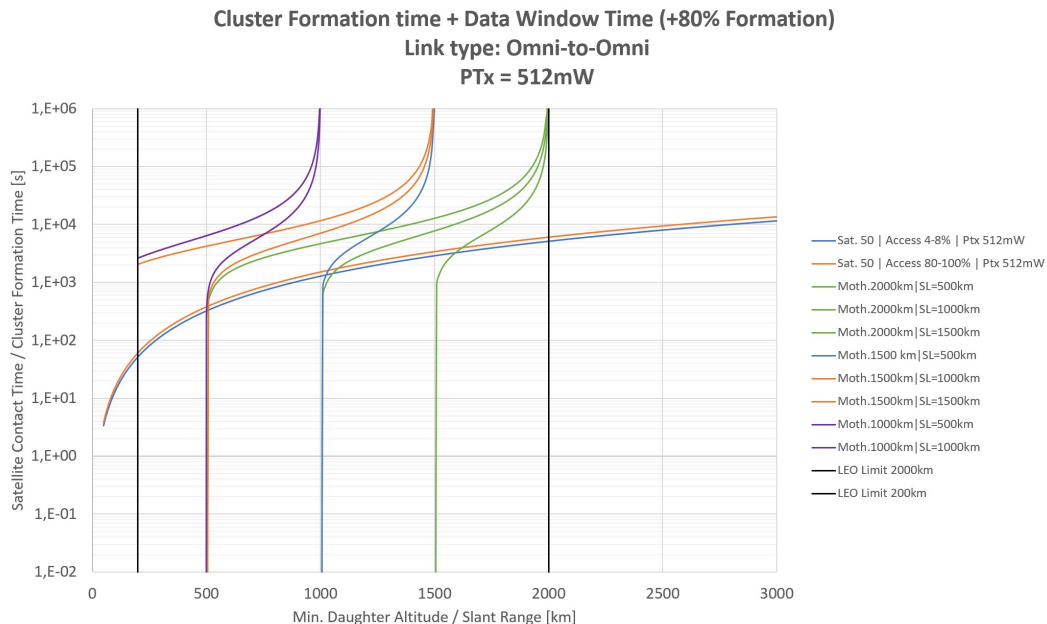
Fig. 9.11 Cluster formation time vs. altitude differences on same orbit plane.

Figures 9.12 and 9.13 show the minimum number of satellites that must form the constellation to keep a communication link in function of MND supposing an homogeneous distribution of satellites respectively over the same orbit plane and same altitude with all possible inclination values. This distribution represent statistical satellite position where satellites are placed in orbit without a releasing strategy nor a preliminary constellation strategy. These specific cases not represent the ideal working condition of our algorithm as the required communication ranges are too high if compared with the communication hardware commonly available on CubeSats.
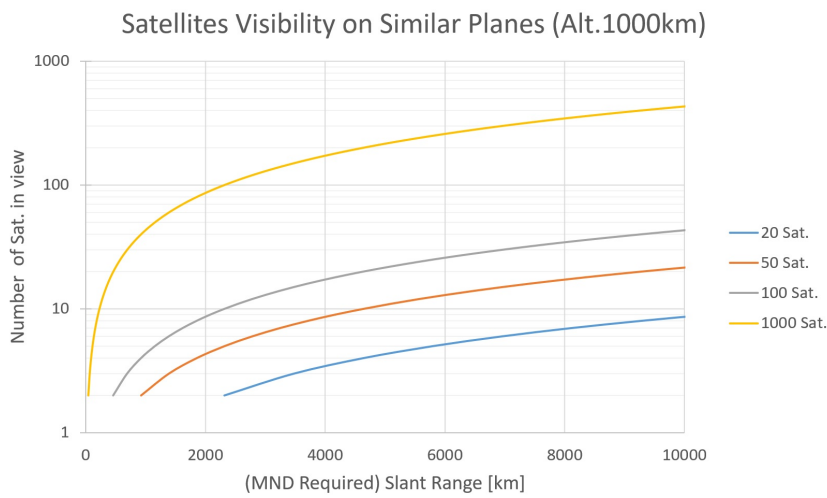
Fig. 9.12 Required Satellites vs MND.
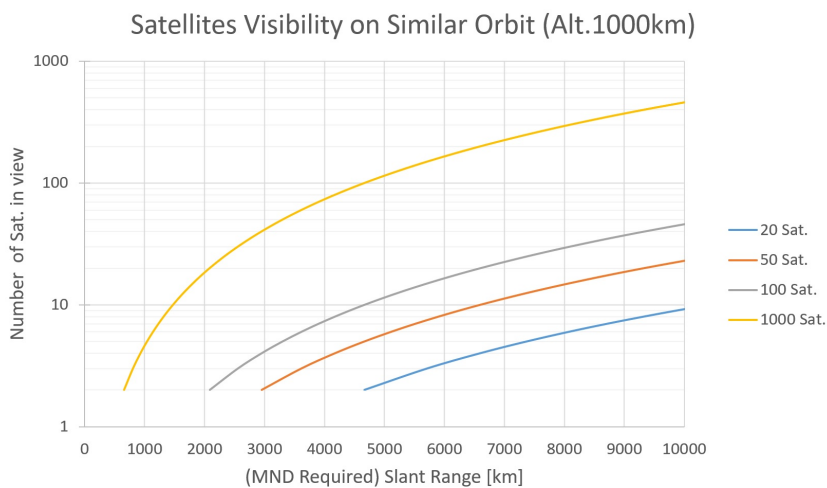
Fig. 9.13 Required Satellites vs MND.

Chapter 10

Data Volume Improvements

In this chapter we present the proposed antenna configuration on CubeSats. The goal is to build up a space-to-space and space-to-ground antenna configuration able to to sensibly increase and optimize the total data volume from the constellations topologies previously presented.

10.1 Ground-link / Space-link data rate - Ratio considerations

In previous chapters we have introduced different antenna types and we performed link budget analysis for several antenna combinations: in general, the ground-link results more performing than every space-link analyzed because of the higher gain provided by the antenna on ground station. Therefore, in most of the cases is not convenient to establish any space-link among CubeSat to download data toward ground station when access (CubeSat-GS) is guaranteed. Ground-links analyzed offer channel capacity able to support bigger throughput than every space-links presented, hence, result unnecessary to perform space-link communication when CubeSats are in view with the ground station, even if access time CubeSat-to-GS is short. Significant data volume that can be directly downloaded (or uploaded) results sensibly bigger than a combined data movement action among CubeSat provided by space-links. In general, data must be downloaded/uploaded directly toward the ground despite eventual short access time windows.

However, particular attention must be given to space-links configurations 2 and 3 previously presented: *patch-to-array* and *array-to-array*. Using these configurations space-links data rate levels results comparable (2 to 4 times lower) with groun-link data rate of omni-directional antenna. Hence, the ratio between ground-links and space-links assumes an important meaning in terms of communication channel design.

To define conditions in which space-links are convenient we focus on the data rate ratio and we consider also the "uncovered" window, i.e. the period in which CubeSats are not in view with the ground station but can exchange data each others.

We introduce and define the *data rate ratio* as:

$$DR_{Ratio} = \frac{GL_{DR}}{SL_{DR}} \tag{10.1}$$

where:
GL_{DR} is the ground-link data rate relative to the CubeSat-to-GS EIRP considered.
SL_{DR} is the space-link data rate relative to the CubeSat-to-CubeSat EIRP considered.

DR_{Ratio} represents the first value to consider to design constellations in terms of allowed distances, altitudes and orbits by taking into account the communication features relative to hardware configurations. It can be interpreted as maximum number of satellite that can communicate in real time with a CubeSat that re-send information toward the GS i.e. the real-time concept of *data mule* satellites introduced in *Flower* and *SSRGT* constellations.

According to our proposed algorithm, a local behavior that a constellation assume is the mother-to-daughters (cluster-head/cluster-members) cluster, where one satellite is elected as mother-ship (cluster-head) and others assumes the daughter-ships role (cluster-members / cluster-guests). Usually mother-ship communicate with the GS, collects data from daughters and download them toward GS or, receive data from GS and distribute them to daughters. Mother-to-daughters configuration represents the basic local satellite topology of our constellation analysis.

10.2 The proposed antenna configuration for Cube-Sat

By analyzing DR$_{Ratio}$ values it's clear that space-link among CubeSat is not convenient in most of the cases. Usually, download data toward the ground station during the access windows is the most convenient solution because of the high data rate levels achievable. The low data rate levels of space-links do not justify the design effort and the costs to set up the cross-link capability However, considering certain communication capabilities, space-link can be a powerful strategy to sensibly increase the total data volume transfer from/to constellation to/from GS.

The antenna pointing operations to maintain the communication, the CubeSats attitude control and attitude requirements for the mission, battery-charge cycles etc.. are the some of the several factor that must be considered to design a functional antenna configuration able to manage constellations space-links and ground-link.

The ground-link analysis shows that omni-directional antennas provide sufficient data rate levels due to the the relative proximity with the ground station of CubeSats in LEO. Considering a 5-meter parabolic antenna receiver on the ground station we can guarantee data rate levels of down-link between 4 Mbps and 100 kbps when altitudes range is between 500 km and 2150 km and transmission power is between 16mW and 2W (figure 10.1).
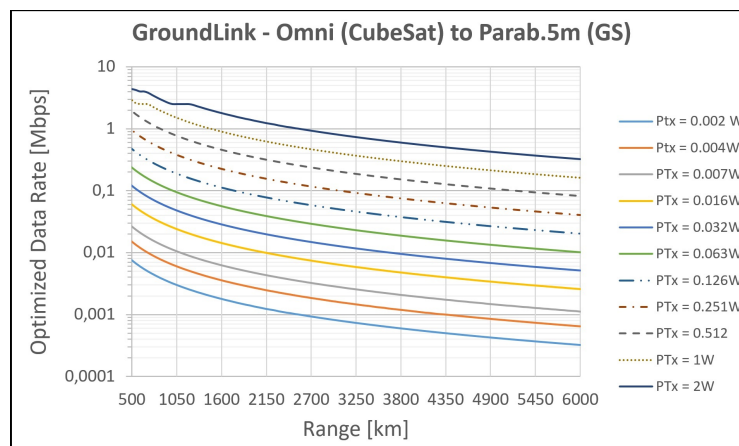
Fig. 10.1 Ground-Link - Isotropic Omni-directional to 5-m Parabolic at different transmission power.

In next data volume analysis we consider the isotropic omni-directional antenna to establish the ground-link. The semi-spherical radiation pattern typical of this antenna brings great advantages in terms of CubeSats attitude mobility freedom. The wide field of view of omni-directional antenna (ideally +/- 90°) allows CubeSat to perform attitude control strategies by maintaining a reliable link with the ground station.

Phased arrays represent our proposed solution to establish space-links. Phased arrays relax the CubeSat attitude control required to establish links thanks to their ability to electronically steer their beam.
Therefore, the overall antenna configuration proposed reduces the impact on the attitude control strategy required for CubeSats. In terms of communication channel, the omni-directional antenna presents link performances comparable with the space-link data rate obtained by exploiting phased arrays.

Figures 10.2 shows the simulation of the antennas configurations proposed.

In red, the beam of the isotropic antenna pointed toward the ground station. The multi-colour beam represents the phased array, it performs pointing operations until reach the maximum steering angle.
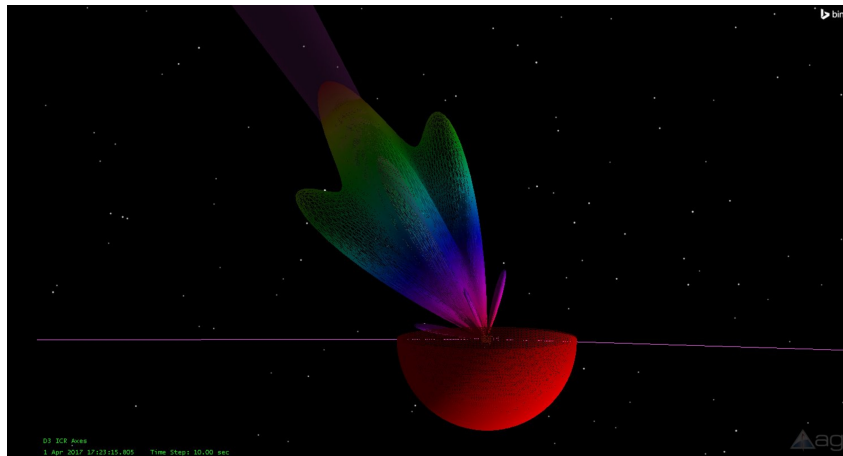
(a) P.Array + isotropic configuration.
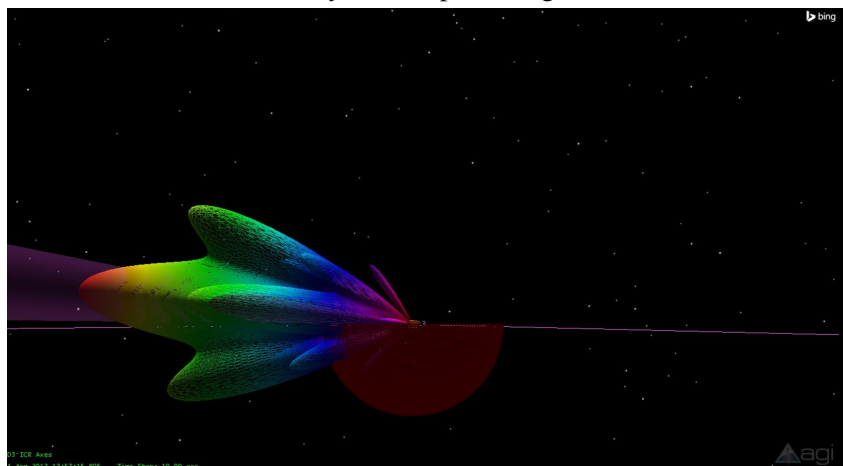
(b) P.Array (pointing) + isotropic configuration.

Fig. 10.2

10.2.1   Attitude Control

Attitude control of CubeSat represent an important stage of the link creation and maintenance if phased array steering action is not able to point the beam toward a specific direction. Furthermore, it can be used also to optimize and maintain cluster structure during the cluster formation and maintenance process. Most of common attitude control in CubeSat applications are the reaction wheel [62] and a magnetic torquer, a system that react with the Earth magnetic fiel to orient the CubeSat in the desired position, an example is described in [63].

10.3   Constellations analysis and data volume improvements

The access and data volume analysis has been performed considering the same transmission settings utilized to simulate the clustering algorithm as shown in table below. We reported the access information performed in chapter *Constellation Topologies* and we calculated the data volume improvements achievable thanks to the proposed antenna configuration.

All the access timing in this chapter and in chapter 5 have been obtained thanks to AGI STK [64] simulation software, considering the proposed antenna configuration we calculated the data volume and the data volume improvements obtained thanks to the inter-satellite links.

When *sensor* satellites are not in view with the ground station but can communicate with *sink* satellites the communication link is established according to the link limitations constraints defined (60° field of view on *sink*) and a certain amount of data volume is flows from *sensor* to *sinks*. Afterwards, these amount of data are sent from *sink* satellites to the ground station. The total data volume that flows from *sensor* to the ground station represent the data volume improvement, i.e. the additional amount of data earned thanks to the space-link creation between CubeSats. In next sections we analyze the data volume improvements of the three constellation topologies analyzed.

Table 10.1 Simulation Configuration.

Description	Value
Tx Antenna	Omni-directional
Rx Antenna	Omni-directional
Tx Power	512[mW]
EIRP	27,09 dBm
Working freq.	2.4 [GHz]
Modulation Scheme	QPSK
Coding Scheme	LDPC 1/2, 4/5, 7/8

10.4   Equatorial Topology: Data volume Improvements

Considering store & forward communication from D3, D6, D7, D8 to D1, then from D1 to GS we calculate the total average access from daughters to GS. Table 10.2 shows the total average access to GS earned in relation to direct access from daughters to GS.

Table 10.2 Equatorial Sensor total Access to GS.

Satellite	Access to GS [h]	Access to Sink (60° sens.)[h]	Total Monthly Access[h]	Average Daily Access[h]	Access Improve-ment[%]
Equatorial Sens 3,6,7,8	68,067	11,562	79,629	2,65	+ 16,99%

10.5   Flower / Sink Topology: Data volume Improvements

Figure 10.3 resumes the access timing values presented in flower /sink constellation topology. The store and forward method can move data from *sensor* to *sink* satellites and significantly improve the total access that *sensor*s have with the ground station through *sinks*. For each *sensor* is reported the direct access to GS and the total access to *sinks* when they are not in view with GS.
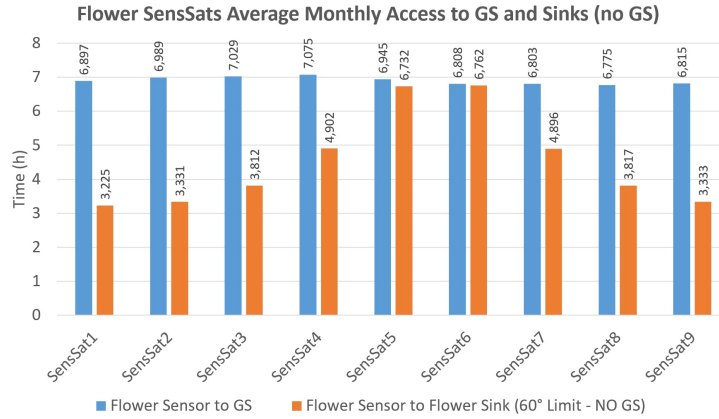
Fig. 10.3 Flower Sensors access to GS and Sink (sensor 60°).

To calculate the improvement in terms of access time we define:

- $T_{SensorGS}$: Total access time from Flower Sensors to Ground Station

- $T_{SensorSink}$: Total access time from Flower Sensor to the 60° cone on the Flower Sinks when Flower Sensors are not in view with the ground station.

- T_{SinkGS}: Total acces time from Sinks satellites to GS

Total access from Sensors to Ground Station is:

$$T_{tot} = T_{SensorGS} + min|T_{SensorSink}, T_{SinkGS}| \qquad (10.2)$$

For each Sensor Satellite we obtain total access timing reported in table 10.3. Sink to GS access guarantees that data volume moved from Sensors to Sinks can be downloaded toward the GS according to ratio table, balance between channels is provided.

Table 10.3 Flower Sensor total Access to GS.

Satellite	Access to GS [h]	Access to Sink (60° sens.)[h]	Total Monthly Access[h]	Average Daily Access[h]	Access Improve-ment[%]
Flower Sens 1	6,897	3,224	10,122	0,337	+ 46,75%
Flower Sens 2	6,988	3,330	10,319	0,343	+47,66%
Flower Sens 3	7,028	3,811	10,840	0,361	+54,23%
Flower Sens 4	7,075	4,902	11,977	0,399	+69,29%
Flower Sens 5	6,945	6,732	13,676	0,455	+96,93%
Flower Sens 6	6,808	6,762	13,570	0,452	+99,32%
Flower Sens 7	6,802	4,896	11,698	0,389	+71,98%
Flower Sens 8	6,775	3,817	10,592	0,353	+56,34
Flower Sens 9	6,815	3,333	10,148	0,338	+48,91%

In Flower / Sink constellation the space-link communication allows to increase the total access time to the ground station from 1,5 to 2 times.
In conclusion, total access is strongly related to the orbital parameters of the constellation's elements, despite the information about the communication link, a deep study must be done to define the achievable performances in relation to the position and evolution of constellations.

Figure 10.4 shows the orbits of Flower Sensors (violet), orbit of Flower Sinks and their relative 60° cone sensors (green) and the 3000km line of sight between Sensors and Sinks (red). Connections for *data links* is not represented by a line, detail 10.4b shows *data links* established between Flower-Sink-8 with Flower-Sens-7,Flower-Sens-8,Flower-Sens-9, they fall inside the sensor cone view.
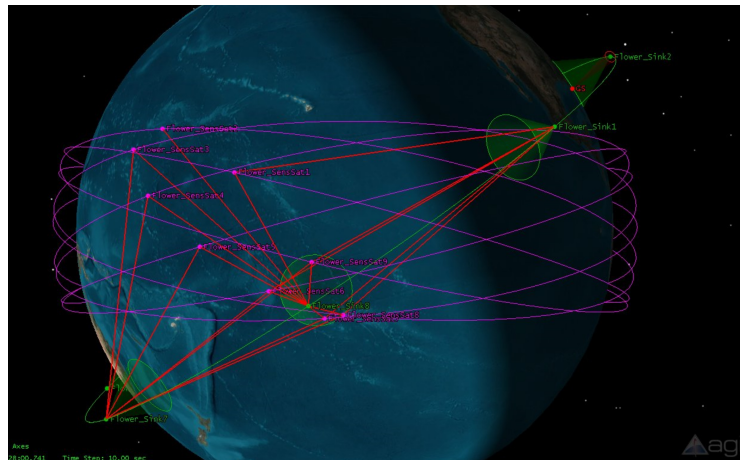
(a) Flower access picture.
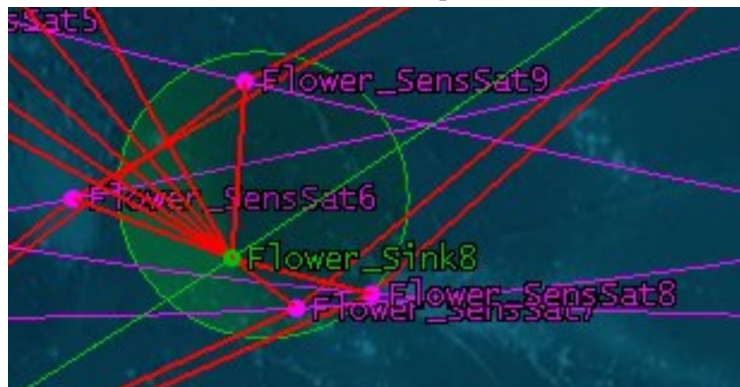
(b) Flower access picture detail.

Fig. 10.4 Flower Access Types.

10.6   SSRGT / Sink Topology: Data volume Improvements

We apply formula 10.2 to calculate the maximum achievable access from SSRGT Sensors to GS trough the store and forward communication service provided by SSRGT Sinks. Also for SSRGT/Sink constellation, Sink to GS access guarantee that data volume moved from Sensors to Sinks can be downloaded toward GS because the constellation communication hardware is coherent with its relative ratio table, therefore balance between data channel is provided. Total access table is shown in 10.4.

Table 10.4 SSRGT Sensor total Access to GS.

Satellite	Access to GS [h]	Access to Sink (60° sens.)[h]	Total Monthly Access[h]	Average Daily Access[h]	Access Improve-ment[%]
SSRGT Sens 1	12,713	5,414	18,128	0,60	+ 42,59%
SSRGT Sens 2	12,7172	5,328	18,045	0,60	+41,90%
SSRGT Sens 3	12,8119	5,371	18,184	0,61	+41,93%
SSRGT Sens 4	2,711	5,392	18,103	0,60	+42,42%
SSRGT Sens 5	12,721	5,397	18,118	0,60	+42,43%
SSRGT Sens 6	12,752	5,351	18,103	0,60	+41,96%
SSRGT Sens 7	12,697	5,398	18,096	0,60	+42,52%
SSRGT Sens 8	12,772	5,394	18,166	0,61	+42,23
SSRGT Sens 9	12,770	5,284	18,054	0,60	+41,38%

Given the linear orbit characteristics the access improvements is results to be around 42% for each SSRGT Sensor satellite.

10.7 Mission Design: real-time hop-to-hop access optimization

The analyzed constellation topologies represent an useful example to underline the potentiality of space to space communication abilities. To build a complete tool, able to design constellations and optimize the inter-satellite links, we must consider a limit case in which one (or more) sensor satellites that are not in view with GS are able to communicate with one (or more) sink satellite(s) that are in communication with GS as shown in figure 10.5. In this specific case is possible to establish an hop-to-hop communication and guarantee a real-time access from sensors to GS despite they result not in GS's field of view: the goal is to calculate the maximum number of sensor satellite that can transmit data to the Sink without saturate the down-link (Sink to GS) channel.
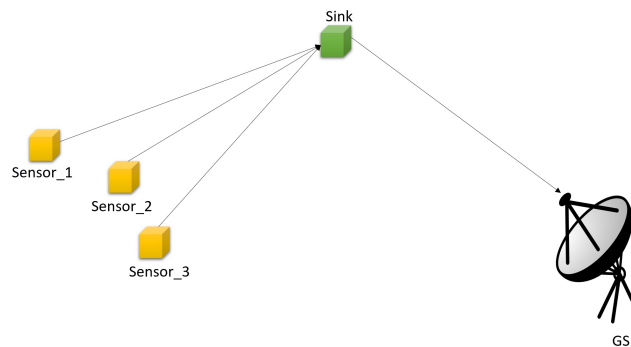
Fig. 10.5 Real-time hop-to-hop communication: Sensors to Sink / Sink to GS.

Due to the satellite distribution pattern, in SSRGT constellation is not possible that more than one sensor satellite communicates with same Sink. In this case, the down-link channel do not risk to be saturated. Flower constellation presents situations where up to three/four satellites communicate with the same sink at the same time.
In order to simply the design process of constellations and avoid down-link channel saturation of sink satellites due to multiple sensor satellite communication we consider the following parameters to create a graphic design tool:

- N: Number of Satellites in that communicate at the same time with a Sink

- α: Sink Satellite field of view aperture (60° degree toward Earth in our analysis)

- DR$_{Ratio}$

Figure 10.6 shows an example of the dynamic graphs constellation design tool. It indicates how many sensor satellites can communicate whit the same sink satellite and at which altitude range when the real-time hop-to-hop condition previously introduced occurs.
Parameters selected are: N = 4, α = 60° and DR$_{Ratio}$ is relative to our proposed hardware and antennas communication configuration with transmission power fixed for both space-link and ground-link at 512mW. Curves refers to all possible altitudes and Data Rates combinations with this parameter configuration.

Constellation Spacing and Data Rate Trade
GL(par5m - Patch)/SL(Array - Array)
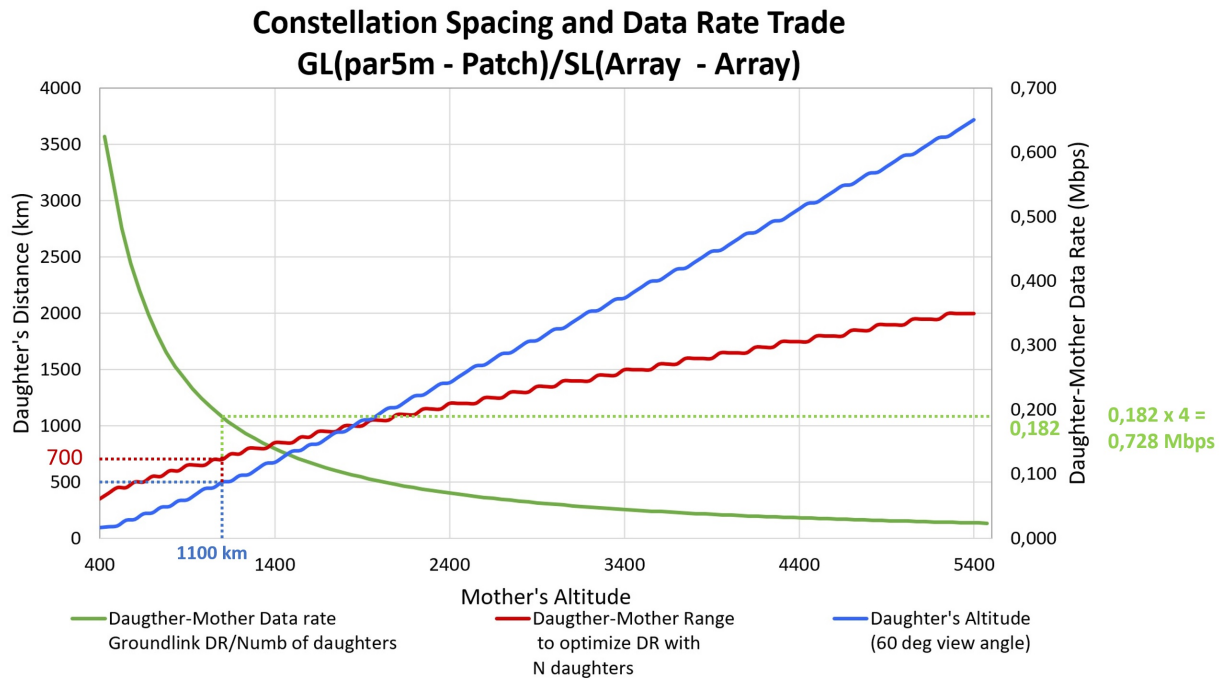
Fig. 10.6 Constellation Design Tool (communication Analysis).

Considering a 4 daughter-ship (sensor satellites) cluster in view with a single Sink (mother-ship) satellite at the same time, the Sink can be placed as high as 1100km, with a down-link rate at 728 kbps to ground station during all the access window. That means the daughter-ship can be talking to the mother at 182 kbps each at a maximum range of 700 km away from the mother, which coincides with the maximum range of the 60° deg field of view cone from sinks to sensors satellites. This tool can be used to define how many satellites can be managed by a single sink satellites in case of hop-to-hop real-time access to GS, sinks correspond to our cluster-heads of our proposed clustering algorithm.

Chapter 11

Conclusions

In this dissertation we faced the communication networks in CubeSat constellations in terms of communication strategies, data link optimizations and access increasing to the ground station. We started from the constellation management strategies represented by clustering algorithms and we went deeper until we designed the communication system in detail.

After a preliminary analysis on existing clustering algorithms and a selection of specific algorithms that can be useful to our applications we have introduced, design and simulate a clustering algorithm able to create communication links between satellites depending on hardware and mobility characteristics of the constellation elements.

In presence of strong communication link performances, the communication between satellites results able to create reliable connection, on which route informations to optimize the constellation behavior and facilitate the achievement of mission's goals. Also in non optimal conditions due to particular mobility factors, results possible to establish communication links, despite hop-to-hop communication is required. The main side effect related to the creation and maintenance of a MANET has been faced and mitigated thank to a strategy who prefers the limitation of the energy consumption and maintain under control flooding effect like the ripple effect of the re-clustering.

Due to the communication limitation, a preliminary analysis must be performed to understand if the constellation orbital parameters respect the total required time to execute the clustering of satellites. The assumption of mutual satellite access reduce the set of applicable cases where algorithm can be applied. We conclude that a

random distribution of satellites around a common plane can require communication capabilities that aren't usually available on CubeSat. However, we can assume that in next future CubeSat constellations will be composed by more and more satellites thus providing opportunity to increase the algorithm application conditions.

The design of the communication system for CubeSat constellations start from the analysis of the hardware configurations for antennas available for CubeSat technologies, focusing on low cost, and reliable solution by considering the available CubeSat's surface and low power supply capabilities that characterize these small satellites.

By selecting a set of candidate antennas configurations to establish communication links, we focused on the absolute data rate performances achievable depending on distances and transmission power levels involved, with a special focus on data rates related to the inter-satellite link (ISL) or space-link.

From a first analysis we noticed that, for satellites orbiting in LEO, the ground-link data rate values result to fit for our purposes despite the low power levels involved and the use of patch or isotropic omni-directional antennas. This because of the relative proximity of satellite to Earth. Moreover, unlike patch antennas, isotropic omni-directional antennas allow to maintain the link also at non-optimal CubeSat inclinations / pointing.

Data rates analyzed for ground-links are related to many factors, we can achieve values from 1kbps to 5 Mbps depending on antennas, transmission power and distances.

The particular attention to the space-link analysis bring us to the conclusion that phased array are one of the best solution to establish space-link given their greater antenna gain if compared to other solutions. Their ability to steer the beam guarantee to CubeSats a certain level of attitude freedom of movement and relax constraints in terms of the overall mission attitude strategy. Moreover, data rates achievable between CubeSats results comparable with ground-link data rates when phased arrays are involved: if we consider any ground-link analyzed and we compare it with a space-link performed without phased arrays we can conclude that establishing space-link is not efficient. Given the data rate differences is better to download data toward ground.

Nevertheless, by using phased arrays data rates results "comparable", and is possible to hypothesize use of space-link as tool to move data between CubeSat constellations in LEO orbit by performing store and forward data operations or hop-to-hop communications. Depending on the power supply levels considered we cross-compare

ground-links and space-links data rates and the relative maximum achievable distances in order to find a zone in which establishing space-links can bring us advantages in terms of total data volume transferable.

Afterwards, we analyzed three different constellations considering the proposed antenna configuration for space-link performed by phased array and groun-link communication performed by an isotropico omni-directional antenna, both transmission with a transmission power of 512 mW. These constellation topologies refer to specific missions for Earth observation and performs data movements through the use of mule satellite techniques: we simulated each constellations to obtain information about satellites mutual access and GS access to understand the improvements in terms of data volume transferable from constellation to ground and vice versa thanks to the mules (Sink Satellites).

The next step has been to use access to perform a data volume analysis considering specific communication constraints we introduced.

In most of cases, the total access time from constellations to ground station considerably increased: depending on constellation, satellites can increase the total access from 40% up to 99% more. The average daily volume downloadable in the best case scenario results to be 63 / 64 Gb in an Equatorial constellation; 14/15 Gb in a Flower/Sink constellation and 26 / 27 Gb in a SSRGT constellation.

However, we cannot compare constellations topologies by relying only on the total access performances: constellations design process involve the consideration of several factors. The constellation mission/s is the first element that must be considered to define the topology: earth observation, specific target or observation area, particular payloads and specific combined action of elements of constellations (e.g.: Tandem-X / TanderSAR constellation topology [65]) cannot be ignored or partially scarified in favor of data flow optimization strategies.

The communication optimization results a critical factor in a constellation design process but not the unique. Therefore, we combine measurements and simulation performed to for a dynamic graph able to facilitate the constellation design process in terms of communication optimization. This tool can be used as support of the decision of orbital parameters once the communication performances are established or vice-versa.

References

[1] H. Heidt, J. Puig-Suari, A. Moore, S. Nakasuka, and R. Twiggs. Cubesat: A new generation of picosatellite for education and industry low-cost space experimentation. *In Procedings of the 14th AIAA/USU Small Satellite Conference. SSC00-V-5. August 2001.*

[2] J.Bouwmeester and J.Guo. Survey of worldwide pico- and nano- satellite missions, distributions and subsystem technology. *Acta Astronaut. 67(7–8)(2010)854–862.*

[3] J.Bouwmeester, G.F.Brouwer, E.K.A.Gill, G.L.E.Monna, and J. Rotteveel. Design status of the delfi-next nanosatellite project. *Proceedings of the 61st International Astronautical Congress, 2010,pp.1–13.*

[4] K.Sarda, C.Grant, S.Eagleson, D.Kekez, and R.Zee. Canadian advanced nanosatellite experience 2 orbit operations: Two years of pushing the nanosatellite envelope. *Proceedingsofthe 61st International AstronauticalCongress, 2010.*

[5] A. Aydinliogluand and M.Hammer. Compass-1picosatellite:mag- netic coilsforrattitudecontrol. *Proceedingsofthe2ndInter- national ConferenceonRecentAdvancesinSpaceTechnologies, 2005, pp.90–93.*

[6] F.M.Pranajaya and R.E.Zee. Advancednanosatellitedevelopment at spaceflightlaboratory. *Proceedingsofthe1stIAACon- ference onUniversitySatelliteMissions,2011.*

[7] C. E. Perking. *Ad Hoc Networking.* 2001.

[8] J. M. Kahn, R. H. Katz, and K. S. J. Pister. Mobile networking for 'smart dust'. *Proc. 5th IEEE/ACM MOBICOM*, Aug. 1999.

[9] P. Guptar and P. R. Kumar. The capacity of wireless networks. *IEEE Trans. Info. Therory, vol. -IT 46.2*, Mar. 2000.

[10] K. X. Xu, X. Y. Hong, and M. Gerla. An ad hoc mobile network with mobile backbones. *Proc. IEEE ICC'2002, vol. 5*, Apr.-May 2002.

[11] E. M. Belding-Royer. Hierarchical routing in ad hoc mobile networks. *Wireless communications and mobile comp., vol. 2 n. 5*, 2002.

[12] E. M. Belding-Royer. Virtual dynamic backbone for mobile ad hoc network. *Proc. IEEE ICC'01, Vol. 1, p 250-55*, 2001.

[13] M. R. Pearlman and Z. J. Has. Determining the optimal configuration for the zone routing protocol. *IEEE JSAC, vol. 17, p. 1395-414*, 1999.

[14] J. Wu and H. L. Li. On calculatin connected dominating set for efficient routing in ad hoc wireless networks. *3rd int. Wksp. Discrete Algorithms and Methods for Mobile Comp. and Communication*, 1999.

[15] C. Chiang et al. Routing in cluster multihop, mobile wireless networks with fanding channel. *Proc. IEEE SICON'97*, 1997.

[16] M. Gerla and J. T. Tsai. Multiuser, mobile, multimediaradionetwork. *Wireless Networks, vol. 1*, Oct. 1995.

[17] J. Y. Yu and P. H. J. Chong. 3hbac (3-hop between adjacent clusterheads): a novel non-overlapping clustering algorithm for mobile ad hoc networks. *Proc. IEEE Pacrim,vol.1*, Aug. 2003.

[18] P. Basu, N. Khan, and T. D. C. Little. A mobility based metric for clustering in mobile ad hoc networks. *Proc. IEEE ICDC-SW'01*, Apr. 2001.

[19] A. D. Amis and R. Prakash. Load-balancing clusters in wireless ad hoc networks. *Proc. 3rd IEEE ASSET*, 2000.

[20] J. Wu et al. On calculating power-aware connected dominationg sets for efficient routing in ad hoc wireless networks. *J. COmmunication and Networks, vol.4 n.1*, 2002.

[21] M. Chatterjee, S. K. Das, and D. Turgut. An on-demand weighted clustering algorithm (wca) for ad hoc netwoks. *Proc. IEEE Globecom*, 2000.

[22] T. J. Kwon et al. Efficient flooding with passive clusterign - an overhead-free selective forward mechanism for ad hoc/sensor networks. *Proc. IEEE vol.91 n.8*, Aug. 2003.

[23] A. Iwata et. al. Scalable routing strategies for ad hoc wireless networks. *IEEE JSAC, vol.17, pp. 1369-79*, Aug. 1999.

[24] W. Chen et. al. Anmp: Ad hoc networks management protocol. *IEEE Journal on Selected Areas in Communications, vol. 17*, 1999.

[25] C. R. Lin and M. Gerla. Adaptive clustering for mobile wireless networks. *IEEE JSAC, vol.15, pp.1466-75*, Sept. 1997.

[26] A. B. McDonald and T. F. Znati. Design and performance of a distribuited dynamic clustering algorithm for ad-hoc networks. *34th Annual Symp.,pp.27-35*, Apr. 2001.

[27] C. R. Lin and M. Gerla. A distribuited control scheme in multi-hop packet radio networks forvoice/data traffic support. *Proc. IEEE ICC,pp. 1238-42*, 1995.

[28] T. C. Hou and T. J. Tsai. An access-based clustering protocol for multihop wireless ad hoc network. *IEEE JSAC , vol.19, pp.1201-10*, 2001.

[29] Jane Y. Yu and Peter H.J. Chong. A Survey of Clustering Schemes for Mobile Ad Hoc Networks. *IEEE Communications Surveys, first quarter 2005, Volume 7, No.1*, 2005.

[30] Ian D. Chakeres and Elizabeth M. BeldingRoyer. The utility of hello messages for determining link connectivity. *Wireless Personal Multimedia Communications. The 5th International Symposium on Wireless Personal Multimedia Communications*, 2002.

[31] A. Ephremides, J. E. Wieselthier, and D. J. Baker. A design concept for reliable mobile radio networks with frequency hopping signals. *Proc. IEEE vol. 75*, 1987.

[32] Ian D. Chakeres and Elizabeth M. BeldingRoyer. Recomendation itu-r p.676-10. attenuation by atmospheric gases. *International Telecommunication Union*, 09/2013.

[33] S. Speretta, L.M. Reyneri, C. Sansoé, M. Tranchero, C. Passerone, and D. Del Corso. Modular architecture for satellites. *58th International Astronautical Congress , Hyderabad, India. - IAC-07-B4.7.09*, 24 - 28 September 2007.

[34] Patch Antenna 1.4"x1.4" Data Sheet ADC-0509251107. http://www.antdevco.com/.

[35] J.Sauder et. al. Ultra-compact ka-band parabolic antenna deployable antenna for radar and interplanetary cubesats. *29th Annual AIAA/USU)*.

[36] Alessandra Babuscia et. al. Inflatable antenna for cubesat: Fabrication, deployment and results of experimental tests. *Aerospace Conference, 2014 IEEE*, 1-8 March 2014.

[37] Richard E. Hodges, Daniel J. Hoppe, Matthew J. Radway, and Nacer E. Chahat. Novel deployable reflectarray antennas for cubesat communications. *Microwave Symposium (IMS), 2015 IEEE MTT-S International*, 2015.

[38] Andrew Klesh and Joel Krajewski. Marco: Cubesats to mars in 2016. *29th Annual AIAA/USU Conference on Small Satellites*, 2015.

[39] R. G. Gallager. Low-density parity-check codes. *IRE TRANSACTIONS ON INFORMATION THEORY*.

[40] NASA Space Technology Mission Directorate (STMD). Low-density parity-check codes for high data rate receivers.

[41] CCSDS. Low-density parity-check codes for use in near-earth and deep space aplications, experimental specification. *CCSDS 131.1-O-2*, sept 2007.

[42] CCSDS. Flexible advanced coding and modulation scheme for high rate telemetry applications. *CCSDS 131.1-B-1*, March 2012.

[43] Eb / N0 Curves figure 4.1(a). https://www.dsprelated.com/showarticle/136.php.

[44] Eb / N0 Curves figure 4.1(b). http://file.scirp.org/html/7-9700275/6ea762d3-3451-4cbd-95c6-bee5834beec3.jpg.

[45] Alexandru Budianu, Teodoro J. Willinks Castro, Arjan Meijerink, and Mark J. Bentum. Itersatellite links for cubesats. *IEEEAC Paper 2276, Version 5*, 01/2013.

[46] Najeeb ul Hassan, Michael Lentmaier, and Gerhard P. Fettweis. Comparison of ldpc block and ldpc convolutional codes based on their decoding latency. *Vodafone Chair Mobile Communications Systems Dresden University of Technology (TU Dresden), 01062 Dresden, Germany.*

[47] Paul Muri, Janise McNair, Joe Antoon, Ann Gordon-Ross, Kathryn Cason, and Norman Fitz-Coy. Topology design and performance analysis for networked earth observing small satellites. *The 2011 Military Communications Conference - Track 5 - Communication and Network Sysstems*, 2011.

[48] R. Shah, S. Roy, S. Jain, and W. Brunette. Data mules: Modeling and analysis of a three-tier architecture for sparse sensor networks. *Ad Hoc Networks, vol. 1, no. 2-3, pp. 215–233, 2003.*

[49] D. Mortari and M. Wilkins. Flower constellation set theory. part i:compatibility and phasing,. *erospace and Electronic Systems, IEEE Transactions on, vol. 44, no. 3, pp. 953–962, 2008.*

[50] J. Wertz, H. Meissinger, L. Newman, and G. Smit. Mission geometry; orbit and constellation design and management. *Kluwer Academic Publishers, El Segundo, CA, 2001.*

[51] V. Salomonson and A. Park. An overview of the landsat-d project with emphasis on the flight segment. *LARS Symposia, 1979, p. 236.*

[52] P. Slater. Survey of multispectral imaging systems for earth observations. *Remote Sensing of Environment, vol. 17, no. 1, pp. 85–102, 1985.*

[53] G. Tyc, J. Tulip, D. Schulten, M. Krischke, and M. Oxfort. The rapideye mission design. *Acta Astronautica, vol. 56, no. 1-2, pp. 213–219, 2005.*

[54] G. Bruni and L. Reyneri. Development and testing of innovative solar panels with deployable structure for aramis satellite platform. Master's thesis, Politecnico di Torino, 2016.

[55] AraMis thermal analysis. 1b641.v1.0.i3 satellite thermal analysis.

[56] AraMis thermal analysis. 1b6411.v1.0.i1 structure thermal analysis.

[57] S.V. Shell and W.A. Gardner. High resolution direction finding. *Chapter 17,Handbook of Statistic 10 - Signal Processing and Application, ed. Bose,N.K., and Rao,C.R.,pp.755-817,1993.*

[58] R.O. Schmidt. Multiple emitter location and signal parameter etimation. *Procedings of RADC Spectrum Estimation Workshop ,Griffiss AFB,NY, 243-258,1979.*

[59] Paulraj A., Roy R., and Kailath T. A subspace rotation approach to signal parameter estimation. *Preceedings of the IEEE, vol. 74, pp.1044-1045,july 1986.*

[60] Isamu Chiba, Nobuo Kumagae, Rumiko Yonezawa, Ken ichi Hariu, and Naoya Morita. Phased array antenna calibration method in operating condition- rev method -. *International Telecommunication Union*, 09/2013.

[61] Netlogo Simulator. https://ccl.northwestern.edu/netlogo/.

[62] Espen Oland and Rune Schlanbusch. Reaction wheel design for cubesats. *Department of Scientific Computing, Electrical Engineering and Space Technology Narvik University College Narvik, Norwayl.*

[63] Anwar Ali, M. Rizwan Mughal, Haider Ali, Leonardo M. Reyneri, and M. Naveed Aman. Design, implementation, and thermal modeling of embedded reconfigurable magnetorquer system for nanosatellites. *IEEE Transactions on Aerospace and Electronic Systems. Volume: 51 Issue: 4.*

[64] System Tool Kit by AGI. https://www.agi.com/news/blog/april-2017/stk-11-2-is-here-download-now.

[65] Gerhard Krieger et. al. Tandem-x: A satellite formation for high-resolution sar interferometry. *IEEE Transactions on Geoscience and Remote Sensing (Volume: 45, Issue: 11, Nov. 2007).*